

# Integration of Active and Passive Sampling Techniques for Characterization of Non-point Source Contamination from Septic Systems in Rural Ontario Hamlets

by

Maria Digaletos

A thesis  
presented to the University of Waterloo  
in fulfillment of the  
thesis requirement for the degree of  
Master of Science  
in  
Earth Science

Waterloo, Ontario, Canada, 2019

©Maria Digaletos 2019

## **AUTHOR'S DECLARATION**

This thesis consists of material all of which I authored or co-authored: see Statement of Contributions included in the thesis. This is a true copy of the thesis, including any required final revisions, as accepted by my examiners.

I understand that my thesis may be made electronically available to the public

## **Statement of Contributions**

Chapters 2 and 3 of this thesis will be submitted as journal articles. The majority of the contributions (sample collection, laboratory work, figure preparation, and writing) were completed by me. Laura Groza and YingYing Liu contributed to the results section in Chapter 2. My supervisors, Dr. Carol Ptacek and Dr. Janis Thomas, and committee members, Dr. Chris Parsons and Dr. David Blowes, contributed helpful edits and comments to improve the quality of the chapters.

## Abstract

Excessive nutrient loading to surface water bodies can lead to the development of eutrophic conditions, including deterioration of water quality and ecological stability. Sources of nutrient loading include wastewater treatment plants, agricultural activities, and to a lesser extent, septic systems. Septic systems are commonly used to dispose of domestic waste in rural areas where access to a municipal wastewater treatment system is not practical. When homes are closely spaced in rural communities forming hamlets, there are increased risks of nutrient impacts. Direct assessment of anthropogenically-derived nutrient loading from septic systems can involve costly and time-consuming investigations of subsurface releases. There is a need for indirect assessment of septic system releases through measurement of wastewater indicators within surface receiving waters. This thesis describes two studies on characterizing nutrient and contaminant concentrations in rural headwater streams: (1) a study sampling the upstream (US) and downstream (DS) locations of streams flowing through three rural hamlets for nutrients and organic tracers; and (2) the application of passive sampling techniques to determine time weighted average concentrations of an organic anthropogenic wastewater tracer and dissolved phosphorus.

Several anthropogenic tracers were used to delineate septic system discharge in rural hamlets. The selected suite included an artificial sweetener acesulfame-K (ACE-K), pharmaceuticals caffeine (CAF), carbamazepine (CBZ), gemfibrozil (GEM), ibuprofen (IBU), naproxen (NAP), and sulfamethoxazole (SMX), and a human specific biological indicator *Bacteroides* (BacHum) to determine wastewater impacts on the streams. Additional water quality parameters and nutrient concentrations were also measured, including soluble

reactive phosphorus (SRP) and total ammonia and ammonium nitrogen ( $\text{NH}_{3+4}\text{-N}$ ). Three rural hamlets in the Grand River Watershed (Ontario) were selected for this study based on varying characteristics including home density and location relative to streams, stream geometry, and overburden material. The US and DS locations for each hamlet were sampled up to two times monthly between April 2017 and March 2018. Results indicate that non-point source contamination by septic systems is present in these areas, with downstream locations showing elevated concentrations of anthropogenic tracers. The tracers with the most elevated concentrations consistently across all three sites were ACE-K concentrations ( $\sim 54 \mu\text{g L}^{-1}$ ) and BacHum abundances ( $\sim 10^7$  counts  $100 \text{ mL}^{-1}$ ). The Spearman Rank Order Sum test significant ( $P < 0.05$ ) results indicate that tracer concentrations are increasing along the streams. Elevated nutrient concentrations were also observed, including SRP concentrations up to  $1.72 \text{ mg L}^{-1}$  and  $\text{NH}_{3+4}\text{-N}$  concentrations up to  $5.51 \text{ mg L}^{-1}$ . These results suggest that in densely populated rural areas near streams, elevated nutrient concentrations may be derived from septic systems. The nutrient-organic tracer correlation results were frequently insignificant or were not very strong, which indicates that it is difficult to quantify the extent of nutrient contamination by wastewater based on the nutrient and organic tracer concentrations.

Passive sampling techniques were applied to these headwater streams during two-week deployments in the spring, summer, and fall, followed by an intensive two-week study at one site. The polar organic chemical integrative sampler (POCIS) was used to target ACE-K, and a modified peeper filled with Fe-coated sand (P-Trap) was used to accumulate dissolved phosphorus. The samplers include two membranes secured around a receiving

phase placed parallel to flow in the surface waters. Both samplers are designed to linearly uptake the contaminants and provide time weight average (TWA) concentrations which can be compared to average grab sample concentrations. The POCIS extract TWA concentrations of ACE-K ( $< 2 \text{ ng L}^{-1}$  to  $11 \text{ ng L}^{-1}$ ) were up to three orders of magnitude lower than the mean grab sample concentrations ( $< 140 \text{ ng L}^{-1}$  to  $2.7 \text{ } \mu\text{g L}^{-1}$ ). The results indicate that the POCIS utilized are not ideal for targeting ACE-K in surface waters. Issues with accumulation of debris and biofouling were observed on the POCIS and P-Traps upon collection, which may have hindered the interaction between the water and the membranes. The 14-day P-Trap TWA concentrations of dissolved P (US =  $29.4 \text{ } \mu\text{g L}^{-1}$ , DS =  $45.5 \text{ } \mu\text{g L}^{-1}$ ) more closely approximated the mean grab sample concentrations (US =  $27.1 \text{ } \mu\text{g L}^{-1}$ , DS =  $31.4 \text{ } \mu\text{g L}^{-1}$ ) compared to the 8-day results (TWA: US =  $40.2 \text{ } \mu\text{g L}^{-1}$ , DS =  $53.6 \text{ } \mu\text{g L}^{-1}$ ; mean grab: US =  $22.9 \text{ } \mu\text{g L}^{-1}$ , DS =  $26.0 \text{ } \mu\text{g L}^{-1}$ ). Overall, the P-Trap performed better in the rural streams compared to the POCIS.

The results of this thesis suggest that headwater streams flowing within rural hamlets warrant increased attention to help mitigate nutrient loading and implement strategies to reduce septic system impacts. The use of a conservative tracer, like ACE-K, and a fecal indicator that is host specific, like *Bacteroides*, is recommended for future studies monitoring surface waters in rural areas. The use of passive sampling techniques shows potential as an environmental monitoring method in shallow streams, but requires selection of an appropriate phase, and actions are taken to minimize fouling.

## Acknowledgements

I would first like to acknowledge the Ontario Ministry of Environment, Conservation and Parks for providing support and funding for this project through the Canada-Ontario Great Lakes Agreement (Project ID #1300).

I would like to express my great appreciation to Dr. Carol Ptacek and Dr. Janis Thomas, my co-supervisors, for their support, valuable suggestions, edits, and help planning and developing this project.

I am also indebted to YingYing Liu and Laura Groza– thank you for running my pharmaceutical analyses and for teaching me new analytical techniques with enthusiasm. I would also like to thank Joy Hu for running ICP-OES analyses, and Linden Fairbairne for helping me in the lab. I am also grateful for the encouragement I received in the lab– thank you, Sara Fellin, Janice Cooper and Krista Elena for helping me, teaching me, and making me laugh!

This field work would not have been completed without the help of numerous other people. From the Ministry of the Environment, Conservation and Parks: thank you, Sarah MacKell, Laura Benakoun, and Erin Nicholls. From the University of Waterloo: thank you, Nicole Russell, YingYing Liu, Brent Verbuyst, and Shawn Wheatley.

Finally, I would like to thank my committee members, Dr. Chris Parsons and Dr. David Blowes, for their insight and recommendations.

## **Dedication**

For my wonderful and supportive fiancé Shawn.



## Table of Contents

AUTHOR'S DECLARATION .....	ii
Statement of Contributions.....	ii
Abstract .....	iv
Acknowledgements .....	vii
Dedication .....	viii
Table of Contents .....	ix
List of Figures .....	xii
List of Tables.....	xix
List of Abbreviations.....	xxii
Chapter 1 Introduction.....	1
1.1 Introduction .....	1
1.2 Dissolved Nutrients in the Environment .....	2
1.3 Wastewater Released from Septic Systems.....	5
1.3.1 Dissolved Nutrients .....	5
1.3.2 Release of Other Contaminants in the Environment .....	6
1.4 Using Organic Tracers to Track Wastewater .....	7
1.5 Passive Sampling Techniques .....	9
1.6 Research Objectives .....	10
1.7 Thesis Organization.....	10
Chapter 2 Characterization of Non-point Source Contamination from Septic Systems in Rural Ontario Hamlets.....	13
2.1 Introduction .....	13
2.1.1 Non-point Source Contamination in Rural Hamlets.....	14
2.1.2 Tracing Nutrients in Rural Catchment Areas .....	15
2.1.3 Study Objectives.....	17
2.2 Methods.....	17
2.2.1 Field Site Descriptions and Sampling Design .....	17
2.2.2 Water Sampling and Field Analysis .....	18
2.2.3 General Water Quality Analysis.....	20
2.2.4 Tracer Analysis.....	21
2.2.5 Statistical Analysis .....	26

2.3 Results.....	26
2.3.1 Stream Characterization and Spatial-temporal Patterns in Water Quality .....	26
2.3.2 US–DS Statistical Comparison .....	36
2.3.3 Correlations between Dissolved Nutrients, FIB, and Tracers .....	39
2.4 Discussion.....	41
2.4.1 Characterization of Non-point Source Contamination in Rural Streams .....	41
2.4.2 Tracking Nutrients in Surface Waters Using Tracers .....	48
2.4.3 Potential Pathways for Wastewater Contamination in the Environment .....	50
2.4.4 Evaluation of a Combined Tracer Approach .....	55
2.5 Conclusions.....	60
Chapter 3 Using Passive Samplers POCIS and P-Traps to Measure Trace Acesulfame-K and Total Dissolved Phosphorus Concentrations in Headwater Streams.....	77
3.1 Introduction.....	77
3.1.1 Research Objectives.....	79
3.2 Methods.....	79
3.2.1 POCIS Specifications.....	79
3.2.2 P-Trap Specifications.....	80
3.2.3 Field Site Characterization and Study Design .....	81
3.2.4 Field Sampling Methods .....	83
3.2.5 Laboratory Methods.....	84
3.2.6 Solutes and Solvents .....	84
3.2.7 POCIS Extraction and Sample Preparation.....	85
3.2.8 ACE-K Analysis .....	86
3.2.9 P-Trap Extraction and Analysis .....	86
3.3 Results.....	87
3.3.1 QA/QC Results .....	87
3.3.2 Seasonal Study (POCIS) Results .....	90
3.3.3 Two-week Study (POCIS, P-Trap) Results .....	92
3.4 Discussion.....	93
3.4.1 Confidence in TWA POCIS Concentrations.....	93
3.4.2 Confidence in P-Trap TWA Concentrations.....	96
3.5 Conclusions.....	97

Chapter 4 Conclusions.....	106
4.1 Summary of Findings .....	106
4.1 Future Research and Recommendations.....	107
References .....	110
Appendix A: QA/QC Results for Chapter 2.....	128
Appendix B: Additional Figures/Tables for Chapter 2 .....	132
Appendix C: Equations for Calculations in Chapter 2 .....	149
Appendix D: Additional Figures/Tables for Chapter 3 .....	150

## List of Figures

- Figure 1-1 - Schematic showing a typical on-site septic system. Household waste is deposited in a septic tank located in the unsaturated zone. The wastewater separates into solid waste (sinks) and liquid waste. The wastewater is eventually released in an adjoining drain field. The wastewater includes contaminants, such as organic compounds and microorganisms (e.g., *E. coli*), which percolate down (red arrow), and may eventually reach the groundwater (blue arrow). The groundwater eventually reaches surface waters (e.g. streams). ..... 12
- Figure 2-1 – Map of the study sites (inlet maps) within the Grand River Watershed as Site A. (top, orange), Site B (middle, red), and Site C (bottom, black). Catchment areas were delineated and streams, sample sites (stars), and buildings (red squares) were overlaid on an overburden map\*. The main map (right) of the Grand River Watershed includes the main channel, the Grand River, which discharges into Lake Erie, and WWTPs within the watershed were overlaid (triangles) to show the placement relative to the inlet maps..... 62
- Figure 2-2 - Spatial-temporal multiple line plots of annual fluctuations in rain (mm) and flow ( $\text{m}^3 \text{s}^{-1}$ ) between April 1, 2017 and March 31, 2018, followed by multiple scatter plots of annual data for Site A (SA) upstream (US), SA downstream (DS), SB-US, SB-DS, SC-US, and SC-DS, for: temp., pH, DO, SPC, turb., alk., DOC, TS, and Cl. The high rainfall event (HRE) and high flow event (HFE) are highlighted on all the plots..... 63
- Figure 2-3 - Spatial-temporal multiple line plot of annual fluctuations in rain (mm) and flow ( $\text{m}^3 \text{s}^{-1}$ ) between April 1, 2017 and March 31, 2018, followed by multiple scatter plots of annual data for Site A (SA) upstream (US), SA downstream (DS), SB US, SB DS, SC US, and SC DS, for:  $\text{SO}_4$ , Ca, K, Mg, Na, Ba, Fe, Mn, and Zn. The high rainfall event (HRE) and high flow event (HFE) are highlighted on all plots. The Mn plot is displayed as a log scale (exponents are shown). ..... 64
- Figure 2-4 - Spatial-temporal multiple line plot of annual fluctuations in rain (mm) and flow ( $\text{m}^3 \text{s}^{-1}$ ) between April 1, 2017 and March 31, 2018, followed by multiple scatter

plots of annual data Site A (SA) upstream (US), SA downstream (DS), SB US, SB DS, SC US, and SC DS for: TP, TDP, SRP, TN, NO<sub>3</sub>-N, NO<sub>2</sub>-N, NH<sub>3+4</sub>-N, *E. coli*, and BacGen. The high rainfall event (HRE) and high flow event (HFE) are highlighted on all the plots. Note all parameter scales are displayed as log (exponents are shown). Dashed line represents the MDLs for *E. coli* and BacGen.

..... 65

Figure 2-5 - Spatial-temporal multiple line plot of annual fluctuations in rain (mm) and flow (m<sup>3</sup> s<sup>-1</sup>) between April 1, 2017 and March 31, 2018, followed by multiple scatter plots of annual data for Site A (SA) upstream (US), SA downstream (DS), SB US, SB DS, SC US, and SC DS for: BacBov, BacHum, ACE-K, CAF, CBZ, GEM, IBU, NAP, and SMX. The high rainfall event (HRE) and high flow event (HFE) are highlighted on all the plots. Scales are log (exponents are shown) except for CAF and CBZ plots. Dashed lines represent the calculated MDLs for all target FIB and tracers. .... 66

Figure 2-6 - Bar graphs showing the frequency of detection (% samples > MDL) of the target compounds 1. *E. coli* (> 4 CFU 100 mL<sup>-1</sup>), 2. BacGen (> 10 C 100 mL<sup>-1</sup>), 3. BacBov (> 10 C 100 mL<sup>-1</sup>), 4. BacHum (> 10 C 100 mL<sup>-1</sup>), 5. ACE-K (> 140 ng L<sup>-1</sup>), 6. CAF (> 0.162 ng L<sup>-1</sup>), 7. CBZ (> 0.438 ng L<sup>-1</sup>), 8. GEM (> 0.032 ng L<sup>-1</sup>), 9. IBU (> 0.228 ng L<sup>-1</sup>), 10. NAP (> 0.254 ng L<sup>-1</sup>), and 11. SMX (> 0.394 ng L<sup>-1</sup>) over the course of the sampling period between April 21, 2017 and March 31, 2018 at Site A (SA), Site B (SB), and Site C (SC) at the upstream (US), downstream (DS). The final bar graph displays the combined (SA+SB+SC) % of sample frequency > MDL for all 11 target compounds. .... 67

Figure 2-7 - Box and whisker plots displaying a statistical analysis of the annual concentrations of the nutrients TP, TDP, SRP, TN, NO<sub>3</sub>-N, NO<sub>2</sub>-N, and NH<sub>3+4</sub>-N at Sites A, B, and C upstream and downstream sites. The points represent outliers in the dataset and the dotted and solid lines represent the mean and median respectively. The P-values for the Mann Whitney Rank Sum Order tests are displayed on each graph, and the results obtained from a student's t-test are

marked with an asterisk (\*). N values vary and may be found in Appendix B. Bolded P-values are statistically significant ( $P < 0.05$ ). Note that the y-axes are in log scale (exponents shown). ..... 68

Figure 2-8 - Box and whisker plots displaying a statistical analysis of annual concentrations of the FIB *E. coli*, BacGen, BacBov, and BacHum at Sites A, B, and C upstream and downstream sites. The points represent outliers in the dataset and the dotted and solid lines represent the mean and median respectively. The MDLs are shown using dashed lines. The P-values for the Mann Whitney Rank Sum Order tests are displayed on each graph, and the results obtained from a student's t-test are marked with an asterisk (\*). N values vary and may be found in Appendix B. Bolded P-values are statistically significant ( $P < 0.05$ ). Note that the y-axes are in log scale (as exponents). ..... 69

Figure 2-9 - Box and whisker plots displaying a statistical analysis of the annual concentrations of the artificial sweetener ACE-K, and pharmaceuticals CAF, CBZ, GEM, IBU, NAP, and SMX at Sites A, B, and C upstream and downstream sites. The points represent outliers in the dataset and the dotted and solid lines represent the mean and median respectively. The MDLs are shown using dashed lines. The P-values for the Mann Whitney Rank Sum Order tests are displayed on each graph, and the results obtained from a student's t-test are marked with an asterisk (\*). N values vary and may be found in Appendix B. Bolded P-values are statistically significant ( $P < 0.05$ ). Note that the y-axes are in log scale (as exponents). ..... 70

Figure 2-10 - Bar graphs of the measurements or concentrations of specific conductance (SPC), total solids (TS), chloride (Cl), sodium (Na), soluble reactive phosphorus (SRP), ammonia and ammonium-nitrogen ( $\text{NH}_{3+4}\text{-N}$ ), BacHum, and ACE-K at the upstream, storm drain, and downstream sites at Site B over six sampling occasions between June 20, 2017 and February 21, 2018. Note that some data are displayed using a log scale (exponents shown). ..... 71

Figure 3-1 - Multi-line plots of the ambient air temperature (red) and water temperature (blue) through the sampling period. The first column displays the Spring 2017 seasonal POCIS deployment (May 17-31, 2017). The second column displays the Summer 2017 seasonal POCIS deployment (July 12-26, 2017). The third column displays the Fall 2017 seasonal POCIS deployment (November 15-29, 2017). The fourth column displays the 2-week study results for SA only (May 8-22, 2018). The rows represent sample sites, from the top: SA-US, SA-DS, SB-US, SB-DS, SC-US, and SC-DS. The graphs without a blue line were not subject to POCIS deployment..... 98

Figure 3-2 - Scatter plot showing the measured vs. expected concentrations of the QC samples (Blank, 0.5, 1, and 2  $\mu\text{g L}^{-1}$ ) analyzed with the three POCIS batches. A regression line was fit through the data, with a correlation coefficient value of 0.9936..... 99

Figure 3-3 – Bar graphs of the average grab sample and POCIS ACE-K concentrations for the Spring, Summer, and Fall 2017 seasonal study excursions. The grab sample and POCIS MDLs are displayed with dashed and solid lines respectively. POCIS were not deployed at SA-US during the Spring and Summer, nor at SA-DS during the Summer (denoted with “NA”)..... 100

Figure 3-4 – Scatter-plot of the calculated seasonal POCIS Rs values for ACE-K during the spring, summer, and fall 2017 for SA-US, SA-DS, SB-US, SB-DS, SC-US, and SC-DS. The mean calculated Rs values are also displayed. The values were calculated using the mass (ng) of ACE-K measured in each POCIS sample and the mean grab sample ACE-K concentrations for each deployment/retrieval... 101

Figure 3-5 – Stair plots of the ACE-K grab sample concentrations (blue solid line) collected on Day 0, 2, 4, 6, 8, 10, 12, and 14 during the 2-week study at SA-US (A) and SA-DS (B). The solid lines represent the grab sample concentrations (dark blue) and the POCIS TWA concentrations (light blue), and dashed lines show the respective MDLs and average grab sample concentrations. .... 102

Figure 3-6 – Stair plots of the TWA TDP and grab sample TDP concentrations for SA-US and SB-DS. The TWA concentrations calculated for the first 8 days (A and B), and for 14 days (C and D) were plotted as red solid lines. The solid blue line and dashed blue line represent the grab sample concentrations and the mean respectively. .... 103

Figure B-1 - Spatial-temporal multiple line plot displaying annual fluctuations in rain (mm) and flow ( $m^3 s^{-1}$ ) between April 1, 2017 and March 31, 2018, followed by multiple scatter plots displaying annual data for Site A (SA) upstream (US), SA downstream (DS), Site B (SB) US, SB DS, SC US, and SC DS for: Al, Be, Cd, Co, Cu, Li, Mo, Sr, Ti, U, and V. Note all parameter scales are displayed as log (exponents are shown). Dashed lines represent the MDLs. The high rainfall event (HRE) and high flow event (HFE) are noted on the multiple line plot.... 132

Figure B-2 - Box and whisker plots of the annual proportions of TDP:TP, SRP:TDP,  $NO_3-N$ :TN,  $NO_2-N$ :TN, and  $NH_{3+4}-N$ :TN for SA, SB, and SC US and DS concentrations. The solid and dashed lines represent the median and mean respectively. The dotted lines represent outliers in the dataset..... 133

Figure B-3 - Scatter plot displaying the proportion of BacGen that is BacBov (%) and BacHum (%) at the upstream and downstream of Site A (SA), Site B (SB), and Site C (SC) between April 26, 2017 and March 28, 2018. .... 134

Figure B-4 - Box and whisker plots displaying the annual measurements and concentrations of temperature, pH, DO, SPC, turbidity, alkalinity, DOC, TS, Cl,  $SO_4$ , Ca, K, Mg, and Na at Sites A, B, and C upstream and downstream sites. The points represent outliers in the dataset and the dotted and solid lines represent the mean and median respectively. The MDLs were not displayed on the graphs as all data points were measured above the MDL. The P-values for the Mann Whitney Rank Sum Order tests are displayed on each graph, and the results obtained from a student's t-test are marked with an asterisk (\*). Bolded P-values are statistically significant ( $P < 0.05$ )..... 135



Figure B-5 - Box and whisker plots displaying the annual concentrations of Al, Ba, Be, Cd, Co, Cu, Fe, Li, Mn, Mo, Sr, Ti, U, V, and Zn at Sites A, B, and C upstream and downstream sites. The points represent outliers in the dataset and the dotted and solid lines represent the mean and median respectively. The MDLs were not displayed on the graphs as all data points were measured above the MDL. The P-values for the Mann Whitney Rank Sum Order tests are displayed on each graph, and the results obtained from a student's t-test are marked with an asterisk (\*). Bolded P-values are statistically significant ( $P < 0.05$ ). ..... 136

Figure B-6 - Bar graphs showing the measurements or concentrations of alkalinity (Alk.), pH, turbidity (Turb.), dissolved organic carbon (DOC), sulfate (SO<sub>4</sub>), total phosphorus (TP), total dissolved phosphorus (TDP), total nitrogen (TN), nitrate-nitrogen (NO<sub>3</sub>-N), nitrite-nitrogen (NO<sub>2</sub>-N), *E. coli*, BacGen, and BacBov at the upstream, storm drain, and downstream sites at Site B over six sampling occasions between June 20, 2017 and February 21, 2018. Note that some data are displayed using a log scale. Samples were not taken for DOC on December 6, 2017, January 30, 2018, or February 21, 2018. .... 137

Figure B-7 - Bar graphs showing the concentrations of trace metals: aluminum (Al), barium (Ba), beryllium (Be), calcium (Ca), cadmium (Cd), cobalt (Co), copper (Cu), iron (Fe), potassium (K), lithium (Li), magnesium (Mg), manganese (Mn), molybdenum (Mo), strontium (Sr), titanium (Ti), uranium (U), vanadium (V), and zinc (Zn) at the upstream, storm drain, and downstream sites at Site B over six sampling occasions between June 20, 2017 and February 21, 2018. Note that some data are displayed using a log scale. Measurements of silver, bismuth, chromium, nickel, lead, tin, and zirconium are not displayed as the concentrations were consistently below the MDLs. The MDLs on the graphs are displayed using a dashed line. .... 138

Figure B-8 – Schematic of the higher-permeability pathways that may exist in hamlets and may be interacting with drain fields, providing preferential pathways for contaminants to reach surface waters prior to attenuation or removal. .... 139

Figure D-1 – Schematic of a POCIS with two stainless steel washers securing two filter membranes and a receiving phase (sorbent). ..... 150

Figure D-2 – A. mixture of sand and ferric nitrate; B. after the addition of NaOH; C. slurry after supernatant water was removed; D. dried Fe-coated sand; E; P-Trap outer plate overlain with filter membrane paper and secure to the main plate; F. addition of sand and ultrapure water into the P-Trap; G. addition of the second filter membrane paper and the outer plate. Photos taken by Maria Digaletos (2018). ..... 151

Figure D-3 -Placement of the passive samplers within a wire cage in a stream (SA-DS). The membranes of the POCIS and P-Traps are placed parallel to the flow of the stream to allow interaction with both sides of the samplers. Photos taken by Maria Digaletos (2017). ..... 152

Figure D-4 – Three POCIS removed from the stream (SA-DS) after a 14-day deployment. The POCIS may have been exposed to the air during a portion of the deployment period, as shown by the inconsistent lines and fouling on the membranes. Photos taken by Maria Digaletos (2017). ..... 153

## List of Tables

- Table 2-1 - Land-use information (drainage, lakes, and wetland area; % agricultural or domestic; dwelling size), hydrometric information (annual temperature/precipitation), and hydrogeological characterization (overburden thickness, dominant material, and permeability) of Site A, Site B, and Site C. The number of buildings (including homes) was manually determined using Google Earth satellite imagery..... 72
- Table 2-2 - Spearman Rank Order statistical test results for correlation coefficients ( $\rho$ ) obtained for Site A (SA), Site B (SB), and Site C (SC) upstream (US) and downstream (DS). Only significant ( $P < 0.05$ )  $\rho$  values are tabulated (bolded) between the nutrients TP, TDP, SRP, TN,  $\text{NO}_3\text{-N}$ ,  $\text{NO}_2\text{-N}$ , and  $\text{NH}_{3+4}\text{-N}$  and the FIB/tracers *E. coli*, BacGen, BacBov, BacHum, ACE-K, CAF, CBZ, GEM, IBU, NAP, and SMX. NS: not significant. The results were interpreted as: 0.2–0.4 = weak, 0.4–0.6 = moderate, and 0.6–0.8 = strong. .... 73
- Table 2-3 - Spearman Rank Order statistical test results for correlation coefficients ( $\rho$ ) obtained for Site A (SA), Site B (SB), and Site C (SC) upstream (US) and downstream (DS). Only significant ( $P < 0.05$ )  $\rho$  values are tabulated (bolded) between FIB/tracers *E. coli*, BacGen, BacBov, BacHum, ACE-K, CAF, CBZ, GEM, IBU, NAP, and SMX. NS: not significant. The results were interpreted as: 0.2–0.4 = weak, 0.4–0.6 = moderate, and 0.6–0.8 = strong. .... 75
- Table 3-1 – Average measurements/concentrations for the parameters measured in the field or laboratory for target water quality indicators, including includes the average concentrations for samples retrieved in Spring 2017, Summer 2017, and Fall 2017, for SA, SB, and SC US and DS samples where applicable. Samples for SA-US during Spring 2017 and Summer 2017, along with SA-DS in Summer 2017 were not included because POCIS were not deployed at these sites during the sampling excursions. The ACE-K mean concentrations are italicized..... 104
- Table 3-2 – Table showing the daily grab sample averages for Days 1, 2, 4, 6, 8, 10, 12, and 14 for SA-US and SA-DS during the 2-week study for a variety of water quality

parameter measurements or concentrations. The weekly average for each parameter is also calculated. The ACE-K and TDP concentrations are italicized.

..... 105

Table B-1 - Statistical summary table for general water quality, FIB, and organic tracer concentrations measured at Site A Upstream and Downstream sample sites. Min. = minimum; Max. = maximum; Med. = median; Std. Dev. = standard deviation; n = count. Results measured below detection limits for the target parameter are reported as < MDL. .... 140

Table B-2 - Statistical summary table for general water quality, FIB, and organic tracer concentrations measured at Site B Upstream and Downstream sample sites. Min. = minimum; Max. = maximum; Med. = median; Std. Dev. = standard deviation; n = count. measured below detection limits for the target parameter are reported as < MDL. .... 142

Table B-3 - Statistical summary table for general water quality, FIB, and organic tracer concentrations measured at Site C Upstream and Downstream sample sites. Min. = minimum; Max. = maximum; Med. = median; Std. Dev. = standard deviation; n = count. measured below detection limits for the target parameter are reported as < MDL. .... 144

Table B-4 - Table summarizing the Spearman Rank Order statistical test results for correlation coefficients ( $\rho$ ) obtained for Site A (SA) upstream (US) and downstream (DS) between the nutrient concentrations and the tracer concentrations. The tabulated values represent the output  $\rho$ -value with the P-value underneath for the correlation values between the nutrients TP, TDP, SRP, TN, NO<sub>3</sub>-N, NO<sub>2</sub>-N, and NH<sub>3+4</sub>-N and the FIB/tracers *E. coli*, BacGen, BacBov, BacHum. ACE-K, CAF, CBZ, GEM, IBU, NAP, and SMX. Significant values (P < 0.05) are bolded. --: no output (< MDL). The results were interpreted as: 0.2–0.4 = weak, 0.4–0.6 = moderate, and 0.6–0.8 = strong. .... 146

Table B-5 - Table summarizing the Spearman Rank Order statistical test results for correlation coefficients ( $\rho$ ) obtained for Site B (SB) upstream (US) and downstream (DS) between the nutrient concentrations and the tracer concentrations. The tabulated values represent the output  $\rho$ -value with the P-value underneath for the correlation values between the nutrients TP, TDP, SRP, TN, NO<sub>3</sub>-N, NO<sub>2</sub>-N, and NH<sub>3+4</sub>-N and the FIB/tracers *E. coli*, BacGen, BacBov, BacHum. ACE-K, CAF, CBZ, GEM, IBU, NAP, and SMX. Significant values ( $P < 0.05$ ) are bolded. --: no output ( $< MDL$ ). The results were interpreted as: 0.2–0.4 = weak, 0.4–0.6 = moderate, and 0.6–0.8 = strong ..... 147

Table B-6 - Spearman Rank Order statistical test results for correlation coefficients ( $\rho$ ) obtained for Site C (SC) upstream (US) and downstream (DS) between nutrient concentrations and tracer concentrations. The tabulated values represent the output  $\rho$ -value with the P-value underneath for the correlation values between the nutrients TP, TDP, SRP, TN, NO<sub>3</sub>-N, NO<sub>2</sub>-N, and NH<sub>3+4</sub>-N and the FIB/tracers *E. coli*, BacGen, BacBov, BacHum. ACE-K, CAF, CBZ, GEM, IBU, NAP, and SMX. Significant values ( $P < 0.05$ ) are bolded. --: no output ( $< MDL$ ). The results were interpreted as: 0.2–0.4 = weak, 0.4–0.6 = moderate, and 0.6–0.8 = strong. 148

## List of Abbreviations

ACE-K	acesulfame-K
Al	aluminum
alk.	alkalinity
Ag	silver
Ba	barium
BacBov	bovine <i>Bacteroides</i>
BacHum	human <i>Bacteroides</i>
BacGen	general <i>Bacteroides</i>
Be	beryllium
Bi	bismuth
C <sub>w</sub>	time weighted average concentration
Ca	calcium
CAF	caffeine
CBZ	carbamazepine
Cd	cadmium
CCV	continuing calibration verification
Cl	chloride
Co	cobalt
Cr	chromium
Cu	copper
DO	dissolved oxygen
DOC	dissolved organic carbon
DS	downstream
<i>E. coli</i>	<i>Escherichia coli</i>
Fe	iron
GEM	gemfibrozil
HFE	high flow event
HRE	heavy rainfall event

IBU	ibuprofen
IC	ion chromatography
IC-MS/MS	ion chromatography tandem mass spectrometry
ICP-OES	inductively coupled plasma optical emission spectroscopy
IS	internal standard
K	potassium
LaSB	Laboratory Services Branch
LC-MS/MS	liquid chromatography tandem mass spectrometry
Li	lithium
M <sub>s</sub>	mass of target analyte
MDL	method detection limit
Mg	magnesium
Mn	manganese
Mo	molybdenum
N	nitrogen
Na	sodium
NAP	naproxen
NH <sub>3+4</sub> -N	ammonia and ammonium nitrogen
Ni	nickel
NO <sub>2</sub> -N	nitrite nitrogen
NO <sub>2+3</sub> -N	nitrite and nitrate nitrogen
NO <sub>3</sub> -N	nitrate nitrogen
P	phosphorus
P-Trap	phosphorus trap
POCIS	polar organic chemical integrative sampler
Pb	lead
PRC	performance reference compound
QA	quality assurance
QC	quality control

R <sub>s</sub>	uptake rate constant
RSD	relative standard deviation
SA	Site A
SB	Site B
SC	Site C
SD	storm drain
SMX	sulfamethoxazole
Sn	tin
SPC	specific conductance
SO <sub>4</sub>	sulfate
Sr	strontium
SRP	soluble reactive phosphorus
SS	seasonal study
t	time
TDP	total dissolved phosphorus
temp.	temperature
Ti	titanium
TN	total nitrogen
turb.	turbidity
TS	total solids
TWA	time weighted average
U	uranium
US	upstream
UW	University of Waterloo
V	vanadium
WWTP	wastewater treatment plant
Zn	zinc
Zr	zirconium



# Chapter 1

## Introduction

### 1.1 Introduction

Septic systems are a cost-effective way to manage domestic wastewater in rural areas or towns that are without centralized wastewater treatment facilities. Septic systems are designed to treat domestic waste in-situ through a sequence of anaerobic and aerobic processes followed by reintroducing the wastewater back into the shallow subsurface environment and eventually into the groundwater system. Household wastewater encompasses a plethora of household water sources including sewage, kitchen and food waste, along with laundry and dishwasher wastewater. Therefore, septic tanks are continuously loaded with wastewater containing nutrients, personal care products, microorganisms, trace organic compounds, detergents, food residue, etc. that may not be fully removed during the anaerobic and aerobic processes and infiltration processes. A review by Schaidler et al. (2017) noted that removals reported for domestic waste by septic tank systems, including artificial sweeteners and pharmaceuticals, are similar to removal percentages by WWTPs.

Typical domestic septic systems are designed to treat waste in two treatment steps. The primary treatment step is the anaerobic digestion of compounds in the septic tank, and settling of floatable solids which could clog the infiltration bed. Effluent then leaves the tank and infiltrates the leach field and released into the soil, where it percolates down into the shallow groundwater system (*see* Figure 1-1). Extensive groundwater contamination occurs when there is inadequate treatment caused by clogging or an insufficient residence time in

the unsaturated zone. When compounds reach the water table, wastewater contaminants are transported by the physical processes of advection, dispersion, and diffusion, and by geochemical processes promoted by the anoxic and aerobic environments created by the wastewater (Wilhelm et al., 1994). If these loads are discharged into surface waters it can be difficult to track the proportions of contaminants and nutrients sourced from septic systems versus other sources (e.g. WWTPs, agricultural runoff).

## 1.2 Dissolved Nutrients in the Environment

Eutrophication of major surface water bodies by excessive nutrient loading has become a global issue. Natural and anthropogenic loading of nutrients (i.e. nitrogen and phosphorus species) by non-point and point sources can lead to the development of eutrophic conditions, stimulate plant growth, and promote algal blooms. Harmful algal blooms can greatly reduce the quality of drinking water resources and compromise aquatic health (CCME, 2004), ultimately threatening ecosystem stability. Some recent global examples of impacted surface waters by harmful algal blooms include the coastal regions of Qingdao (China) and the Gulf of Mexico (USA), and freshwater systems such as the Everglades (USA) and Lake Erie (Canada) in the Great Lakes Basin.

Beginning in the 1960s, the water quality of the Great Lakes was under public scrutiny as reports emerged concerning the extreme eutrophication of these water bodies by nutrient loading. In response, Canadian and United States governments banded together to mitigate nutrient inputs by implementing the Great Lakes Water Quality Agreement in 1972. The agreement was amended in 2012 to enhance water quality programs related to point and non-point source inputs affecting the biological, physical, and chemical integrity of the Great

Lakes system (GLWQA, 2012). One of the main targets is to develop action plans and strategies by 2018 to diminish phosphorus (P) concentrations (Annex 4 of GLWQA). The current objective is to reduce P concentrations to  $10 \mu\text{g L}^{-1}$  in the central and eastern basins of Lake Erie and a total load target of 11,000 metric tons of total P per year (Annex 4 of GLWQA).

Natural sources of P and N are found in the environment and are vital for plant and animal growth. These nutrients are found in soils, plants, atmospheric deposition, surface water and groundwater, minerals, as well as in human and animal waste products. Phosphorus commonly occurs in nature in the form of orthophosphate (o- $\text{PO}_4$ ). More specifically, o- $\text{PO}_4$  occurs as  $\text{H}_3\text{PO}_4$ ,  $\text{H}_2\text{PO}_4^-$ ,  $\text{HPO}_4^{2-}$ ,  $\text{PO}_4^{3-}$ , but since speciation is pH dependent and natural ground and surface waters are within the neutral pH range,  $\text{H}_2\text{PO}_4^-$  and  $\text{HPO}_4^{2-}$  are the predominant species (Stumm and Morgan, 1996). Polyphosphates ( $\text{P}_2\text{O}_7^{4-}$  and  $\text{P}_3\text{O}_{10}^{5-}$ ) are found in household products but are unstable in natural environments and convert to o- $\text{PO}_4$  (Lusk et al. 2017). Total Phosphorus (TP) refers to both dissolved phosphorus and non-soluble P (particulate P) fractions. The filterable portion of orthophosphate, denoted soluble reactive phosphorus (SRP), is readily taken up by plants and riparian vegetation, therefore waters near or containing abundant vegetation normally have a higher particulate P fraction. Furthermore, it is well-established that P tends to adsorb onto soil particles; specifically, P adsorbs onto clay minerals, iron (e.g. goethite) and aluminum (e.g. gibbsite) oxide minerals, as well as calcium carbonates such as limestone (Lusk et al., 2017). Overall, groundwater transport of P has been extensively studied and found to be generally negligible in zones where adsorption and riparian uptake processes dominate (*see*

Lusk et al., 2017). However, a study on o-PO<sub>4</sub> transport in septic plumes by Robertson et al. (1998) observed that the extent and rate of o-PO<sub>4</sub> transport is controlled by the aquifer material. For example, o-PO<sub>4</sub> transport in calcareous sands (~ 1 m year<sup>-1</sup>) was observed more than 10 m from the source compared to o-PO<sub>4</sub> transport in non-calcareous sediments (< 0.3 m year<sup>-1</sup>) with smaller grain sizes (silt, clay) observed only within 3 m of the source. Similarly, Domagalski and Johnson (2011) found that in subsurface environments where o-PO<sub>4</sub> is not entirely taken up by plants or the soil biogeochemistry is not suitable for sorption processes, o-PO<sub>4</sub> may be found in nearby surface waters at elevated concentrations. Overall, the P cycle is simpler than the N cycle. Nitrogen species are found in the environment in many naturally-occurring forms: nitrate (NO<sub>3</sub><sup>-</sup>), nitrite (NO<sub>2</sub><sup>-</sup>), ammonia (NH<sub>3</sub>), ammonium (NH<sub>4</sub><sup>+</sup>), nitrous oxide (N<sub>2</sub>O), organic N, and as nitrogen gas (N<sub>2</sub>).

Nitrate is also an essential nutrient for plant growth, but unlike P, does not sorb onto aquifer materials. Although NO<sub>3</sub><sup>-</sup> is stable in aerobic conditions, it is commonly denitrified to N<sub>2</sub> under anaerobic conditions. Denitrification is microbially mediated and involves an electron donor (organic carbon), with intermediate products found in the environment such as NO<sub>2</sub><sup>-</sup> and N<sub>2</sub>O. Ammonia is found in reducing conditions and will transform into NO<sub>2</sub><sup>-</sup> and NO<sub>3</sub> by the process of nitrification, which is caused by oxidation of organic matter by bacteria. In the presence of oxidizing groundwater, these anions transport readily through the subsurface and eventually discharges into surface waters. Although the P and N cycles naturally occur, the extra loads caused by human activities are believed to greatly disturb nutrient balances in surface water systems, and water quality may improve with decreases in anthropogenic loads (*see* Conley et al., 2009).

The main anthropogenic sources of P and N in surface water are wastewater treatment plant (WWTP) effluent (Carey and Migliaccio, 2009) and agricultural runoff of manure and fertilizers (IJC, 2018). Another less studied source of anthropogenic loading is by septic systems in rural areas. Recent research has concluded that quantifying contributions of domestic wastewater, especially in areas where there are large clusters of septic tank systems near streams and rivers with low dilution capacity, is deserving of more attention (Jarvie et al., 2010; Palmer-Felgate et al., 2010; Withers et al., 2011).

### **1.3 Wastewater Released from Septic Systems**

#### **1.3.1 Dissolved Nutrients**

Owing to processes such as adsorption, denitrification, and precipitation, nutrients are expected to become attenuated in receiving aquifers prior to reaching surface waters nearby where eutrophic conditions may develop (Lusk et al., 2017). Robertson and Harman (1999) found that if  $\text{o-PO}_4$  leaving a septic tank system is not retained in the unsaturated zone and reaches shallow groundwater, it may persist and eventually discharge into nearby surface waters. Wilhelm et al. (1994) found that  $\text{NO}_3^-$  did not undergo complete denitrification before reaching groundwater and suggested that nitrate loads to groundwater may be an issue in areas with dense septic tank development. Ptacek (1998) observed  $(\text{NO}_3+\text{NO}_2)\text{-N}$  concentrations as high as  $80 \text{ mg L}^{-1}$ , and concentrations of  $\text{NH}_4\text{-N}$  greater than  $15 \text{ mg L}^{-1}$ , measured 20 m downgradient from the septic source. The most elevated  $\text{o-PO}_4\text{-P}$  reported in the study was  $1.5 \text{ mg L}^{-1}$  downgradient from the septic system. In receiving surface waters, Withers et al. (2011) measured SRP and  $\text{NH}_4\text{-N}$  concentrations downstream of a septic

system as high as 0.21 and 0.55 mg L<sup>-1</sup> respectively. In areas with very dense septic system development or poor septic system design, the proportions of o-PO<sub>4</sub> and NO<sub>3</sub>-N released into the environment are currently unknown and may be an important source of loading into surface water bodies.

### **1.3.2 Release of Other Contaminants in the Environment**

Water affected by septic plumes may be characterized by high specific conductance, suspended solids, turbidity, and elevated concentrations of chloride. Domestic wastewater released from drain fields is comprised of many other potential pollutants including fecal waste derivatives, cleaning products, and pharmaceuticals (Wilhelm et al., 1994; Richards et al., 2015, 2017a). Human waste includes *E. coli* and other pathogens or viruses. Fecal coliforms and *E. coli* have been noted at concentrations between 10<sup>3</sup> and 10<sup>7</sup> CFU 100 mL<sup>-1</sup> in septic effluent (Richards et al., 2016b). Other microcontaminants include certain trace metals derived from household cleaning products and detergents (Richards et al., 2015). Certain organic compounds such as pharmaceuticals (e.g. caffeine, ibuprofen) and artificial sweeteners (e.g. acesulfame-K, sucralose) are part of a class of emerging contaminants found within the environment that are associated with domestic effluent (Buerge et al., 2003; Schaider et al., 2017; Snider et al., 2017). The ubiquitous presence of these organic compounds have been found in impacted groundwaters (Conn et al., 2006), receiving waters (Liu et al., 2014), and coastal waters (Jiang et al., 2014).

## 1.4 Using Organic Tracers to Track Wastewater

Tracing nutrient inputs to their original sources may be problematic due to the numerous sources in the environment. The use of human-specific compounds found in domestic wastewater can be used to characterize sources of effluent. There have been multiple studies on the fate and occurrence of emerging contaminants in septic tank plumes for compounds such as personal care products, pharmaceuticals, and artificial sweeteners (Conn et al., 2006; Carrara et al., 2008; Robertson et al., 2013). These compounds are anthropogenically derived; therefore, they can be used to track septic system contamination.

Artificial sweeteners are generally considered human-specific as they are not found naturally in the environment and are predominantly consumed by humans, although some have been reported in animal feed (Buerge et al., 2011). Artificial sweeteners are found in food and drink products such as candies and soda pop marketed as healthier alternatives, as a substitute for sugar in caffeinated beverages, and consumed by diabetics. Artificial sweeteners pass through the human digestive system without being transformed and are excreted relatively unchanged with recoveries of acesulfame-K (ACE-K) reported at 100-101% (Buerge et al., 2009). The presence of prescribed and un-prescribed pharmaceutical compounds has been reported in shallow groundwater systems impacted by septic tank wastewater (Godfrey et al., 2007; Carrara et al., 2008). More recently, researchers have recommended and used pharmaceutical compounds as domestic wastewater indicators, including caffeine (CAF), carbamazepine (CBZ), gemfibrozil (GEM), ibuprofen (IBU), naproxen (NAP), and sulfamethoxazole (SMX) (Hoque et al., 2014; Liu et al., 2014; Richards et al., 2017a).

A more traditional method of screening for contamination by septic systems is with fecal indicator bacteria (FIB). FIB are routinely monitored in areas where groundwater is used to supply drinking water as they provide a good indication of fecal contamination, and are associated with waterborne illnesses (WHO, 2001). Fecal matter is excreted by humans and animals and contains many microbes, and potentially pathogens, that may pose a health risk if not adequately treated. Therefore, FIB (e.g. *Escherichia coli*) are widely accepted and used as indicators of recent fecal contamination (e.g. WHO, 2001; Lee et al., 2014; Richards et al., 2017a). A member of the coliform group, *E. coli* is a rod-shaped bacterium found in the gut of humans and other warm-blooded animals. *E. coli* is widely accepted as an indicator in source water monitoring because it is source specific (e.g. of fecal origin) and quantifiable (WHO, 2001). However, *E. coli* cannot be used to differentiate between animal types, for example between farm animal manure versus septic effluent.

More recently, host-specific biological markers have been used to differentiate between humans and animal species (Peed et al., 2011; Tambalo et al., 2012; Lee et al., 2014). The use of *Bacteroides* is more indicative than *E. coli* as it can be separated out into different strains. For example, human and bovine sources can be differentiated to determine if the fecal source is domestic waste or agriculturally-sourced. Lee et al. (2014) measured host-specific (bovine and human) *Bacteroides* counts in the Grand River (Ontario) and found that upstream locations near farm sites had higher bovine *Bacteroides* counts and samples downstream from WWTP discharge sites had higher human *Bacteroides* counts. The use of a host-specific (*Bacteroides*) domestic waste indicator coupled with a widely-accepted



indicator (*E. coli*) has previously been used to observe potential loading to surface waters by septic systems in rural watersheds (Peed et al., 2011).

Ultimately, research suggests that the use of co-tracers is the most effective way to determine sources of contamination (Liu et al., 2014; Richards et al., 2017a). Van Stempvoort et al. (2013) calculated correlation coefficients between ACE-K and CBZ equal to 0.69, and a value of 0.91 between ACE-K and chloride. Further investigations are required to assess the usefulness of co-tracers in the environment.

### **1.5 Passive Sampling Techniques**

Passive sampling techniques are increasingly used in conjunction with grab samples for environmental monitoring (Metcalf et al., 2014; Criquet et al., 2017). Passive sampling works by the movement of chemicals (net flux) from the water (sample medium) to the passive sampling device (receiving phase) by differences in concentration between the medium and the phase (chemical potential) (Lord, 2017). The main advantage of using passive sampling is that the calculated concentrations are generally more representative of the average concentrations of the study site, as the samplers capture major and base events reported as time weighted average (TWA) concentrations that may reduce the variability (Criquet et al., 2017). Surface waters would need to be intensively sampled to obtain the same resolution of water quality data that passive samplers produce. Consequently, it is more cost effective to visit the field sites less often and obtain a more representative sample. The use of passive samplers may eliminate the issue of sediment interference during sampling and analysis, as the membranes only allow freely dissolved particles to enter and accumulate

on a sorbent (Alvarez, 2010). Finally, the detection limits for passive samplers are typically lower than those reported for grab samples (Lord, 2017). The main disadvantage of passive sampling is that the samplers are left in the environment without surveillance over an extended period (e.g. 14 days). Long deployments increase risk of vandalism, biofilm accumulation, and high-water events that may displace the installation (Alvarez, 2010).

## **1.6 Research Objectives**

The objective of this thesis is to use a suite of anthropogenic tracers, including host-specific fecal indicator bacteria, an artificial sweetener, and pharmaceuticals to identify potential impacts of septic systems on surface water quality in rural areas. A secondary objective is to compare passive sampling techniques to discrete sample concentrations of soluble reactive phosphorus and acesulfame-K. Surface water samples were collected upstream and downstream of three small rural communities that are serviced exclusively by septic systems. Few research studies have identified the occurrence of wastewater in watersheds exclusively on septic systems with no other known wastewater discharges.

## **1.7 Thesis Organization**

The following thesis is organized as four research chapters representing two separate studies related to detecting septic system impacts in surface waters in rural hamlets, followed by a concluding chapter. The first chapter titled “Introduction” presents the thesis layout, background information pertaining to the research, and the thesis research objectives. The second chapter, “Characterization of Non-point Contamination by Septic Systems in Rural Ontario Hamlets”, describes an in-depth study into the use of a combined-tracer approach to

ascertain domestic wastewater contamination downstream of three rural hamlets. The third chapter, “Using Passive Samplers POCIS and P-Traps to Measure Trace Acesulfame-K and Total Dissolved Phosphorus Concentrations in Headwater Streams”, describes a study in which passive sampling techniques are compared to discrete samples collected during seasonal sampling events and an intensive two-week field study with an emphasis on the emerging contaminant ACE-K and dissolved nutrient SRP. The fourth Chapter entitled “Conclusions” is a summary of the findings for the two studies, their implications from a water management perspective, and future directions.

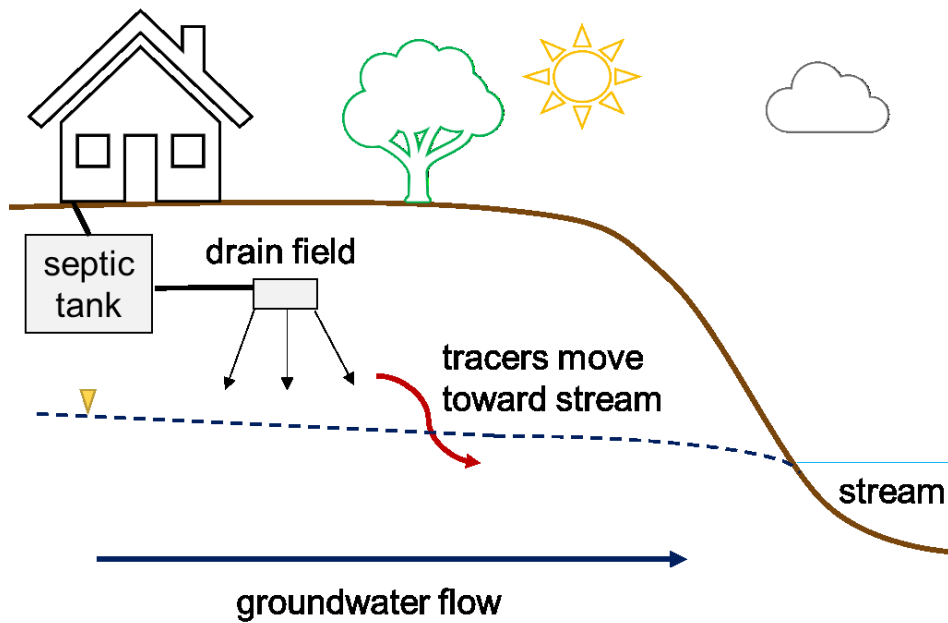


Figure 1-1 - Schematic showing a typical on-site septic system. Household waste is deposited in a septic tank located in the unsaturated zone. The wastewater separates into solid waste (sinks) and liquid waste. The wastewater is eventually released in an adjoining drain field. The wastewater includes contaminants, such as organic compounds and microorganisms (e.g., *E. coli*), which percolate down (red arrow), and may eventually reach the groundwater (blue arrow). The groundwater eventually reaches surface waters (e.g. streams).

## **Chapter 2**

### **Characterization of Non-point Source Contamination from Septic Systems in Rural Ontario Hamlets**

#### **2.1 Introduction**

Eutrophication of surface water bodies is linked to excessive loading of nutrients (P, N) from anthropogenic activities including agriculture and domestic waste products. The contribution of nutrients from treated effluent sourced from wastewater treatment plants (WWTPs) to receiving waters has been well documented (e.g. Chambers et al. 1997; Gibson & Meyer, 2007). In rural areas where WWTPs are not a feasible option for treatment, on-site domestic wastewater treatment in the form of septic systems are frequently used. In the United States, more than one in five homes use on-site treatment systems resulting in more than 15,000,000 L of sewage treated each day (USEPA, 2014). In 2009, 13% of Canadians reported using on-site septic systems to treat their domestic wastewater (Environment Canada, 2009) with 25,000 new installations per year (including replacements) in Ontario alone (Council of Canadian Academies, 2009).

Septic system nutrient contributions to water sources are often assumed to be of minor significance compared to those derived by agricultural activities. Most research pertains to septic plumes affecting groundwater quality, with less focus on the fate of nutrients and their load contributions to surface waters. Previous works have identified elevated concentrations of P and N species in groundwater in sand aquifers associated with septic plumes in Ontario (Harman et al., 1996; Ptacek, 1998; Robertson et al. 1998). Research on surface water contamination by septic systems in Ontario is limited (e.g. Spoelstra et al., 2017), although evidence of impacts on stream water quality has been

studied in the United Kingdom (Keegan et al., 2014; Richards et al., 2016) and the United States (Sowah et al., 2017). Septic systems have been identified as a potentially important diffuse source of contaminants to surface waters in catchment areas with high dwelling density and low dilution capacity related to high residence time (Jarvie et al., 2010; Withers et al., 2011). Further information on the effects of septic systems on stream water quality in rural areas in Ontario is crucial for the proper development of water management guidelines to maintain ecosystem health, as well as for assuring safe sources of water for drinking and recreational activities.

### **2.1.1 Non-point Source Contamination in Rural Hamlets**

Nutrient loading in surface waters by septic systems is difficult to characterize due to the presence of multiple rural sources including agricultural practices occurring in proximity to the homes and businesses in hamlets. The relative nutrient contributions from agricultural activities, such as fertilizer application, manure storage and spreading, and grazing animals, are difficult to quantify due to variable factors affecting the leaching of P and N into the environment such as site-specific hydrogeology, fertilizer/manure loading and timing (seasonality), climatic conditions, crop type, and grazing activities (e.g. Arheimer and Lide, 2000; Schoumans et al. 2014). Likewise, natural attenuation of septic-derived nutrients is also highly dependent on the site-specific characteristics (soil type, water-table depth, oxidation/reduction zones), and nutrient loading is based on individual household contributions, location, number of systems, and on proper maintenance of the systems. Nutrient contributions by septic systems are difficult to quantify relative to other

contributions in areas with multiple nonpoint sources, as nutrients are not easily source tracked.

### **2.1.2 Tracing Nutrients in Rural Catchment Areas**

Previous studies have used stable isotopes to determine the main nitrate sources, although these only pertain to groundwater quality and areas where information on agricultural practices and location of septic systems was well understood (Aravena et al., 1993; Minet et al., 2017). Additionally, this method is limited to N concentrations and not P, the latter of which is recognized as the limiting nutrient for triggering eutrophic conditions (Schindler, 1977). The traditional use of chloride (Cl) as a wastewater tracer may not be effective in rural hamlets due to road salt application. Other constituents found in domestic waste include pathogens, household cleaning products, and organic chemicals. Fecal indicator bacteria (FIB) *Escherichia coli* (*E. coli*) has been used as a domestic waste tracer to identify municipal waste and septic effluent in receiving waters (Glassmeyer et al., 2005; Richards et al., 2017a), but is limited as a tracer in rural areas with multiple sources of fecal contamination, including farming activities and wildlife. The use of host-specific FIB, such as *Bacteroides*, has been recognized as a more valuable tool for differentiating between fecal contamination sources (Odagiri et al., 2015; Somnark et al., 2018). In the Grand River (Ontario), bovine and human markers were used to measure contaminants in relation to both upstream mixed agricultural and septic system inputs, and WWTP sources (Lee et al., 2014). The use of these host-specific markers may help further differentiate between manure and domestic wastewater inputs in isolated headwater streams with no WWTP effluent.

Wastewater tracer studies have emphasized the usefulness of organic chemicals that are resistant to biodegradation and are persistent in the environment, including artificial sweeteners (e.g. acesulfame-K) and pharmaceuticals (e.g. carbamazepine). Groundwater sources of these compounds include landfills (Clarke et al., 2015) and septic systems (Carrara et al., 2008; Spoelstra et al., 2017), surface water inputs are from WWTPs (Buerge et al., 2003) and direct septic discharges (Richards et al., 2017a). In rural areas with no known WWTP or landfill impacts upstream, select organic tracers may provide indications of septic wastewater impacts in surface waters. Previous studies have suggested using a co-tracer approach to track domestic waste effluent in the environment (Liu et al., 2014; Richards et al., 2017a).

Ideal tracers should be source-specific, measured above detection limits, have continuous inputs, and be conservative in ground and surface waters (Buerge et al., 2009; James et al., 2016). The sweetener acesulfame-K (ACE-K) is known to be recalcitrant in the environment and has been identified as an ideal tracer in the aquatic environment (Buerge et al., 2009; Van Stempvoort et al., 2011a). The ubiquitous use of the recreational pharmaceutical caffeine (CAF) identifies it as a continuous input within the environment. In this work, these two tracers are studied alongside five other pharmaceutical compounds: carbamazepine (CBZ), gemfibrozil (GEM), ibuprofen (IBU), naproxen (NAP), and sulfamethoxazole (SMX). Previous studies have identified these organic tracers in septic plumes (Carrara et al., 2008; Robertson et al., 2013; Snider et al., 2017), and in receiving surface waters (Liu et al., 2014).



### **2.1.3 Study Objectives**

The main objective of this study was to use a suite of anthropogenic tracers to determine domestic wastewater contamination in rural headwater streams in three hamlets that exclusively use on-site systems (septic systems) for wastewater disposal. The co-tracer approach in this study is unique, as it contains a human-specific fecal indicator bacteria *Bacteroides*, a conservative artificial sweetener, and six pharmaceuticals. Additionally, this study assesses the usefulness of using organic tracer concentrations to track nutrient concentrations, that may also be derived from septic systems, as well as identify which tracers are the most useful for detecting septic inputs in receiving streams.

## **2.2 Methods**

### **2.2.1 Field Site Descriptions and Sampling Design**

In this study, three small headwater streams located in rural areas (1.16-3.69 km<sup>2</sup>, Table 2-1) in the Grand River Watershed (GRW, Ontario, Canada) were sampled over a one-year period between April 2017 and March 2018. Samples were collected one to two times per month to capture seasonal variations in water quality and variable climatic conditions (e.g. snowmelt, baseflow, rain events). These sites were selected to represent varying hydrogeological conditions, home density, and land-use characteristics (Table 2-1). Samples were collected at upstream (US) and downstream (DS) locations in streams with low dilution capacity (Figure 2-1). Site A (SA) should have little to no impact by septic effluent at the US compared to the DS because of the lack of homes upgradient, with abundant agricultural activities potentially affecting the US. Site B (SB) and Site C (SC) had a few homes located upgradient from the

US sampling locations, and SC had a more complicated stream geometry including a junction located between the US and DS sites. A storm drain (SD) located between the US and DS at SB was also sampled on six occasions. The finer grained material comprising SA and SB contrasted the coarser grained overburden material found at SC (Figure 2-1).

Flow measurements were not measured directly at the field sites; however, a nearby flow gauging station (Figure 2-1) was used to assess peaks in flow potentially affecting the stream water concentrations. Historical flow data ( $\text{m}^3 \text{s}^{-1}$ , 15-minute intervals) between April 2017 and March 2018 were obtained from a hydrometric station (Station ID: 02GA005, Environment Canada) located near the study sites ( $43^\circ 41' 36'' \text{ N}$ ,  $80^\circ 26' 43'' \text{ W}$ ). Historical rainfall data (mm, daily total) were obtained from a local weather station (Station ID: 6142402, Environment Canada). For this study, missing data cells were not assigned a value, and data were available for all 17 sampling days.

### **2.2.2 Water Sampling and Field Analysis**

Each sampling excursion (approximately six samples per outing, 17 outings) involved collecting water samples using a grab pole or by wading to the center of the stream, always ensuring samples were collected upstream with minimal interference. All samples were collected at the US prior to the DS to reduce the distance between samples for better comparison and to reduce DS contamination in US samples. After water samples were collected, a water quality multi-probe (YSI ProPlus handheld, Hoskin Scientific) was used to collect measurements of temperature, pH, specific conductivity (SPC), dissolved oxygen (DO), and turbidity using individually calibrated probes (no. 15B105053, 15C100538, 15C101265, and 15B104975).

Each sampling occasion included the same suite of samples collected for: alkalinity, total solids (TS), dissolved organic carbon (DOC), anions ( $\text{Cl}^-$ ,  $\text{SO}_4^{2-}$ ), trace metals (Ag, Al, Ba, Be, Bi, Ca, Cd, Co, Cr, Cu, Fe, K, Li, Mg, Mn, Mo, Na, Ni, Pb, Sn, Sr, Ti, U, V, Zn, and Zr); dissolved nutrients: total nitrogen (TN), nitrite nitrogen ( $\text{NO}_2\text{-N}$ ), nitrite and nitrate nitrogen ( $\text{NO}_{2+3}\text{-N}$ ), ammonia and ammonium nitrogen ( $\text{NH}_{3+4}\text{-N}$ ), total dissolved phosphorus (TDP), and soluble reactive orthophosphate (SRP); an unfiltered measurement for total phosphorus (TP); filtered samples for pharmaceuticals: caffeine (CAF), carbamazepine (CBZ), gemfibrozil (GEM), ibuprofen (IBU), naproxen (NAP), and sulfamethoxazole (SMX), an artificial sweetener acesulfame-K (ACE-K); and unfiltered samples for fecal indicator bacteria (FIB) including *Escherichia coli* (*E. coli*) and *Bacteroides*: general (BacGen), host-specific bovine (BacBov), and human (BacHum) abundances.

All general water quality samples were collected in high-density polyethylene containers, except for water collected for dissolved nutrients and TP (glass), DOC and pharmaceuticals (amber glass). Approximately 1 L of sample was collected for alkalinity and TS (unfiltered), trace metals, anions, DOC, and dissolved nutrients, which were filtered using 0.45  $\mu\text{m}$  membrane filters and disposable polyethylene syringes, and ACE-K which was filtered with 0.2  $\mu\text{m}$  PVDF (Chromatographic Specialties Inc.) filters. An additional 1 L of sample was filtered with 0.45  $\mu\text{m}$  nylon filters (Pall® Corporation) and glass syringes for pharmaceutical analysis. Pharmaceutical and DOC samples were acidified ( $\text{pH} < 2$ ) with concentrated  $\text{H}_2\text{SO}_4$ , and trace metals with  $\text{HNO}_3$  ( $\text{pH} < 2$ ). An additional 35 mL sample aliquot was collected for TP. Two 250 mL unfiltered samples were collected for FIB

analyses in 300 mL sterile bottles containing sodium thiosulfate for preservation. All samples were transported in a cooler on ice to either the Ontario Ministry of the Environment, Conservation and Parks (MECP) laboratories in Dorset, and Etobicoke, ON, or to the University of Waterloo (UW). All samples were stored at 4 °C, except for trace metals (room temperature), and anions and ACE-K (frozen at -22 °C).

### **2.2.3 General Water Quality Analysis**

Alkalinity, TS, trace metals, dissolved nutrients (except TDP), and FIB abundances, were analyzed by the MECP Laboratory Services Branch (LaSB) in Etobicoke, Ontario. A 10-mL sample volume was used to determine the fixed end-point alkalinity (as mg L<sup>-1</sup> CaCO<sub>3</sub>) using an automated titration programmed for the volume of titrant added to the sample (MOE, 2015a). Total solid concentrations were determined by gravimetry techniques previously published (MOE, 2014a), whereby known volumes of sample aliquots were weighed and dried in the oven, and then reweighed to determine the concentration of TS in each sample. Trace metal concentrations were measured using inductively coupled plasma-optical emission spectroscopy (ICP-OES) using a previously published method (MOE, 2014b). Dissolved nutrient concentrations were measured by colourimetry techniques using a San++ Automated Wet Chemistry Analyzer (MOE, 2014c). The TP and TDP concentrations were measured at the MECP LSB in Dorset, ON, using a colourimetry technique (MOE, 2015b). Briefly, two 35 mL surface water sample aliquots were digested in sulfuric acid-persulfate, autoclaved at 121 °C for 30 minutes, and analyzed using a Technicon AutoAnalyzer II. The anion and DOC concentrations were determined at UW using an ion-chromatography system (IC) (Dionex ICS-5000+, Mississauga, Canada) and a TOC analyzer (Aurora 1030W)

respectively. *E. coli* was analyzed within 24 hours at the MECP LaSB. Briefly, the samples (100 mL final) were passed through a 0.45 µm mixed cellulose ester membrane (Pall, Canada), and plated on mFC-BCIG agar, ensuring no air bubbles, inverted, and transferred to an incubator at  $44.5 \pm 0.2$  °C for 22-24 hours. The culture plates were then examined and target colonies (blue-green colour) were enumerated (Ciebin et al., 1995; Lee et al., 2014; APHA, 2018). Additional information on the quality control measures taken for laboratory analysis can be found in Appendix A.

## **2.2.4 Tracer Analysis**

### 2.2.4.1 Bacteroides analysis

The *Bacteroides* genetic markers (BacGen) were measured using previously published methods (Lee et al., 2010, 2014) at the MECP LaSB. In short, 100 mL of the water was filtered through a 0.45 µm cellulose-ester membrane, and the membrane subsequently transferred to a tube containing a buffer and placed on a shaker (70 rpm) for one hour to remove the cells from the filter. Samples were then centrifuged to remove debris and the DNA extracted with a buffer solution. Samples were run using TaqMan real-time quantitative Polymerase Chain Reaction (qPCR) assays at 50 °C for 10 minutes, 40 15-second cycles at 95 °C and 1-minute cycles at 60 °C. Data was collected for total *Bacteroides* (BacGen), human-specific (BacHum), and bovine-specific (BacBov). Additional information on the quality control measures taken for laboratory analysis can be found in Appendix A.

#### 2.2.4.2 Solutes and solvents

The native compounds for the artificial sweetener ACE-K and the six target pharmaceuticals, CAF, CBZ, GEM, IBU, NAP, and SMX, were purchased from Sigma-Aldrich (Oakville, Canada). Dry powder isotope-labelled compounds were obtained in the form of CAF-d3, CBZ-d10, IBU-d3, GEM-d6, and [<sup>13</sup>C]-NAP (Cambridge Isotope Laboratory Inc., USA), along with SMX-d4 and ACE-K-d4 (Toronto Research Chemicals Inc., Canada). HPLC-grade methanol and acetonitrile were purchased from Fisher Scientific™ (Toronto, ON), and formic acid and ammonium acetate were supplied by Sigma-Aldrich (Oakville, Canada). Ultrapure water was generated by a MilliQ A10 water system (18.2 MΩ cm @ 25 °C).

Two sets of analyte and internal standard (IS) stock solutions were made: one for ACE-K only, and the other a mixture containing the six pharmaceutical compounds. The ACE-K stocks were made with ultrapure water and the pharmaceutical mixtures with 50:50 by volume methanol and ultrapure water. Each analyte was dissolved to obtain an original stock solution with a concentration of 1 g L<sup>-1</sup>. This solution was used to make more stock solutions by serial dilution to a final concentration of 1 µg L<sup>-1</sup>. All stock solutions were used to make calibration standards and to spike unknown samples. Each of the isotope-labelled compounds was dissolved with 1000 µL of methanol to a final internal standard (IS) stock solution concentration of 1 g L<sup>-1</sup>. Individual compounds were diluted by serial dilution to a final concentration of 10 µg L<sup>-1</sup>. The final pharmaceutical IS consisted of a mixture of all six compounds. The IS mixtures were used to spike all samples and calibration standards.

#### 2.2.4.3 Artificial sweetener analysis

The artificial sweetener ACE-K was analyzed by direct injection using an ion chromatography (IC) coupled with electrospray tandem mass spectrometry (MS) with a modified version of the method described by Van Stempvoort et al. (2011b). Artificial sweetener samples were prepared by diluting 500  $\mu\text{L}$  of aqueous sample with ultrapure water and spiking with a consistent known concentration of IS. Sample was injected into a Dionex ICS-500 (Sunnyvale, CA, USA) where it was passed through a guard column (Dionex IonPac™ AG20 RFIC™, 2×50 mm) and an analytical column (Dionex RFIC™ IonPac® A520, 2×250 mm). The sample was then injected into an Agilent 6460 QQQ (Mississauga, ON, CA) operating in negative electrospray ionization (ESI -) mode with multiple reaction monitoring (MRM). Source parameters were optimized to provide the best signal to noise ratio and were the same as those reported in (Saurette et al., 2017). The MRM transitions (m/z) were 162.1→81.8 for the analyte and 162.1→78.0 for the IS. The ACE-K retention time was 5.9 minutes. The MDL with the dilution factor applied was 0.14  $\mu\text{g L}^{-1}$ . The QA/QC information can be found in Appendix A. The mean relative and absolute IS recoveries and RSD% for unknown samples were  $53 \pm 17\%$  and  $110 \pm 20\%$  respectively.

#### 2.2.4.4 Pharmaceutical analysis

The target pharmaceutical compounds were measured using solid phase extraction (SPE) techniques followed by high performance liquid chromatography (HPLC) coupled with tandem mass spectrometry (MS) using a slightly modified method by Liu et al. (2014). Each aliquot was made by diluting 300 mL of sample with 300 mL of ultrapure water. Quality control (QC) consisted of 600 mL of ultrapure water spiked with stock solution mixture, and

600 mL ultrapure samples were used as laboratory blanks. Site A US samples were spiked with analyte stock mixture as blind QC samples. All known, unknown, and blanks were spiked with a consistent amount of IS prior to extraction. The samples were passed through Oasis HLB 6cc SPE cartridges (Waters). The cartridges were preconditioned with 2×3 mL methanol, and subsequently washed with 2×3 mL ultrapure water. Samples were loaded under light vacuum not exceeding 6 mL min<sup>-1</sup>. The cartridges were rinsed with 2×3 mL of 5% by volume methanol washing solution and the sorbent was vacuumed dry. The pharmaceutical compounds were extracted by eluting with 2×3 mL methanol, and the eluate was collected in 7 mL amber glass vials (Supelco). The eluates were then evaporated under a gentle nitrogen stream, reconstituted with 600 µL methanol, well mixed by vortex, and transferred to 2 mL amber glass HPLC injection vials (Supelco). The final extracts were concentrated 500 times and were stored at 4 °C until analysis.

The samples were injected in an Agilent 1100 HPLC (Agilent Technologies, Mississauga, ON) coupled with tandem mass spectrometry on a 4000 Q TRAP (Applied Biosystems, Foster City, US). Samples were passed through a Zorbax Eclipse XDB C18 analytical column (4.6×150 mm). Electrospray ionization positive (ESI+) mode was used to target CAF, CBZ, and SMX, while negative (ESI-) mode was used for IBU, GEM, NAP. The mobile phases for + mode consisted of 5 mM ammonium acetate in ultrapure water with 0.1% formic acid (A) and methanol (99.9%) with 0.1% formic acid (B), with an eluent gradient of phase B of 10% for three minutes, followed by 90% to 10 minutes, and held for 10 minutes. For – mode, the phases comprised of 6.9 mM acetic acid in 700 mL ultrapure water and 300 mL acetonitrile (A), and 10% acetonitrile (B). The elution gradient for phase



B started at 12%, increased to 40% to 10 minutes, and was held for 10 minutes. Sample volumes of 15  $\mu\text{L}$  for + mode and 10  $\mu\text{L}$  for – mode were injected at a flow rate of 1000  $\mu\text{L min}^{-1}$ . The source-dependent parameters and gradient and mobile phases were selected to optimize the results. The MDLs considering the concentration factor applied and the dilution, SPE and evaporation processes were ( $\text{ng L}^{-1}$ ): 0.162 for CAF; 0.438 for CBZ; 0.032 for GEM; 0.228 for IBU; 0.254 for NAP; 0.394 for SMX.

The mean accuracies for the calibration standards (0.01-50  $\mu\text{g L}^{-1}$ ) were between 99-103%. The continuing calibration verification samples (0.05-10  $\mu\text{g L}^{-1}$ ) that were run at least every ten samples had mean accuracies that ranged between 97-103%. The instrument and SPE blanks had concentrations consistently below detection limits for all six compounds. The mean absolute IS recoveries for CCV and method blanks ranged between 95-132%. Method QC samples had mean accuracies between 72-74% and mean absolute IS recoveries between 95-152%. Blind spiked samples had mean accuracies between 64-85%, absolute relative recoveries between 71-132%. The unknown samples had mean absolute IS recoveries between 59-108% and mean relative IS recoveries between 99-103%. Except for CAF ( $108 \pm 37\%$ ), all mean absolute IS recoveries were less than 100%, and RSD% ranged between 27-36%. All internal standard recoveries improved using relative IS recovery, which accounts for the matrix effects in the sample water, with lower RSD% values for five of the compounds (not CAF) between 16-29%. Overall, GEM and IBU had the most consistent absolute and relative IS recoveries with the lowest RSD%. NAP and SMX had the lowest mean absolute IS recoveries (59 and 71%), but both improved to 99% for mean relative recovery. Additional information on quality assurance/control may be found in Appendix A.

### **2.2.5 Statistical Analysis**

For this study and the frequent number of samples that had tracer concentrations below the MDLs, samples that did not have concentrations above the MDL were assigned the MDL for statistical analysis. The differences in annual concentrations were assessed using the nonparametric statistical test Mann-Whitney Rank Order Sum ( $P < 0.05$ ). Sample groups that failed a Shapiro-Wilk Normality Test ( $P < 0.05$ ) were compared using the parametric statistical student's t test ( $P < 0.05$ ). Furthermore, correlations between tracers, nutrients, and other water quality parameters were measured using the nonparametric statistical test Spearman Rank Order Correlation ( $P < 0.05$ ). All statistical analyses were accomplished using Sigma Plot (Version 11.0).

## **2.3 Results**

The sample sites were visited one to two times per month, totaling 17 occasions, between April 2017 and March 2018 to collect 47 upstream (US) and 50 downstream (DS) samples. Samples were not collected during August-October 2017 at the upstream (US) of Site C (SC) due to no flow, nor at SA-DS in September 2017 also due to low flow. The complete set of descriptive statistics for all water quality parameters and anthropogenic tracers may be found in Table B-1-Table B-3.

### **2.3.1 Stream Characterization and Spatial-temporal Patterns in Water Quality**

#### **2.3.1.1 Annual general water quality patterns**

The annual ranges of surface water temperature at all six sampling locations were between -0.2 and 20.2 °C and pH between the near-neutral range of 6.76–9.01 (Figure 2-2). These

ranges are typical of streams in southern Ontario. The ranges of DO concentrations over the course of the sampling year were between 4.18 and 20.2 mg L<sup>-1</sup>, which does not follow the solubility of oxygen in water at these temperatures within the pressure range of 700–795 mm Hg: 13.4–15.3 mg L<sup>-1</sup> at 0 °C, and 8.3–9.5 mg L<sup>-1</sup> at 20 °C (Weiss, 1970). The values that are lower than the solubility may suggest consumption of O<sub>2</sub>, whereas the higher values may be indicative of issues with the YSI probe used to take these measurements, with inconsistencies previously reported by the manufacturer (YSI Environmental, 2005). Although the values may be inaccurate, the same probe was used at all sites, thus the reported values were used for statistical comparison. The SPC measurements were highly variable at all three streams, with standard deviations between 114–297 µS cm<sup>-1</sup> (Table B-1; Table B-2; Table B-3). The lowest SPC range was observed at SC–US (320–382 µS cm<sup>-1</sup>) and the highest at SA–DS (537–1940 µS cm<sup>-1</sup>). The turbidity ranges were similar across all three streams, with minimum values between 0.2–4.6 and maximum values between 14–51.1 NTU (Figure 2-2). Alkalinity measurements were variable between 109–416 mg L<sup>-1</sup> as CaCO<sub>3</sub>, and the DOC concentrations ranged between 2.7 and 85 mg L<sup>-1</sup> (Figure 2-2). Elevated alkalinity concentrations were not unexpected in these geological settings, which are comprised of calcium-rich minerals (LESPRTT, 2008). Some DOC values were higher than anticipated compared to previous measurements in the GRW with a maximum of 25 mg L<sup>-1</sup> (Hutchins, 2011). The TS concentrations were also variable within a range of 211–1530 mg L<sup>-1</sup> (Figure 2-2). Elevated Cl concentrations were detected at SA–DS within the range of 40–333 mg L<sup>-1</sup>, and a low range at the US between 4–104 mg L<sup>-1</sup> (Figure 2-2). The remaining sites had maximum values between 153–202 mg L<sup>-1</sup>. Measurements of SO<sub>4</sub> were similar between sites

with minimum concentrations between 3–6 mg L<sup>-1</sup> and maximum concentrations between 50–65 mg L<sup>-1</sup> (Figure 2-3). Overall, the highest mean values for DO (12 mg L<sup>-1</sup>), SPC (1140 μS cm<sup>-1</sup>), alkalinity (349 mg L<sup>-1</sup> CaCO<sub>3</sub>), TS (753 mg L<sup>-1</sup>), and Cl (153 mg L<sup>-1</sup>) were observed at SA–DS, and the highest mean measurements of turbidity (12 NTU), and SO<sub>4</sub> (28 mg L<sup>-1</sup>) at SB–US.

Maximum concentrations of major cations Ca (157 mg L<sup>-1</sup>) and Mg (45 mg L<sup>-1</sup>) were observed at SC–DS, and maximum concentrations of K (36 mg L<sup>-1</sup>) and Na (268 mg L<sup>-1</sup>) at SB–US and SA–DS, respectively (Figure 2-3). Trace metal concentrations were not elevated, and Ba, Fe, Mn, and Zn were consistently measured greater than their MDLs at all sites (Figure 2-3) and along with continuous measurements above MDLs of Cu, Fe, and U at SB and SC (Figure B-1). The maximum concentrations of Cu (8 μg L<sup>-1</sup>), Sr (805 μg L<sup>-1</sup>) and U (15 μg L<sup>-1</sup>) were observed at SA–DS, and Ba (107 μg L<sup>-1</sup>), Fe (292 μg L<sup>-1</sup>), Mn (1350 μg L<sup>-1</sup>), and Zn (117 μg L<sup>-1</sup>) at SC–DS (Table B-1; Table B-2; Table B-3). The concentrations of trace metals Ag, Bi, Cr, Ni, Pb, Sn, and Zr were always observed less than their MDLs at all six sampling sites DS (Table B-1; Table B-2; Table B-3); negligible trace metal concentrations were expected at these sites, which are not near industrial or mining operations.

Flow measurements were not recorded, but annual rain and flow records from nearby stations indicated a high rainfall event (HRE) and high flow event (HFE) concurrent with sampling occasions on Jun. 20, 2017, and Feb. 21, 2018, respectively (*see* Figure 2-2 to Figure 2-5). The effects of these events on stream water quality were evident in the measurements of SPC, turbidity, alkalinity, TS, Cl (Figure 2-2), SO<sub>4</sub>, Ca, Mg and Na (Figure

2-3). The site-specific minimum measurements of alkalinity ( $109\text{--}155\text{ mg L}^{-1}\text{ CaCO}_3$ ), Cl ( $4.14\text{--}30.8\text{ mg L}^{-1}$ ), and  $\text{SO}_4$  ( $3.06\text{--}5.97\text{ mg L}^{-1}$ ) were associated with samples collected during the HFE. Additionally, minimum measurements of SPC ( $320\text{--}727\text{ }\mu\text{S cm}^{-1}$ ), TS ( $211\text{--}410\text{ mg L}^{-1}$ ), Ca ( $37.9\text{--}57.1\text{ mg L}^{-1}$ ), Na ( $3.82\text{--}56.0\text{ mg L}^{-1}$ ), and Mg ( $9.01\text{--}12.5\text{ mg L}^{-1}$ ) were also associated with this event, except for those collected at SA-DS. The only exception was a maximum SPC measurement at SB-DS ( $1530\text{ }\mu\text{S cm}^{-1}$ ). In contrast, the turbidity measurements were greatest during the HFE at SB ( $51.1\text{ NTU}$ ) and SC ( $37.2\text{ NTU}$ ). Site A DS exhibited a similar response to the HRE and HFE, with the two lowest measurements of SPC, TS, Ca, Na, and Mg, and two highest turbidity measurements recorded during these two events (Figure 2-2; Figure 2-3). Overall, K, Ba, Fe, Mn, and Zn exhibited similar temporal patterns with increasing concentrations in the spring and summer months and decreasing in the autumn and winter months (Figure 2-3).

#### 2.3.1.2 Annual nutrient (P, N) concentration patterns

Nutrient concentrations for TP, TDP, SRP, TN,  $\text{NO}_2\text{-N}$ ,  $\text{NO}_3\text{-N}$ , and  $\text{NH}_{3+4}\text{-N}$  were consistently above MDLs in all surface water samples (Figure 2-4). The proportions of P that is in the dissolved form (TDP) were between  $79.4\text{--}83.5\%$  (as medians), and the proportions of the dissolved form comprised of SRP were between  $85.8\text{--}89.9\%$  (Figure B-2). The greatest concentrations of SRP throughout the year were observed at SB-US ( $316\text{--}1720\text{ }\mu\text{g L}^{-1}$ ) followed by SB-DS ( $152\text{--}948\text{ }\mu\text{g L}^{-1}$ ), and the SA and SC, at the US and DS locations, SRP concentrations were measured between  $12\text{--}259\text{ }\mu\text{g L}^{-1}$  (Figure 2-4). The SRP concentrations were generally lower during the winter and spring compared to the summer and fall (Figure 2-4). At SB, there was a pronounced seasonal effect with elevated

concentrations observed between Jun. 20 and Oct. 17, 2017 during the HRE and baseflow conditions.

The  $\text{NO}_3\text{-N}$  concentrations were calculated by subtracting the  $\text{NO}_2\text{-N}$  from the reported  $\text{NO}_{2+3}\text{-N}$  concentrations (Equation C.1). The TN portions were mostly made up of  $\text{NO}_3\text{-N}$ , with minor proportions of  $\text{NO}_2\text{-N}$  (median between 0.06–2.3%) and  $\text{NH}_{3+4}\text{-N}$  (0.21–17.08%) (Figure B-2). The  $\text{NO}_3\text{-N}$  concentrations were highest at SA (1.8–27.4  $\text{mg L}^{-1}$ ), then SB (0.46–16.43  $\text{mg L}^{-1}$ ), followed by SC (0.03–6.03  $\text{mg L}^{-1}$ ) (Figure 2-4). In general, the highest  $\text{NO}_3\text{-N}$  concentrations were observed during the spring, except for SC–DS, which had elevated measurements in the autumn and winter. The SA–US  $\text{NO}_3\text{-N}$  concentrations were greatest between Apr. and Aug. 2017 (13.6–27.4  $\text{mg L}^{-1}$ ) compared to the rest of the year (4.8–8.7  $\text{mg L}^{-1}$ ). The  $\text{NO}_2\text{-N}$  concentrations were lowest at SA–US (0.003–0.016  $\text{mg L}^{-1}$ ) and highest at SB–US (0.074–1.31  $\text{mg L}^{-1}$ ). There was a similar pattern for  $\text{NH}_{3+4}\text{-N}$  concentrations with a low range of 0.010–0.370  $\text{mg L}^{-1}$  at SA–US, and a high range between 0.525–5.51  $\text{mg L}^{-1}$  at SB–US. Overall, SB–US had the higher TP, TDP, SRP,  $\text{NO}_2\text{-N}$ , and  $\text{NH}_{3+4}\text{-N}$  concentrations and SA–US had higher TN and  $\text{NO}_3\text{-N}$  concentrations (Figure 2-4).

Like other water quality parameters, the effects of the HRE and HFE were pronounced in some of the patterns of P and N species concentrations (Figure 2-4). Elevated or maximum P concentrations were observed during the HRE and HFE at SA–US (210–362  $\mu\text{g L}^{-1}$ ) and DS (147–235  $\mu\text{g L}^{-1}$ ) with concentrations ranging from 1–9.9 times greater than the medians. At SB the P concentrations were variable around the median values. The SC HRE and HFE concentrations were 1.2–3.7 times greater than the median values.

Apart from the  $\text{NH}_{3+4}\text{-N}$  annual concentrations, the N species were elevated in the spring and summer, and low in the fall and winter. At SA-US, the maximum TN ( $31.5 \text{ mg L}^{-1}$ ) and  $\text{NO}_3\text{-N}$  ( $27.4 \text{ mg L}^{-1}$ ) were measured during the HRE, but unlike the P species, SA-DS values were less than the medians. At SB there were maximum concentrations at the US during the HRE, and a concentration three times the median at the DS. The HFE was likely related to dilution of TN and  $\text{NO}_3\text{-N}$  at SA, SB, and SC, with values less than the site medians as well. The HFE had concentrations 0.8–0.9 times and 1.3–1.2 times the TN and  $\text{NO}_3\text{-N}$  median concentrations at SB-US and SB-DS respectively.

The HRE affected all  $\text{NO}_2\text{-N}$  and  $\text{NH}_{3+4}\text{-N}$  concentrations similarly: concentrations were between 0.01–0.37 times the median for  $\text{NO}_2\text{-N}$  and 0.02–0.51 times the median for  $\text{NH}_{3+4}\text{-N}$ . The only exception was the SB-US  $\text{NH}_{3+4}\text{-N}$  concentration which was 3.4 times greater than the median. The HFE concentrations were more variable for  $\text{NO}_2\text{-N}$ : SA-US (1.5 times) and SC-US (1.7 times) were greater than the medians and the remaining sites had concentrations between 0.38–0.87 times the medians. Contrarily, the  $\text{NH}_{3+4}\text{-N}$  HFE concentrations were 2.2–30 times greater than the medians at all sites except for SB-US.

### 2.3.1.3 Occurrence of anthropogenic contamination in headwater streams

The median *E. coli* counts were between  $10^1\text{--}10^4$  CFU  $100 \text{ mL}^{-1}$  (Table B-1; Table B-2; Table B-3). The most elevated counts of *E. coli* were observed at SB with a range of  $10^2\text{--}10^5$  CFU  $100 \text{ mL}^{-1}$  and the lowest *E. coli* abundances were observed at SA-US ( $< 4\text{--}10^3$  CFU  $100 \text{ mL}^{-1}$ ) (Figure 2-4). The median BacGen abundances were two orders of magnitude greater than *E. coli* within the range of  $10^3\text{--}10^6$  C  $100 \text{ mL}^{-1}$ . Like the *E. coli* results, SB-US

had the highest concentration at  $10^7$  C  $100 \text{ mL}^{-1}$ , although the remaining sites exhibited similar maximum counts of  $10^5$ – $10^6$  C  $100 \text{ mL}^{-1}$ , with the lowest counts observed at SA–US.

This study coupled the *E. coli* abundances with host specific *Bacteroides*; the BacGen assays were used to distinguish the proportions (%) from human (BacHum) and bovine (BacBov) hosts (Figure B-3). The abundances of BacHum and BacBov were calculated by multiplying the BacGen abundances by the reported proportion (Equation C.2 and Equation C. 3). The range of abundance for BacBov were between  $< 10^1$ – $10^7$  C  $100 \text{ mL}^{-1}$  and BacHum had a maximum one order of magnitude lower ( $< 10^1$ – $10^6$  C  $100 \text{ mL}^{-1}$ ) (Figure 2-5). Like BacHum, all seven target organic compounds were present in the environment at all three sites, except for CBZ and GEM at SA–US and for GEM and IBU at SC–US (Figure 2-5). Most organic compounds were recorded in the  $\text{ng L}^{-1}$  range, except for occasional ACE-K concentrations and one IBU concentration which were in the  $\mu\text{g L}^{-1}$  range (Figure 2-5).

The artificial sweetener acesulfame-K (ACE-K) concentrations were highest at SB with a maximum of  $54300 \text{ ng L}^{-1}$  (Table B-2). The mean concentrations of ACE-K for SA and SC were  $228 \text{ ng L}^{-1}$  and  $1280 \text{ ng L}^{-1}$  respectively. In this study, ACE-K was found in concentrations one to three orders of magnitude higher than the target pharmaceuticals (not including SA–US) (Figure 2-5). Although ACE-K was detected at SA–US, the mean concentration of the positive hits was 0.10–0.38 times the other site-specific means (for concentrations greater than  $140 \text{ ng L}^{-1}$ ). The most elevated CAF concentrations detected during the year were generally observed at SB ( $11$ – $109 \text{ ng L}^{-1}$ ), with occasional temporal maximums detected at SA–DS ( $15$ – $64 \text{ ng L}^{-1}$ ), and SC–US ( $11 \text{ ng L}^{-1}$ ). The water samples at SA–US had a mean caffeine (CAF) measurement of  $1.95 \pm 1.74 \text{ ng L}^{-1}$ . The antiepileptic



drug carbamazepine (CBZ) exhibited maximum concentrations in the samples collected at SA–DS (4.4–32 ng L<sup>-1</sup>), followed by those at SB–DS (0.65–8.16 ng L<sup>-1</sup>). Similarly, gemfibrozil (GEM), a lipid regulator, had a maximum concentration at SB–DS (67 ng L<sup>-1</sup>). The anti-inflammatory drugs ibuprofen (IBU) and naproxen (NAP) maximum concentrations were also found at SB–DS (1.2 µg L<sup>-1</sup>) and SA–DS (628 ng L<sup>-1</sup>) respectively. Finally, the antibiotic sulfamethoxazole (SMX), had mean concentrations between 0.7–3.9 ng L<sup>-1</sup>, which were lower compared to the other pharmaceuticals, especially at SA–DS and SB; although, the greatest concentration of 11 ng L<sup>-1</sup> was detected at SB–DS. Overall, elevated tracer concentrations were found at SA–DS and SB (Figure 2-5).

#### 2.3.1.4 Spatial-temporal variation in annual FIB and organic tracer concentrations

Maximum BacBov abundances were observed during the spring and winter, and there was no evident pattern in the annual BacHum abundances (Figure 2-5). The patterns in annual organic tracer concentrations were independent of one another. For example, in the summer, there were generally elevated CBZ, GEM, and IBU concentrations, but lower SMX concentrations. The HRE and HFE also exhibited contradicting patterns between sites, and between the different organic tracers.

All maximum concentrations for SA–US (CBZ and GEM were not present), were measured in samples collected on either Feb. 21, 2018 (HFE) or Mar. 28, 2018 (Figure 2-5). The HRE was notably related to the next highest BacHum abundance (10<sup>2</sup>) observed at this site. In contrast, at SA–DS, the HRE was associated with low concentrations of organic tracers: GEM and IBU were less than the MDLs, NAP and SMX were less than the medians, and low concentrations of CAF and CBZ were observed. Tracer concentrations in the HFE

samples, however, were inconsistent, with minimum values of CBZ and SMX, but concentrations of IBU and NAP 4 and 1.7 times greater than their medians.

At SB, there were seasonal differences in organic tracer concentrations, and a notable occurrence of GEM concentrations during the summer and fall at SB-DS, and there were inconsistent trends related to the HRE and HFE concentrations (Figure 2-5). For example, the HRE coincided with the maximum SMX concentration at SB-US, the only GEM concentration greater than the MDL, and with measurements of CAF, CBZ, and NAP between 1.2–7.2 times greater than the median values. However, the IBU concentration measured during the HRE was less than the median, although greater than the MDL, and the BacHum concentration was  $< 10 \text{ C } 100 \text{ mL}^{-1}$ . During the HFE, the SB-US concentrations were sometimes less than the MDLs (CBZ, GEM, SMX), but it is difficult to ascertain that these low concentrations are directly associated with the HFE as they seldom occurred throughout the year. Other organic tracers, CAF, IBU, and NAP, were measured at concentrations 0.43–0.60 times the median concentrations. In contrast, ACE-K and BacHum concentrations measured during the HFE at SB-US were equal to and two orders of magnitude greater than their medians respectively. At SB-DS, the HRE organic tracer concentrations were either less than their MDLs (GEM IBU), a site-specific maximum (SMX), or in between (ACE, CAF, CBZ, NAP). The HFE was associated with concentrations of organic tracers ACE-K, CAF, CBZ, IBU, NAP, and SMX between 0.19–0.40 times their medians. The BacHum abundances during the HRE and HFE at SB-DS were two orders of magnitude less and equal to the median respectively.

At SC, most of selected tracers were not present at concentrations greater than their MDLs. During the HRE at SC-US, BacHum and CAF were the only anthropogenic tracers found at concentrations greater than the MDLs (Figure 2-5). The HRE concentrations at SC-DS was associated with ACE-K and CBZ concentrations 1.2 and 2.3 times greater than their medians, and with elevated BacHum ( $10^3$  C 100 mL<sup>-1</sup>). The maximum NAP and SMX concentrations at both the US and DS were associated with the HFE. Additionally, the concentration of IBU at SC-DS during the HFE was 7 times the median concentration, and there was an elevated BacHum abundance ( $10^4$  C 100 mL<sup>-1</sup>). Maximum concentrations at SC mostly occurred during the HFE (NAP, SMX) and on May 31, 2017 (CAF, CBZ, IBU) which was representative of baseflow at that site. At SC, summer sampling was not possible due to no-flow conditions at the US and DS between Aug. and Oct. 2017.

#### 2.3.1.5 Frequency of FIB, tracer occurrences in surface water samples

The general FIB *E. coli* and BacGen were found in 91% and 100% of the surface water samples respectively (Figure 2-6). This indicated that there was fecal contamination present at detectable levels during most of the year at all three hamlets. Notably, *E. coli* was present in 100% of the DS samples in this study. The host-specific *Bacteroides* BacBov and BacHum markers were measured less frequently, in only 59% and 77% of the stream water samples (Figure 2-6). The proportions of BacGen that were distinguished as BacBov and BacHum markers were variable within 0–230% and 0–52% respectively (Figure B-3). The highest proportion of BacGen identified as the BacBov marker (230%) occurred at SB-DS on Mar. 28, 2018; although a value >100% may occur when the BacGen counts are low, the BacGen abundance for this sample was  $10^7$  C 100 mL<sup>-1</sup>. The BacHum marker proportions were

always less than 100% of BacGen, with a maximum of 52% at SA–US on May 31, 2017; however, the BacGen counts for that sample was low (1200 C 100 mL<sup>-1</sup>). Ranges for percentages of BacHum markers at SB and SC were between 0–36% and 0–9.6% respectively.

Caffeine was the sole anthropogenic tracer in this study that was detected at concentrations greater than the MDL (0.162 ng L<sup>-1</sup>) in 100% of the samples (Figure 2-6). The reported artificial sweetener acesulfame-K (ACE-K) concentrations were detected above the MDL (140 ng L<sup>-1</sup>) in 81% of the samples, with site-specific occurrences between 50% at SA–US and 100% at the DS of SA and SB (Figure 2-6). Occurring less frequently overall at the DS sites were SMX and CBZ. Most SMX concentrations above the MDL were found at SA (88%) and SB (84%). Similarly, CBZ was detected above the MDL (0.438 ng L<sup>-1</sup>) in 100% of the DS samples at SA and SB.

### **2.3.2 US–DS Statistical Comparison**

#### **2.3.2.1 Changes in dissolved nutrient (N, P) concentrations along the streams**

Changes in nutrient concentrations DS of the three hamlets showed variable patterns (Figure 2-7). The P species concentrations DS of SA and SC were significantly higher ( $P < 0.05$ ) apart from SA SRP ( $P = 0.105$ ) and SC TDP ( $P = 0.059$ ); although not significant, the SA–DS concentrations of SRP and TDP were greater in 69% and 79% of the samples, and the removal of the HRE and HFE data yielded significant P-values of 0.040 and 0.029. In contrast, SB was characterized with significantly decreasing ( $P < 0.001$ ) concentrations of TP, TDP, and SRP. Along the streams, the TN and NO<sub>3</sub>–N concentrations exhibited a similar

decreasing pattern: DS concentrations were significantly lower ( $P < 0.001$ ) at SA and SB (TN only). Although not significant ( $P = 0.058$ ), the SB–DS  $\text{NO}_3\text{-N}$  concentrations were less than the US concentrations in 82% of the water samples. There were no significant differences in concentrations at SC.

The more reduced forms of N ( $\text{NO}_2\text{-N}$  and  $\text{NH}_{3+4}\text{-N}$ ) results contrasted the decreasing TN and  $\text{NO}_3\text{-N}$  observations at SA, with significantly higher concentrations along the stream ( $P < 0.001$ ). Similarly, SC–DS  $\text{NO}_2\text{-N}$  concentrations were greater in 71% of the samples even though the result was not significant ( $P = 0.382$ ), and  $\text{NH}_{3+4}\text{-N}$  concentrations were found to be significantly higher ( $P = 0.026$ ). Different than the SA and SC results, the SB–DS  $\text{NO}_2\text{-N}$  concentrations, although not significant ( $P = 0.091$ ), were decreasing in 88% of the instances and  $\text{NH}_{3+4}\text{-N}$  concentrations were significantly lower ( $P < 0.001$ ).

The other water quality parameters and trace metals assessed in this study did not have many instances of significant changes along the streams, although there were parameters that were significantly greater ( $P < 0.05$ ) at the DS at a minimum of two sites for SPC, turbidity, Cl, K, and Na (Figure B-4). Furthermore, SA exhibited the greatest increases in trace metals, including greater Fe ( $P = 0.008$ ) and Mn ( $P < 0.001$ ) concentrations at the DS (Figure B-5).

### 2.3.2.2 Changes in FIB abundances along the streams

At SA, all four parameters (*E. coli*, BacGen, BacBov, and BacHum) were significantly higher ( $P < 0.001$ ) at the DS (Figure 2-8). The *E. coli* at SB exhibited a decrease in concentrations ( $P < 0.001$ ). BacGen counts, although not significantly different, showed a tendency to be lower (65% of the samples) at the DS. The BacBov concentrations were not

different along the stream, although the BacHum concentrations were significantly higher ( $P = 0.007$ ). Finally, the BacHum results at SC increased in 71% of the instances, although were not significant ( $P = 0.188$ ).

### 2.3.2.3 Changes in organic tracer concentrations along the streams

The organic tracer DS concentrations were either significantly higher ( $P < 0.05$ ) or not different compared to the US concentrations (Figure 2-9). Similar to the FIB results, all seven tracers were significantly higher at SA-DS ( $P < 0.001$ ). The tracers CAF and SMX were also significantly higher ( $P < 0.05$ ) at SB-DS and SC-DS. There were significantly higher concentrations of the sweetener ACE-K ( $P < 0.001$ ), along with CBZ ( $P < 0.001$ ), NAP ( $P < 0.001$ ) at SB-DS, and IBU ( $P = 0.003$ ) at SC-DS. The samples with increases/decreases that were not significantly different were further investigated to determine if there were increasing/decreasing trends within the dataset not captured by statistical analysis. At SB, the target compound GEM was less than the MDL in 65% of the samples which may be too low to consider changes along the stream. The IBU concentrations trended towards increasing in 59% of the samples at SB. At SC, the target compounds ACE-K, CBZ, and NAP exhibited increasing trends along the stream in 71%, 64%, and 62% of the samples respectively. Although not statistically different, there was an increasing trend of GEM at SC, with concentrations measured above the MDL at the DS site.

### 2.3.3 Correlations between Dissolved Nutrients, FIB, and Tracers

#### 2.3.3.1 Relationships between nutrients and domestic wastewater indicators

The annual concentrations of TP, TDP, SRP, TN, NO<sub>3</sub>-N, NO<sub>2</sub>-N, and NH<sub>3+4</sub>-N were compared to the abundances of *E. coli*, BacGen, BacBov, and BacHum and the organic tracer concentrations of ACE-K, CAF, CBZ, GEM, IBU, NAP, and SMX for correlations using the Rank Order Sum Test ( $\rho$ ) (Table 2-2). The majority of the  $\rho$  coefficients were not statistically significant ( $P < 0.05$ ). The SA-US correlations were not determined for BacBov, CBZ or GEM due to frequent measurements below the MDLs. For the same reason, SC-DS GEM and IBU correlations were not possible to calculate. The significant correlations were not very strong with absolute  $\rho$  values ranging between 0.49 and 0.79. Complete correlation tables can be found in Table B-4, B-5, and B-6).

Significantly positive correlations were observed between P species and FIB at SA and SC ( $\rho$  between 0.48–0.72), but not at SB. The relationships between P species and the organic compounds exhibited either significantly positive (ACE-K, CBZ, and IBU) or negative (CAF, NAP, and SMX) correlations at SA and SB, but not at SC. There were no significant correlations between GEM and P species in these streams, likely owing to the low instances of GEM. At SA-US, there were strong relationships ( $\rho > 0.60$ ) observed between P species and BacGen and BacHum, but not with organic tracers. Notably, weaker correlations were observed at SA-DS compared to US ( $\rho$  between 0.48–0.59), and BacHum was not significantly correlated with SRP but alternatively with BacBov ( $\rho = 0.49$ ). The only

instances of significant correlations at SA–DS for organic tracers were negative ( $\rho = 0.50$ ) between SMX, TDP and SRP, and at SB–DS between CAF, NAP, and SMX.

The correlations between N species and the FIB, and organic tracers did not exhibit any overarching pattern compared to the P species. The TN and  $\text{NO}_3\text{-N}$  concentrations were notably not correlated with FIB, except for strong negative correlations with *E. coli* at SA–DS. There were no correlations at SA for the remainder of the target compounds. At SB and SC, there was a mixture of negative (ACE-K, CBZ) and positive (SMX) correlations; there were contradicting results for GEM, which were negatively correlated at SB–DS ( $\rho = -0.52$ ) and positively at SC–DS ( $\rho = 0.65$ ). There were no correlations with CAF, IBU, or NAP, similar to the P correlations. The more reduced N forms as  $\text{NO}_2\text{-N}$  and  $\text{NH}_{3+4}\text{-N}$  were found to be more frequently correlated with FIB. The concentrations at SA–DS had positive relationships with BacBov and IBU, but negative correlations with CBZ and SMX. Similarly, SB had positive  $\rho$ -values apart from correlations between BacBov and  $\text{NO}_2\text{-N}$ . The SC results are similar to SA, with both positive (*E. coli*, BacBov, CAF) and negative (BacHum, ACE-K, SMX) correlations. The strongest correlations at SA ( $\rho = 0.76$ ) and SB ( $\rho = 0.79$ ) were between BacBov and  $\text{NH}_{3+4}\text{-N}$ , and between BacBov and  $\text{NO}_2\text{-N}$  at SC ( $\rho = 0.76$ ).

#### 2.3.3.2 Relationships between FIB and organic tracers

The annual FIB and organic tracer concentrations at the sampling locations (except SA–US) were also subject to the Rank Order Sum Test comparison statistical test (Table 2-3). Like the nutrient-tracer correlation analysis, most of the results were not significant. There were significant correlations between *E. coli* and BacGen at all three sites ( $\rho$  between 0.56–0.71).



There were no significant relationships between FIB and CAF, CBZ, or IBU, and no relationships exhibited between *E. coli* and all the organic tracers. There was only one relationship between BacGen and the organic tracer ACE-K ( $\rho = 0.60$ ) and with BacHum and NAP ( $\rho = -0.63$ ). The FIB-tracer correlations occurred the most often with BacBov, although there were more negative correlations ( $n = 3$ ) compared to one positive with SMX ( $\rho = -0.66$ ).

The correlation analysis between the suite of anthropogenic tracers revealed negative and positive  $\rho$ -values between 0.49–0.78. There were only two correlations at SA–DS, both involved CBZ, with a strong correlation observed with ACE-K ( $\rho = 0.66$ ) and a moderate one with SMX ( $\rho = 0.51$ ). At SB, there were multiple positive relationships between organic tracers, but there were a few instances of significant relationships with tracers that were frequently below the MDLs. For example, at SB–US, GEM and SMX were strongly correlated ( $\rho = 0.73$ ) but were seldom detected.

## 2.4 Discussion

### 2.4.1 Characterization of Non-point Source Contamination in Rural Streams

One aim of this study was to characterize water quality in watersheds containing higher densities of septic systems to determine whether there was potential contamination associated with domestic wastewater. In this study, three hamlets were selected based on the location and density of homes along headwater streams. The surface waters were blindly sampled without prior knowledge of the exact number or location of septic systems or any information on the inhabitant's consumption or water usage habits. The sampling period spanned all four

seasons and field observations during sampling provided more details on each study site, with the following important observations: SA–US is located next to an agricultural tile drain, with an adjoining storm drain linked to a nearby primary school that may be mixed with the sample water during high flow, and had multiple storm drains along the stream; SB is characterized by multiple storm drains acting as potential point sources or preferential pathways for contaminants along the stream, including one located adjacent to where the water was sampled at the US; SC had the least amount of observed storm drains and was perceived to be ephemeral as it was not flowing at the US during three of the sampling occasions; and SA–US had consistently cooler water temperatures in the summer and warmer in the winter compared to the DS, which suggests that the stream is predominantly groundwater fed (Figure 2-2).

Testing for the presence of anthropogenically-sourced tracers in surface waters has been used to track the persistence of wastewater downstream from major point sources (e.g. Buerge et al., 2003; Liu et al., 2014) but rarely from a series of smaller wastewater sources, using both biological and chemical tracers (e.g. Richards et al., 2017a). The occurrence of multiple anthropogenic tracers at all three DS sites throughout the sampling year strongly indicated that there were domestic wastewater impacts in streams flowing through all three hamlets, with generally higher concentrations detected at SA–DS and SB. Site A and SB are located on overburden material primarily comprised of a low permeability diamicton (silty clay till), compared to SC which is comprised of diamicton interfingered with high permeability glaciofluvial deposits (sand, gravel) (Figure 2-1) (OGS, 2010).

#### 2.4.1.1 Extent and sources of fecal contamination

In this study, the suite of anthropogenic tracers and FIB provided evidence of fecal contamination. The *E. coli* and BacGen abundances were higher than anticipated, especially at SB with maximum concentrations of  $10^5$  and  $10^6$  C 100 mL<sup>-1</sup> respectively. The abundances of *E. coli* and BacGen at all three sites were comparable to direct sampling results for septic discharge and receiving ponds/lagoons (Knappett et al., 2012; Richards et al., 2016) and aquatic systems affected by wastewater (Schriewer et al., 2010; Lee et al., 2014).

The host-specific *Bacteroides* assays showed that there were elevated BacBov and BacHum abundances at all three sites. BacBov was expected in these areas as agriculture dominates 60–78% of the land-usage (Table 2-1). Surface waters were anticipated to be exposed to fecal bacteria originating from agricultural sources; for example, following application of manure, leaching from manure piles, or livestock-grazing. The prevalence of the BacBov marker observed at SA–DS, SB, and SC are comparable to abundances measured in rural areas in the GRW with counts  $\sim 10^4$ – $10^5$  C 100 mL<sup>-1</sup> (Lee et al., 2010, 2014). There were positive hits of the marker intermittently during the spring and summer months, likely associated with runoff following manure spreading or grazing activities. Previous works observed increased fecal contamination related to agricultural activities (e.g. Marti et al., 2013; Ridley et al., 2014). The DS BacBov abundances were only significantly greater at SA where there were no abundances above the MDL at the US despite an adjacent field, although this field may not have bovine manure applications. This observation, coupled with the lack of significant changes in abundances at SB and SC, strongly indicates that there were agricultural impacts along all three streams during the sampling period.

The human *Bacteroides* marker has been determined a useful tool for assessing fecal contamination in urban areas with WWTPs impacting receiving waters (e.g. Lee et al., 2014), however there is a scarcity of studies using this tool to directly determine septic wastewater impacts. In this work, the BacHum abundances were higher than anticipated ( $10^6$ - $10^7$  C 100 mL<sup>-1</sup>) compared to previous measurements in the GRW ( $\sim 10^5$  C 100 mL<sup>-1</sup>) affected by upstream non-point sources and WWTP effluent (Lee et al. 2014; Marti et al. 2013). The occurrence of this marker at elevated abundances throughout the year at all three sites is highly indicative of domestic wastewater impacting all three streams. Furthermore, there were significantly increasing ( $P < 0.05$ ) abundances at SA and SB and a tendency to increase at SC, which suggests that human-derived contamination increased along the hamlets, and because there were no WWTPs located upstream of these three catchments (Figure 2-1), septic-derived wastewater was identified as the most likely source of this contamination. This finding is congruent with a study by Sowah et al. (2017) that investigated potential impacts of septic systems in rural areas using human-specific *Bacteroides*, although the maximum abundance detected in that study was  $10^3$  C 100 mL<sup>-1</sup>, which is orders of magnitude lower than those obtained in this study. Notably, the BacHum marker was found in samples at SB–US and SC–US, which suggests that the presence of a few homes upgradient from sampling locations may be enough to impact water quality with septic-derived contaminants (Figure 2-1).

Similar trends in concentrations between DS and US were observed in the organic tracer results. With the exception of ACE-K, organic tracer concentrations in this work were generally lower than concentrations reported in previous studies that measured tracers

directly from septic effluent (Conn et al. 2010; Richards et al. 2017a), groundwater septic plumes (Godfrey et al., 2007; Carrara et al., 2008) and waters receiving treated wastewater (Oppenheimer et al., 2011). Maximum concentrations of pharmaceuticals were generally observed at SA–DS (CBZ, NAP, SMX), and SB–US (IBU), and SB–DS (CAF, GEM), which is consistent with the elevated FIB abundances.

Only one pharmaceutical maximum concentration was in the  $\mu\text{g L}^{-1}$  range: IBU,  $\sim 1.2 \mu\text{g L}^{-1}$  at SB–US. This concentration is greater than treated WWTP effluent in the GRW of  $\sim 160 \text{ ng L}^{-1}$  (Liu et al., 2014) and comparable to concentrations downgradient of a septic system in a groundwater plume in Ontario (Carrara et al., 2008). While efforts were made to collect samples with reduced impacts by homes at the US, access to the stream at SB-US left several homes upgradient to the sample site (Figure 2-1). This observation may infer that groundwater septic plumes at SB–US reached the stream prior to complete removal of pharmaceuticals. The consistently low concentrations in this study may be related to low consumption habits of target analytes in these communities or the partial removal of contaminants in groundwater. In a review by Schaidler et al. (2017), removal efficiency for pharmaceuticals (as medians) in septic drain fields were 8% for CBZ, 76% for IBU, and approximately 100% for CAF. Examples of removal mechanisms are sorption (e.g. Conn et al. 2010) and biotransformation (e.g. Stadler and Vela, 2017), although the extent of these removal mechanisms at the field study sites here is unknown.

Contrary to the pharmaceutical concentrations, ACE-K was observed at elevated concentrations similar to those observed in previous studies. For example, Liu et al. (2014) observed concentrations of ACE-K were as high as  $6.5 \mu\text{g L}^{-1}$  in the Grand River, which is in

the same order of magnitude as maximum concentrations measured at SA–DS ( $2.5 \mu\text{g L}^{-1}$ ), SC–US ( $6.9 \mu\text{g L}^{-1}$ ) and SC–DS ( $3.3 \mu\text{g L}^{-1}$ ). Measurements of ACE-K at SB–US and DS were as high as  $54.3$  and  $14.9 \mu\text{g L}^{-1}$ , respectively, which were within the same order of magnitude as seasonal mean concentrations observed in direct septic effluent ( $24\text{--}51 \mu\text{g L}^{-1}$ ) reported in a study by Richards et al. (2016). Previous studies tracking domestic wastewater have reported elevated concentrations of ACE-K compared to other organic tracer concentrations in the environment (Buerge et al., 2009; Graf et al., 2011).

The artificial sweetener and pharmaceutical concentrations exhibited a similar pattern along each stream: the DS sites had elevated concentrations relative to the corresponding US concentrations (Figure 2-9). A study by Richards et al. (2017a) assessed changes in organic tracer concentrations between US and DS of streams impacted by septic effluent, although concentrations were only significantly different at one of two sites studied. Despite the few positive hits for these tracers at SA–US, the consistent trend of significantly greater concentrations ( $P < 0.001$ ) of BacHum and the target organic compounds at SA–DS indicates that there were significant impacts by septic system effluent along the stream. Alternatively, there were multiple instances of positive hits for the target tracers at SB and SC (Figure 2-9). This observation is consistent with the presence of BacHum in these rural headwater streams, which may be impacted by the presence of only a few homes using on-site septic systems. The elevated tracer concentrations located downstream of these two hamlets also strongly suggests that there was likely non-point or point sources reaching the headwaters within the hamlets in addition to the wastewater derived from the homes upgradient to the US sites.

#### 2.4.1.2 Nutrient (P, N) concentrations in rural headwater streams

An understanding of sources of nutrients (P, N) in catchment areas is important to help maintain or mitigate ecosystem health (Withers and Sharpley, 2008). The tracer results in this study revealed that domestic wastewater, likely sourced from septic systems, was present at all three rural hamlets. The indication of domestic wastewater by human-specific tracers may suggest that there are additional nutrient loads reaching these receiving waters in the environment. All three streams were dominated by the dissolved reactive form of phosphorus (SRP), which can trigger eutrophic conditions. The median proportions of TP in the form of SRP in this study were high (63–92%) compared to the range observed in nine rural hamlets in the UK, which had values between 28 and 86% (Jarvie et al., 2010).

The SRP measured at the study sites was between 11.6–1720  $\mu\text{g L}^{-1}$ . The SRP concentrations were lower than those measured in direct septic effluent (Richards et al., 2017) and were more comparable to those measured in receiving waters (Jarvie et al., 2010). Richards et al. (2017) reported direct septic effluent SRP mean concentrations as high as 8.5  $\text{mg L}^{-1}$ , and Jarvie et al. (2010) recorded SRP concentrations as high as  $\sim 1.4 \text{ mg L}^{-1}$  in headwater streams impacted by septic systems and agriculture activities.

The P concentrations increased along the streams at SA and SC, but decreased at SB; however, SB had the most elevated concentrations and exhibited a more pronounced baseflow effect with high concentrations during the summer. Rural headwater streams with low dilution capacity have been previously identified as potentially problematic in areas for eutrophic conditions, especially in areas with high-density septic systems (Jarvie et al., 2010; Withers et al., 2011). Withers et al. (2011) found that nutrient concentrations were

approximately ten times greater in streams with lower dilution, and not just during the summer months.

Domestic wastewater may be contributing to the elevated P concentration in these rural catchment areas. Phosphorus can be derived from both urine and feces, with an estimated production of 0.569 kg person<sup>-1</sup> year<sup>-1</sup> for North Americans (Mihelcic et al., 2011), or in general household waste. In Canada, limits were placed on P concentrations in household detergents, cleaners, dish-washing, and degreasing compounds to help reduce P inputs into the environment indicating these sources may not be of concern. Other potential sources of P in these rural hamlets may be linked to agricultural runoff.

#### **2.4.2 Tracking Nutrients in Surface Waters Using Tracers**

There is difficulty in determining the proportions of P and N sourced from domestic wastewater or from agricultural practices. The selected catchment areas in this study are comprised of densely populated hamlets on lands dominated by agricultural land-use. The capability to track nutrient contributions in the environment would allow regulatory agencies to better recognize and manage anthropogenic-derived sources. In this work, correlation analysis between nutrient concentrations, FIB and selected organic tracers showed that this approach is not effective in distinguishing sources of nutrient inputs in rural headwaters. The correlation results were inconsistent between catchment areas and within each stream.

Significant relationships were rarely observed, and there were incidents of both negative and positive correlations with contradicting patterns. A study reported similar results between CAF and other indicator bacteria and nutrients, with a maximum relationship (*r*) strength of 0.88 with nitrate (Peeler et al., 2006). A more recent study revealed very



strong correlations ( $r$ ) between *E. coli* and SRP (0.95) and between SRP and ACE-K (0.99) at one septic wastewater-impacted site, but only a few less strong correlations at a secondary site (Richards et al., 2017b). The inconsistencies between these studies, and between the three study sites here, may be related to the occurrence of several nutrient sources (natural, agricultural, and anthropogenic) cycling within the environment, while organic tracers are only sourced from wastewater.

An important consideration for nutrient concentrations and forms is the biological uptake processes occurring in the catchment areas. Temporary or permanent nutrient uptake by plants prior to output into surface waters can transform or assimilate nutrients (Gruber and Galloway, 2008; Neilen et al., 2017). Extensive riparian uptake of nutrients in the spring and summer was likely, although the extent of uptake or transformation was not known. In addition, baseflow conditions in receiving waters during the summer have been shown to have elevated sediment pore water SRP concentrations that may affect eutrophication risk downstream (Palmer-Felgate et al., 2010). The variable flow throughout the year may also have affected the degree of nitrification along the stream associated with different residence times (Jarvie et al., 2010). Overall, nutrient cycles are quite complex and difficult to characterize.

As previously discussed, the sources of the selected suite of tracers including BacHum were likely sourced from multiple homes, further complicating the relationship between these tracers and nutrients. The findings in this work indicated that annual non-point source inputs in rural hamlets from domestic waste and agricultural practices may both be dominating nutrient loads during different times and events. The sole use of nutrient and

organic tracer concentrations without any other catchment information is not recommended to track or quantify domestic wastewater contamination in rural headwaters. Ultimately, the complex relationships between the tracer and nutrient concentrations may be partially related to the variable physical pathways affecting transport within the environment.

### **2.4.3 Potential Pathways for Wastewater Contamination in the Environment**

There was evidence at all three hamlets of both agricultural runoff (e.g. fertilizers, manure spreading) and domestic wastewater inputs (e.g. septic systems). Environmental agencies are currently concerned with mitigating contamination associated by agricultural practices in Ontario (e.g. IJC, 2018). Other than nutrient impacts, septic systems have been identified as potentially problematic sources of micropollutants, including ones selected for this study (e.g. ACE -K, *E. coli*) (Buerge et al., 2011; Conn et al., 2011). In this work, potential pathways and triggers were identified including incomplete or poor attenuation of contaminants, high-permeability preferential flow paths, and effects of high flow events.

Septic systems and associated drain fields are designed to adequately attenuate contaminants related to domestic wastewater prior to re-introduction into the groundwater system. However, previous work sampling septic plumes found that there was frequent inadequate attenuation of some contaminants. For example, pharmaceutical compounds (GEM, IBU, NAP) have been shown to persist in plumes where the septic design does not favor target oxidation-reduction zones (Carrara et al., 2008). ACE-K has been noted as relatively resistant to biodegradation processes in septic plumes, and is considered an ideal tracer of septic plumes (Stempvoort et al. 2011). One study measured ACE-K concentrations in distal plume groundwater and found that the tracer persisted for at least 15 years

(Robertson et al., 2013). The ubiquitous occurrence and persistence of ACE-K within the environment may explain the elevated concentrations measured in this study compared to the suite of pharmaceutical compounds. Overall, the occurrence of these tracers in surface water systems, as observed at all three study sites, particularly in elevated concentrations at the DS sites, may be indicative of incomplete attenuation, and elevated septic system contaminant loading in rural communities, which would also affect nutrient cycles/forms (i.e. incomplete nitrification, incomplete P sorption).

In Ontario, the minimum septic system separation distance from surface waters is currently 15 m (O.Reg. 332/12, Building Code), but previous septic plume monitoring studies have noted incomplete immobilization of P or inadequate nitrification at distances exceeding this benchmark distance: relatively elevated concentrations of P have been noted at 20 m downgradient (Ptacek, 1998) and up to 70 m away from the septic bed at concentrations between 0.3 and 2 mg L<sup>-1</sup> (Robertson and Harman, 1999). The homes in these catchments are frequently situated along the banks of the streams (Figure 2-1), and there could be elevated concentrations of P reaching these surface water streams in this study as well. Although there was difficulty in determining the sources and fate of nutrients within the selected catchment areas, the presence of elevated human-specific *Bacteroides* (BacHum) at all sites, which does not transport well through the subsurface, suggests that there may have been incomplete attenuation of contaminants prior to reaching surface waters. The presence of pharmaceuticals within the wastewater may have also inhibited removal of *E. coli*, which was previously observed in sand filtration beds where the addition of pharmaceutically active compounds decreased *E. coli* removal from 95% to 20% (Alessio et al., 2015). In this study,

BacHum, *E. coli*, and organic tracers were not as elevated at SC compared to SA–DS and SB. This could either be related to the higher density or closer proximity of homes to the streams at SA and SB, or perhaps related to hydrogeological differences that may have led to incomplete attenuation or provided preferential flow pathways for the contaminants (at SA and SB).

The study areas were selected for comparison based on their varying hydrogeological conditions. The contaminants were observed at higher concentrations at SA–DS and at SB, which were notably found in areas comprised of finer overburden material compared to SC (Figure 2-1). A field study assessing the survival of fecal indicator bacteria sourced from septic effluent found that *E. coli* and other FIB were relatively stable in groundwater (Bitton et al., 1983). In a coarse-grained aquifer (sand-gravel), *E. coli* has been traced 920 m away from the source, and was recommended as a tool for tracking wastewater in coarser sediments (Sinton, 1980). Filtration is an important mechanism for the removal of bacteria in coarser-grained environments (Pang et al., 2005), and sorption for more fine-grained sediments (Oliver et al., 2007). The presence of FIB and select organic tracers in the streams at SA and SB implied relatively quick transport within the fine overburden material and incomplete sorption to soil particles.

Another physical mechanism that may affect residence time and extent of natural attenuation is the presence of either natural or anthropogenically derived preferential flow paths. Soil macro pores (e.g. fissures, roots, cracks) in the vadose zone may result in flow by-pass as the wastewater quickly percolates into the groundwater (Beven and Germann, 1982). This phenomenon was also discussed in a study that observed transport of *E. coli* through

clay soils, which led to the discussion of macro pores limiting sorption on clay surfaces (Aislabie et al., 2001). Therefore, a possible reason for the presence of these organic tracers and FIB at elevated concentrations at SA and SB may be linked to the presence of macro pores within the fine-grained overburden allowing for rapid transport to the stream directly through these connections.

The introduction of underground infrastructure including domestic wells, pipe systems, and storm drains involves trenching and backfilling, usually with coarser grained material which may act as a high permeability zone (e.g. Sharp, 2010). This mechanism is more frequently studied in urban settings where densely interconnected networks are expected to influence contaminant transport (*see* Bonneau et al., 2017). The introduction of storm drains and tile drains within a watershed may provide lateral conduits for groundwater and contaminants to travel to stream networks (Figure B-8) (Kaushal and Belt, 2012). A study tracing septic effluent in mixed glacial overburden observed 80% of the effluent was transported along a preferential flow pathway along the septic tank wall located in sandy clay loam soil, which provided a pathway for *E. coli* to transfer to groundwater prior to attenuation (Sinton, 1986).

In the studied hamlets, the closely spaced homes with silty clay till soils, near the streams, may have resulted in preferential flow paths for the contaminants. This may be a reason why SA and SB have more contamination compared to SC, which has less densely spaced homes and lower clay content near the stream. In SA and SB, drainage tiles were commonly seen running during times of low flow, which may have been a means for septic contamination to further bypass soil and provide direct transport to the streams. This was

especially probable at SA–US where there were instances of elevated tracers likely associated with mixing with a nearby storm drain: during high flow events at SA–US there was elevated BacHum coupled with elevated ACE-K concentrations, the occurrence of the only positive NAP hit, and IBU concentrations five times greater than the median specified contamination. Additionally, water percolating from and around a storm drain (SD) situated between the US and DS sampling locations at SB was periodically sampled (Figure 2-10). Expectedly, there were elevated measurements of SPC, TS, Na, and Cl which may have been related to road salt application and airborne transport of dust/soil particles. The nutrient SRP and  $\text{NH}_{3+4}\text{-N}$  concentrations were consistently lower than the US and DS sites; however, there was elevated BacHum and ACE-K concentrations from the SD which suggests that there may be a connection to a septic drain field. These observations showed that these human-derived preferential flow paths may be problematic in areas with densely situated septic systems.

In this work, there were instances of both minimum and maximum site-specific concentrations measured during either the HRE or the HFE. Instances of minimal concentrations during these events were attributed to either well designed and maintained septic systems or alluded to the presence of direct discharges. High rainfall or snowmelt associated with high flow may be raising water tables high enough to interfere with drain field mechanics. A mine tailings study by Blowes and Gillham (1988) suggested that capillary fringe effects may be responsible for quick rises in water tables that increase groundwater recharge to streams. The tracer concentrations were not always diluted

compared to annual medians, which suggests that there were greater impacts during these high flow events partly due to do capillary fringe effects.

#### **2.4.4 Evaluation of a Combined Tracer Approach**

A combined tracer approach has been recommended for detecting fecal contamination in ground and surface waters (Liu et al., 2014; Richards et al., 2017). In this work, a comprehensive suite of tracers was used: host-specific FIB, an artificial sweetener, and six pharmaceuticals. The human *Bacteroides* marker is unique to the human gut and is excreted in fecal waste. Artificial sweeteners are commonly used as synthetic dietary replacements for sugar in beverages such as coffee and diet colas, in consumer products such as candy and toothpaste, and pass through the human digestive system relatively unchanged. The widely-used stimulant CAF is found in a variety of beverage products such as carbonated drinks, tea, coffee, and energy drinks, and in food products containing chocolate. The suite of pharmaceuticals in this study included three easily accessible over the counter drugs (GEM, IBU, NAP) and two that required a prescription (CBZ, SMX). Previous research studies have used different combinations of tracers including artificial sweeteners, pharmaceuticals, trace metals, Cl, and FIB, but this is the first study using this specific suite to test for domestic wastewater in surface waters (Peeler and Opsahl, 2006; Van Stempvoort et al. 2013; Richards et al. 2017b). One aim of this study was to assess the usefulness of the selected tracers and recommend a tracer combination for future studies because the use of multiple tracers to establish fecal contamination can be both expensive and time consuming.

Source-specific tracers are recommended to show domestic wastewater in surface waters. In this work, general fecal indicator bacteria such as *E. coli* and BacGen were

correlated at some sites between 0.56 and 0.71, which was anticipated as they both originate from a broad range of non-host-specific fecal sources. Previous work identified similar correlations between *E. coli* and BacGen as well (Lee et al., 2014; Knappett et al., 2012). For example, Knappett et al. (2012) reported a Spearman Rank Order Correlation coefficient ( $\rho$ ) between *E. coli* and BacGen in a receiving pond equal to 0.69, and Lee et al. (2014) detected a correlation range of 0.45 to 0.67 for the Grand River. On their own, *E. coli* and BacGen are not useful in discriminating between fecal sources nor to determine cumulative impacts along streams. For example, at SB, the statistical analysis showed that there was a significant decrease in *E. coli* and BacGen abundances along the stream, but a statistically significant increase in BacHum (Figure 2-8).

In this study, the use of microbial source tracking techniques also helped infer the presence of domestic wastewater inputs and farming-related fecal contamination in the streams; however, the proportions of BacGen identified as the host-specific markers BacHum and BacGen were generally low (Figure B-3). This observation suggests that there were other sources of fecal contamination that were not accounted for, such as other livestock commonly found in these rural areas including horses, swine, along with wildlife and domestic pets. Previously, markers for muskrat, pig, and Canada goose have been prevalent in microbial source tracking studies in eastern Ontario rivers (Marti et al., 2013). Despite the generally low proportions for the markers, there were incidents of the BacBov marker present at concentrations greater than 100% (e.g. 230%) which highlights a limitation of the method.

Although the suite of organic tracers is considered human-specific, there have been instances of artificial sweeteners and pharmaceuticals used in the farming industry. For



example, the common artificial sweetener saccharin has previously been found in pigfeed lots (Buerge et al., 2011), although there is no current information on the use of ACE-K in the agricultural industry in Canada. Additionally, the pharmaceutical SMX has been used in veterinary medicine and found within the environment (e.g. Baydan et al., 2015), although it is unknown whether this particular pharmaceutical is being used to treat the animals in the selected catchments. To help minimize uncertainty in interpretation, further research should include sampling of manure in nearby farms to provide background concentrations of organic compounds. There are limitations with microbial source-tracking and the use of organic tracers, but this study exemplifies the usefulness of using human-specific *Bacteroides* (BacHum) as a human wastewater indicator.

A suitable tracer should be present in concentrations that can be detected using the analytical method. Sampling surface waters impacted by multiple non-point sources may not provide elevated concentrations, nor have consistent proportions of each organic compound. Therefore, tracer concentrations were generally lower than those reported in WWTP studies where there was an emphasis on selecting target compounds that were consumed at a generous rate to be detected in the environment (e.g. Spoelstra et al., 2013; Liu et al., 2014). The lifestyle drug CAF was detected in all samples and has also been previously proposed as a domestic wastewater tracer (Buerge et al., 2003). Previous studies have also reported the presence of CAF but have argued that it may not be an ideal tracer compared to other pharmaceuticals due to the tendency to contaminate field and laboratory blanks (Dickenson et al., 2010).

The second most observed organic tracer was ACE-K which was detected at concentrations one to three orders of magnitude higher than the other organic tracers. The sweetener ACE-K has previously been proposed as an ideal tracer for domestic wastewater effluent due to its conservative behavior in ground and surface waters (Buerge et al., 2009; Liu et al., 2014; Robertson et al., 2013; Stempvoort et al., 2011b) . Furthermore, the analysis of ACE-K was also less-time consuming compared to the pharmaceuticals which required a labor-intensive solid phase extraction step during sample preparation. The use of IC-MS/MS analytical methods instead of LC-MS had its drawback in the study: the surface water samples were diluted to reduce matrix interference which doubled the MDL to 140 ng L<sup>-1</sup>, which is orders of magnitude greater than the pharmaceutical MDLs. In this work, the higher MDL presented an issue for samples collected during the HRE and HFE. For example, during high flow, SB-US and SC ACE-K concentrations were less than the MDL, but that did not mean that they were not present at relevant concentrations compared to the remaining pharmaceuticals, just that they were not equal or greater to 140 ng L<sup>-1</sup>. Therefore, it is recommended to select at least one target analyte that has a low MDL to increase confidence in the results.

The less frequently detected overall tracers GEM, NAP, and IBU were not necessarily “bad” tracers, but were generally more site-specific than the others. For example, at SA-DS, these organic compounds were greater than their MDLs in 88%, 100%, and 76% of the samples respectively. At SB, GEM was detected the least frequently (29%), but the next least detected analyte was IBU, which was detected three times more often (88%). At SC, these compounds were not frequently detected, with hits between 19-50% which affected the

overall assessment of these target tracers. Overall, SC was characterized by the lowest concentrations of tracers and the lowest frequency of samples with concentrations greater than the MDLs. The effect of site-specific differences in tracer concentrations was reflected by the correlation analysis results.

A correlation analysis between the selected suite, including the FIB not specific to human waste (*E. coli*, BacGen, BacBov), revealed limited correlations between tracers and presented inconsistent relationships between sites (Table 2-3). However, other studies using tracers to track WWTP effluent DS have found very strong correlations between tracers (Liu et al. 2014; Scheurer et al. 2011). For example, Liu et al. (2014) reported a  $\rho$ -value of 1.00 between GEM and NAP in the Grand River impacted by wastewater treatment plant effluent.

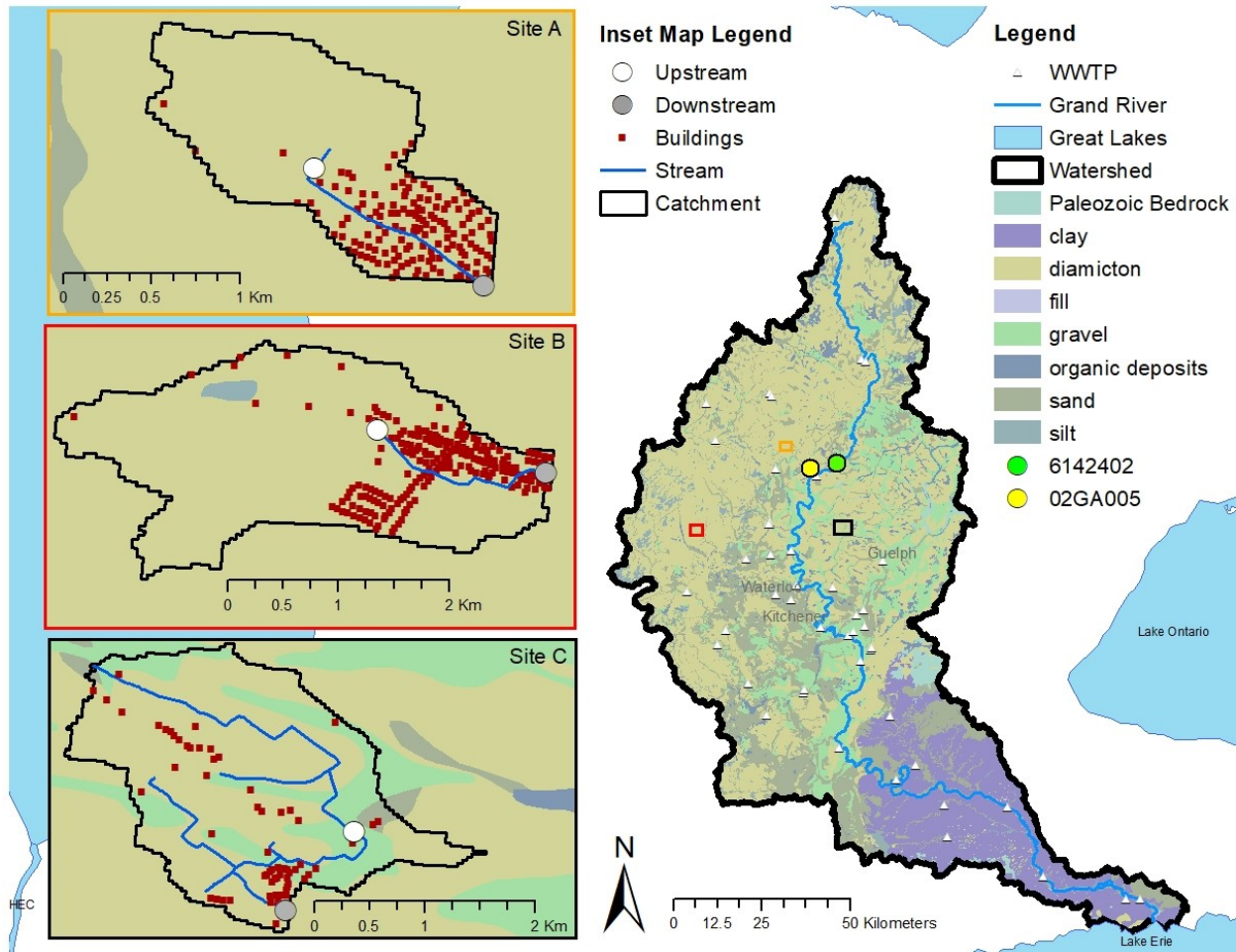
In this study, the strongest significant correlation calculated was 0.78 between IBU and NAP at SC. One reason the correlations may not be as strong between tracers is because there is not one individual contaminant source, but cumulative sources along each stream. The tracer-tracer correlation analysis also showed that ACE-K, CBZ, and SMX show potential as co-tracers at SA, and ACE-K, IBU, and NAP at SB. To eliminate unnecessary analyses and to ascertain consistent hits of organic tracers within rural hamlets, a reconnaissance of the study population's consumption rates and habits is recommended prior to initiating a more detailed study. Overall, BacHum, ACE-K, and the selection of a pharmaceutical such as CBZ or GEM, are suitable as co-tracers in these rural hamlets for establishing the occurrence of domestic wastewater influences in surface waters.

## 2.5 Conclusions

The field study investigated three rural hamlets and found evidence of domestic wastewater contamination year-round, including baseflow in the summer and during high flow events caused by heavy rainfall and snowmelt. The observations suggest that rural hamlets along streams are at higher risk for contamination from domestic wastewater and more studies are warranted in this area. This study suggests that there may be more extensive contamination in high-density hamlets located on finer grained overburden material, such as silty clay tills, due to natural or anthropogenic preferential flow paths. Septic systems may be an underestimated source of contamination in rural hamlets dominated by agricultural activities. Many factors should be considered when studying rural catchments, including dwelling density, location and age of septic systems, hydrogeological conditions, effect of preferential flow pathways, and agricultural activities. Ultimately, it was difficult to discern between the main influencers of the contamination without additional information.

Tying nutrient concentrations back to their sources using a suite of tracers is complex. When considering the source, frequency of detections, concentration patterns, and statistical analyses at each site individually, the following observations were made: (1) BacHum was the most reliable indicator of domestic wastewater impacts; (2) ACE-K was detected at the most elevated concentrations compared to the pharmaceuticals; (3) and each hamlet had a unique set of domestic wastewater signatures. A better approach for future work should include a reconnaissance of the location of septic systems, human consumption rates of selected tracers, and more information on groundwater flow paths. This study supported the

combined-tracer approach, and the human specific *Bacteroides* coupled with a conservative tracer ACE-K are recommended as co-tracers for studies in rural areas.



\*Map created using ArcMap (v.10.6.1); base map (Great Lakes) obtained from Esri; Quaternary geology overburden map layer obtained from the Ontario Geological Survey (OGS); Grand River Watershed boundary shapefile, Grand River shapefile (manipulated), and WWTP points obtained from Grand River Conservation Authority (GRCA); catchment zones delineated using Ontario Flow Assessment Tool (OFAT); and streams and buildings were manually selected using Google Earth satellite imagery

**Figure 2-1** – Map of the study sites (inlet maps) within the Grand River Watershed as Site A. (top, orange), Site B (middle, red), and Site C (bottom, black). Catchment areas were delineated and streams, sample sites (stars), and buildings (red squares) were overlaid on an overburden map\*. The main map (right) of the Grand River Watershed includes the main channel, the Grand River, which discharges into Lake Erie, and WWTPs within the watershed were overlaid (triangles) to show the placement relative to the inlet maps.

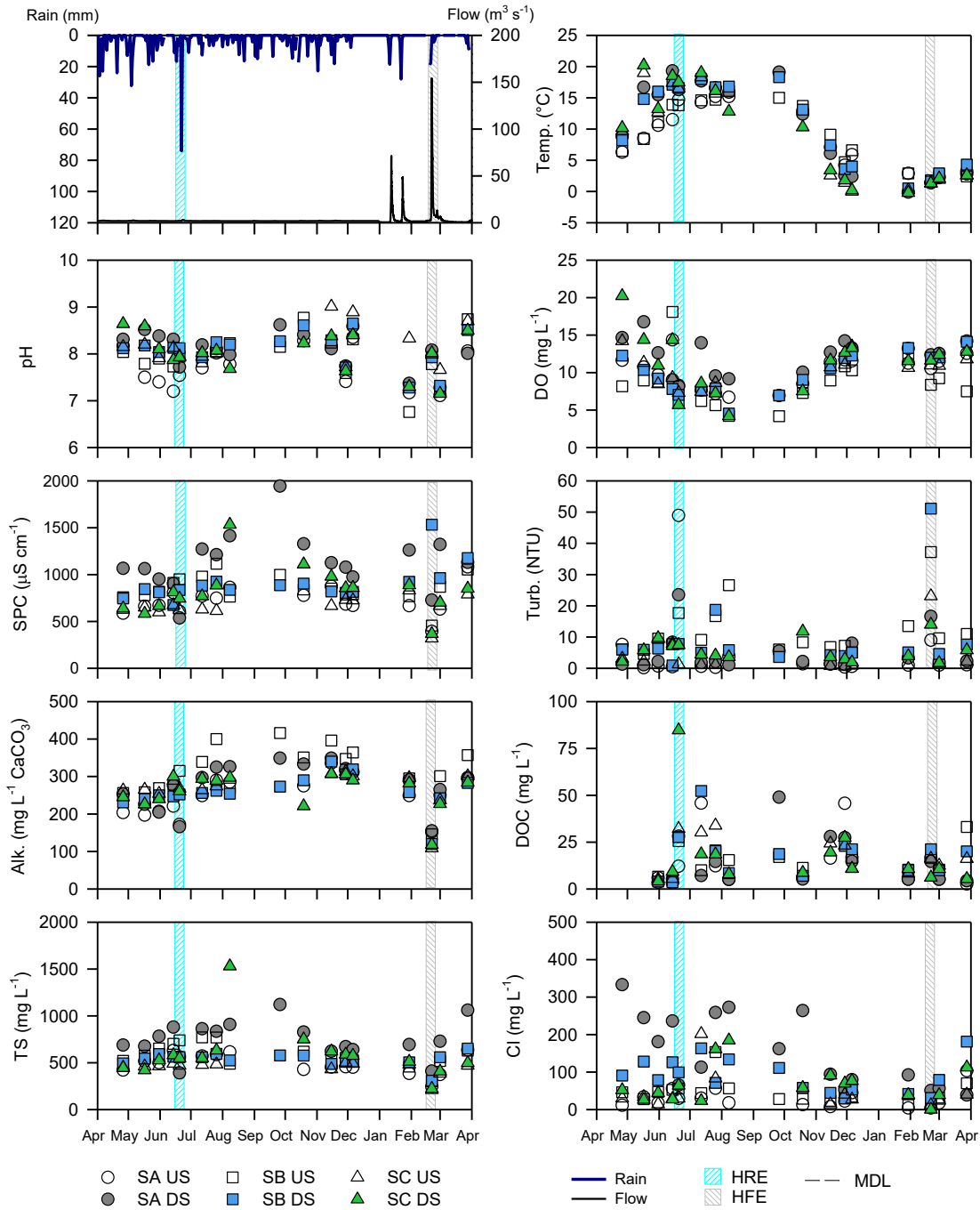


**Figure 2-2** - Spatial-temporal multiple line plots of annual fluctuations in rain (mm) and flow ( $m^3 s^{-1}$ ) between April 1, 2017 and March 31, 2018, followed by multiple scatter plots of annual data for Site A (SA) upstream (US), SA downstream (DS), SB-US, SB-DS, SC-US, and SC-DS, for: temp., pH, DO, SPC, turb., alk., DOC, TS, and Cl. The high rainfall event (HRE) and high flow event (HFE) are highlighted on all the plots.

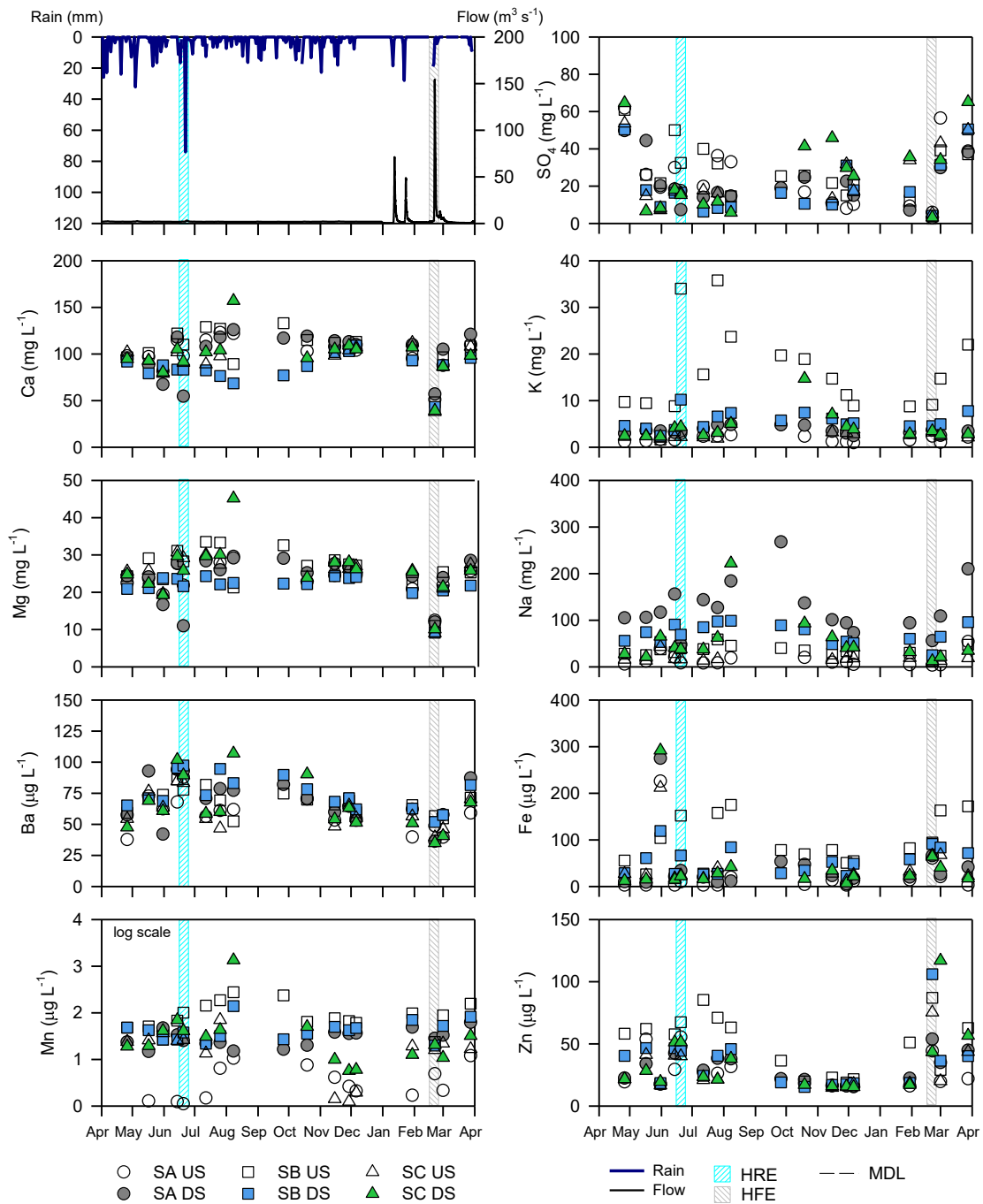


**Figure 2-3** - Spatial-temporal multiple line plot of annual fluctuations in rain (mm) and flow ( $\text{m}^3 \text{s}^{-1}$ ) between April 1, 2017 and March 31, 2018, followed by multiple scatter plots of annual data for Site A (SA) upstream (US), SA downstream (DS), SB US, SB DS, SC US, and SC DS, for:  $\text{SO}_4$ , Ca, K, Mg, Na, Ba, Fe, Mn, and Zn. The high rainfall event (HRE) and high flow event (HFE) are highlighted on all plots. The Mn plot is displayed as a log scale (exponents are shown).



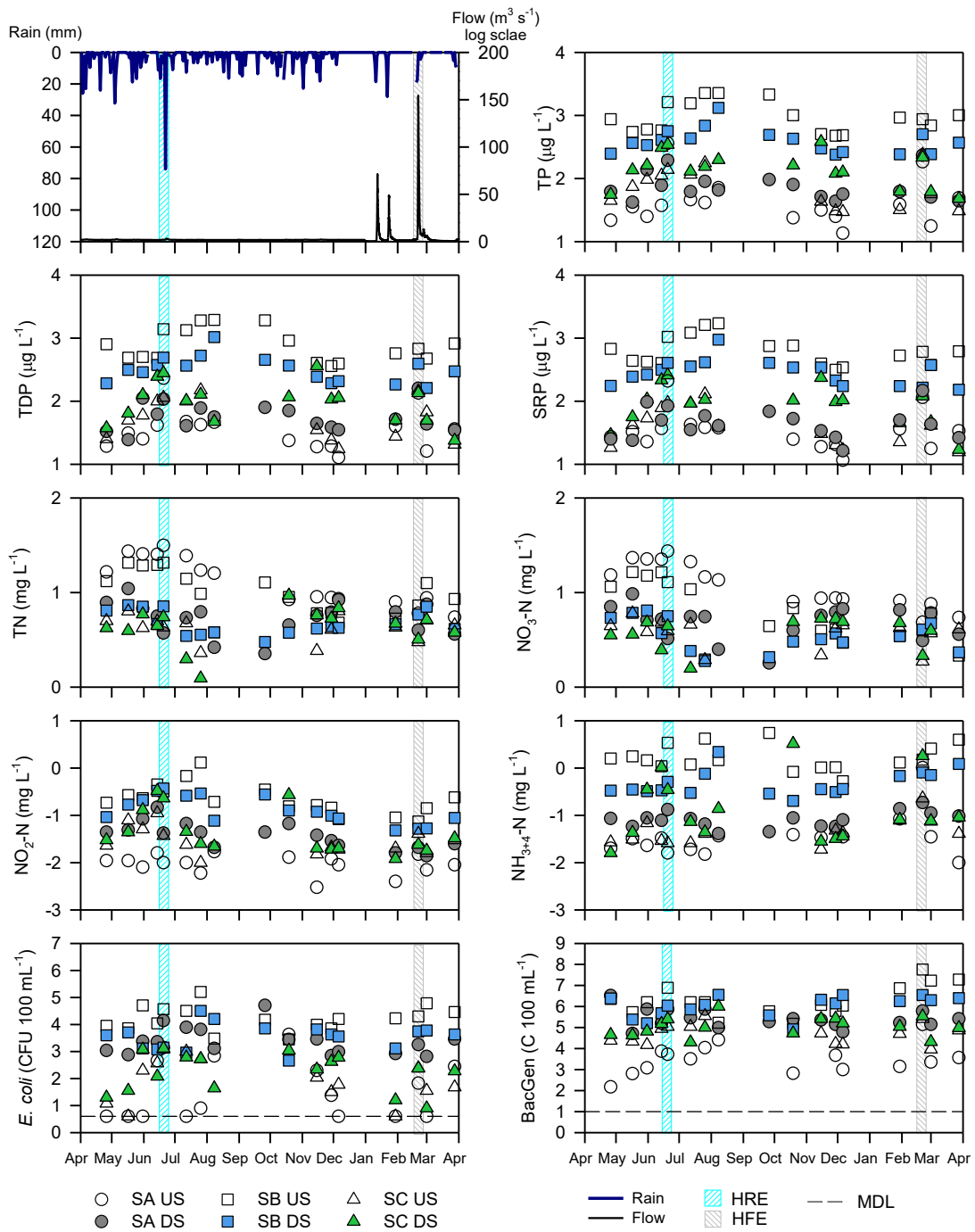


**Figure 2-4** - Spatial-temporal multiple line plot of annual fluctuations in rain (mm) and flow ( $m^3 s^{-1}$ ) between April 1, 2017 and March 31, 2018, followed by multiple scatter plots of annual data Site A (SA) upstream (US), SA downstream (DS), SB US, SB DS, SC US, and SC DS for: TP, TDP, SRP, TN,  $NO_3-N$ ,  $NO_2-N$ ,  $NH_{3+4}-N$ , *E. coli*, and BacGen. The high rainfall event (HRE) and high flow event (HFE) are highlighted on all the plots. Note all parameter scales are displayed as log (exponents are shown). Dashed line represents the MDLs for *E. coli* and BacGen.

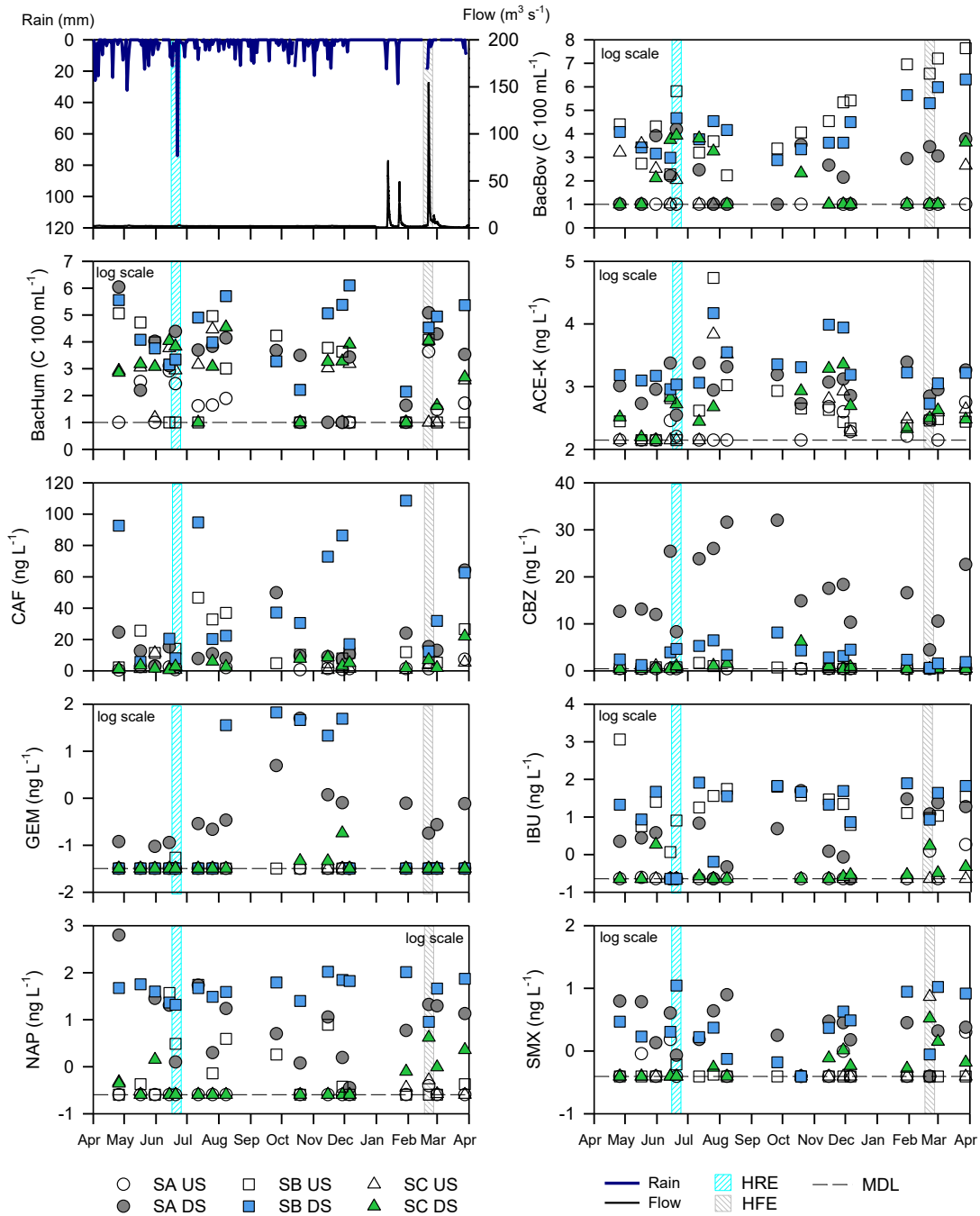


**Figure 2-5** - Spatial-temporal multiple line plot of annual fluctuations in rain (mm) and flow ( $\text{m}^3 \text{s}^{-1}$ ) between April 1, 2017 and March 31, 2018, followed by multiple scatter plots of annual data for Site A (SA) upstream (US), SA downstream (DS), SB US, SB DS, SC US, and SC DS for: BacBov, BacHum, ACE-K, CAF, CBZ, GEM, IBU, NAP, and SMX. The high rainfall event (HRE) and high flow event (HFE) are highlighted on all the plots. Scales are log (exponents are shown) except for CAF and CBZ plots. Dashed lines represent the calculated MDLs for all target FIB and tracers.

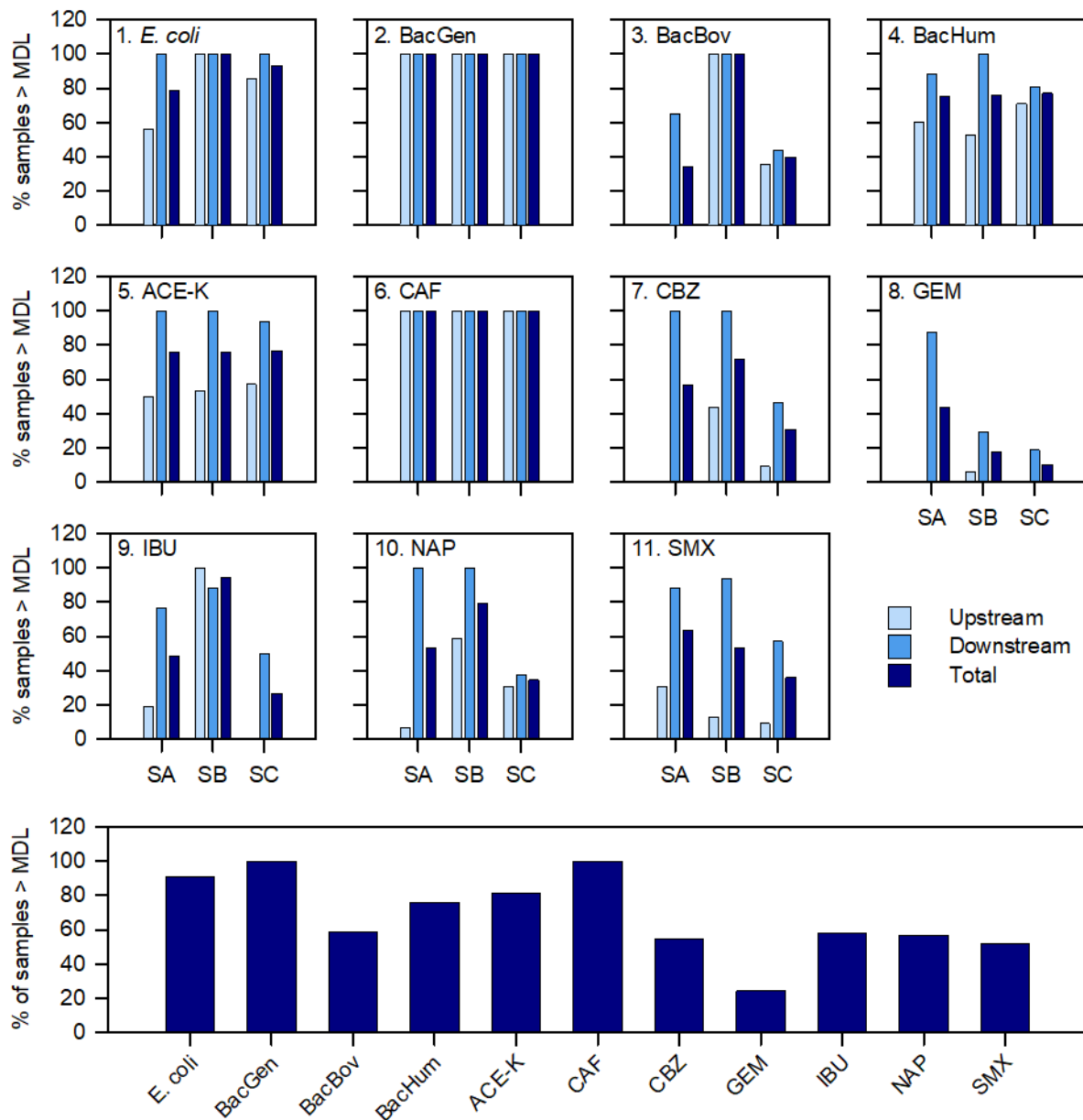


**Figure 2-6** - Bar graphs showing the frequency of detection (% samples > MDL) of the target compounds 1. *E. coli* (> 4 CFU 100 mL<sup>-1</sup>), 2. BacGen (> 10 C 100 mL<sup>-1</sup>), 3. BacBov (> 10 C 100 mL<sup>-1</sup>), 4. BacHum (> 10 C 100 mL<sup>-1</sup>), 5. ACE-K (> 140 ng L<sup>-1</sup>), 6. CAF (> 0.162 ng L<sup>-1</sup>), 7. CBZ (> 0.438 ng L<sup>-1</sup>), 8. GEM (> 0.032 ng L<sup>-1</sup>), 9. IBU (> 0.228 ng L<sup>-1</sup>), 10. NAP (> 0.254 ng L<sup>-1</sup>), and 11. SMX (> 0.394 ng L<sup>-1</sup>) over the course of the sampling period between April 21, 2017 and March 31, 2018 at Site A (SA), Site B (SB), and Site C (SC) at the upstream (US), downstream (DS). The final bar graph displays the combined (SA+SB+SC) % of sample frequency > MDL for all 11 target compounds.

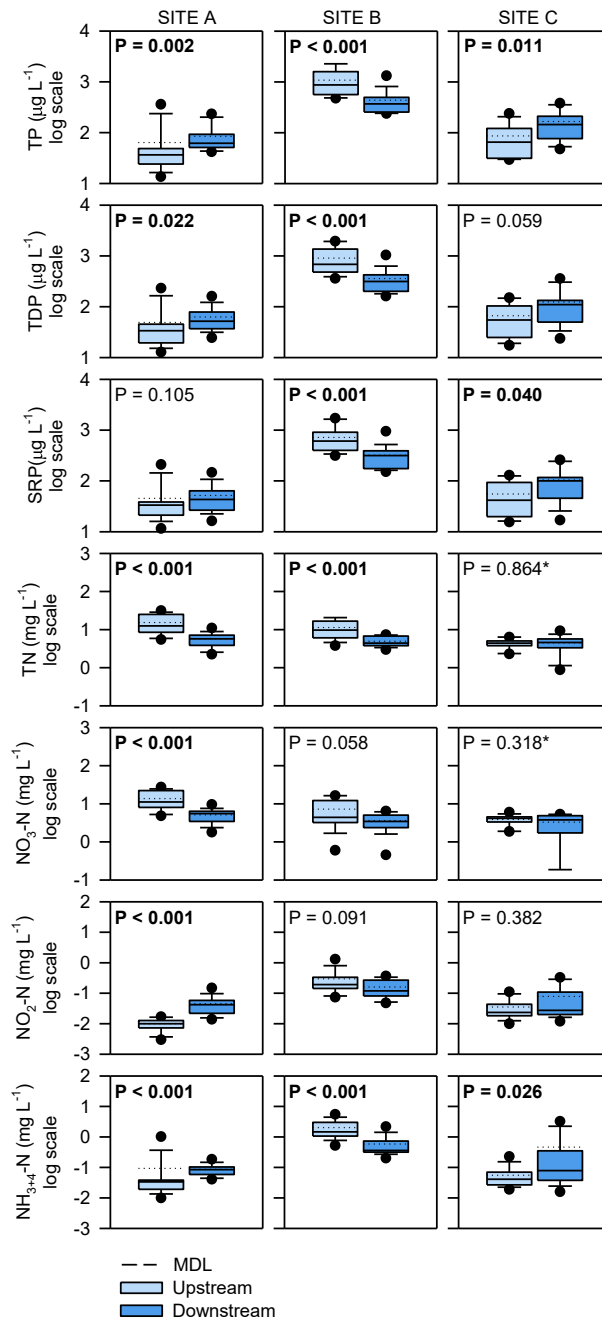


**Figure 2-7** - Box and whisker plots displaying a statistical analysis of the annual concentrations of the nutrients TP, TDP, SRP, TN, NO<sub>3</sub>-N, NO<sub>2</sub>-N, and NH<sub>3+4</sub>-N at Sites A, B, and C upstream and downstream sites. The points represent outliers in the dataset and the dotted and solid lines represent the mean and median respectively. The P-values for the Mann Whitney Rank Sum Order tests are displayed on each graph, and the results obtained from a student's t-test are marked with an asterisk (\*). N values vary and may be found in Appendix B. Bolded P-values are statistically significant (P < 0.05). Note that the y-axes are in log scale (exponents shown).

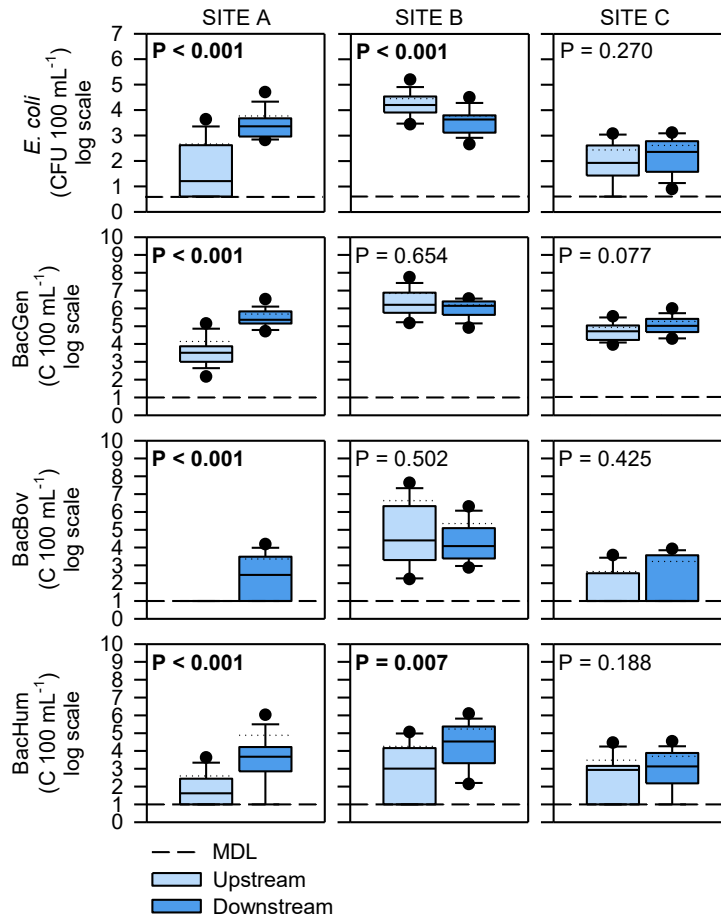


**Figure 2-8** - Box and whisker plots displaying a statistical analysis of annual concentrations of the FIB *E. coli*, BacGen, BacBov, and BacHum at Sites A, B, and C upstream and downstream sites. The points represent outliers in the dataset and the dotted and solid lines represent the mean and median respectively. The MDLs are shown using dashed lines. The P-values for the Mann Whitney Rank Sum Order tests are displayed on each graph, and the results obtained from a student's t-test are marked with an asterisk (\*). N values vary and may be found in Appendix B. Bolded P-values are statistically significant ( $P < 0.05$ ). Note that the y-axes are in log scale (as exponents).

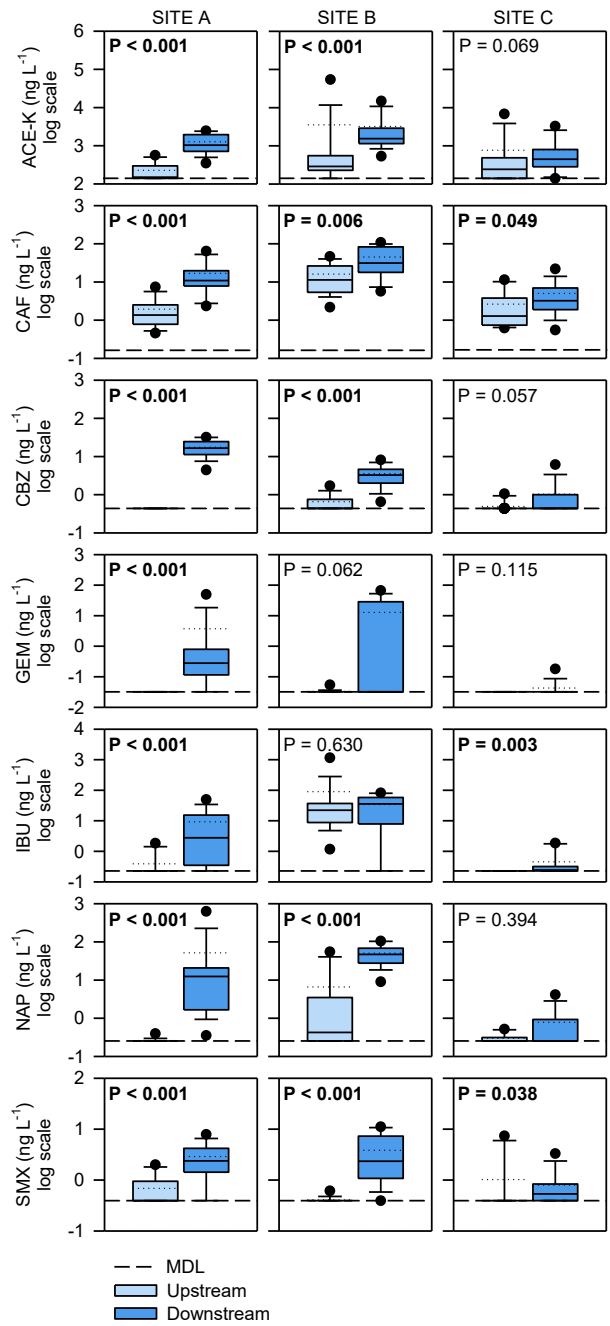


**Figure 2-9** - Box and whisker plots displaying a statistical analysis of the annual concentrations of the artificial sweetener ACE-K, and pharmaceuticals CAF, CBZ, GEM, IBU, NAP, and SMX at Sites A, B, and C upstream and downstream sites. The points represent outliers in the dataset and the dotted and solid lines represent the mean and median respectively. The MDLs are shown using dashed lines. The P-values for the Mann Whitney Rank Sum Order tests are displayed on each graph, and the results obtained from a student's t-test are marked with an asterisk (\*). N values vary and may be found in Appendix B. Bolded P-values are statistically significant ( $P < 0.05$ ). Note that the y-axes are in log scale (as exponents).

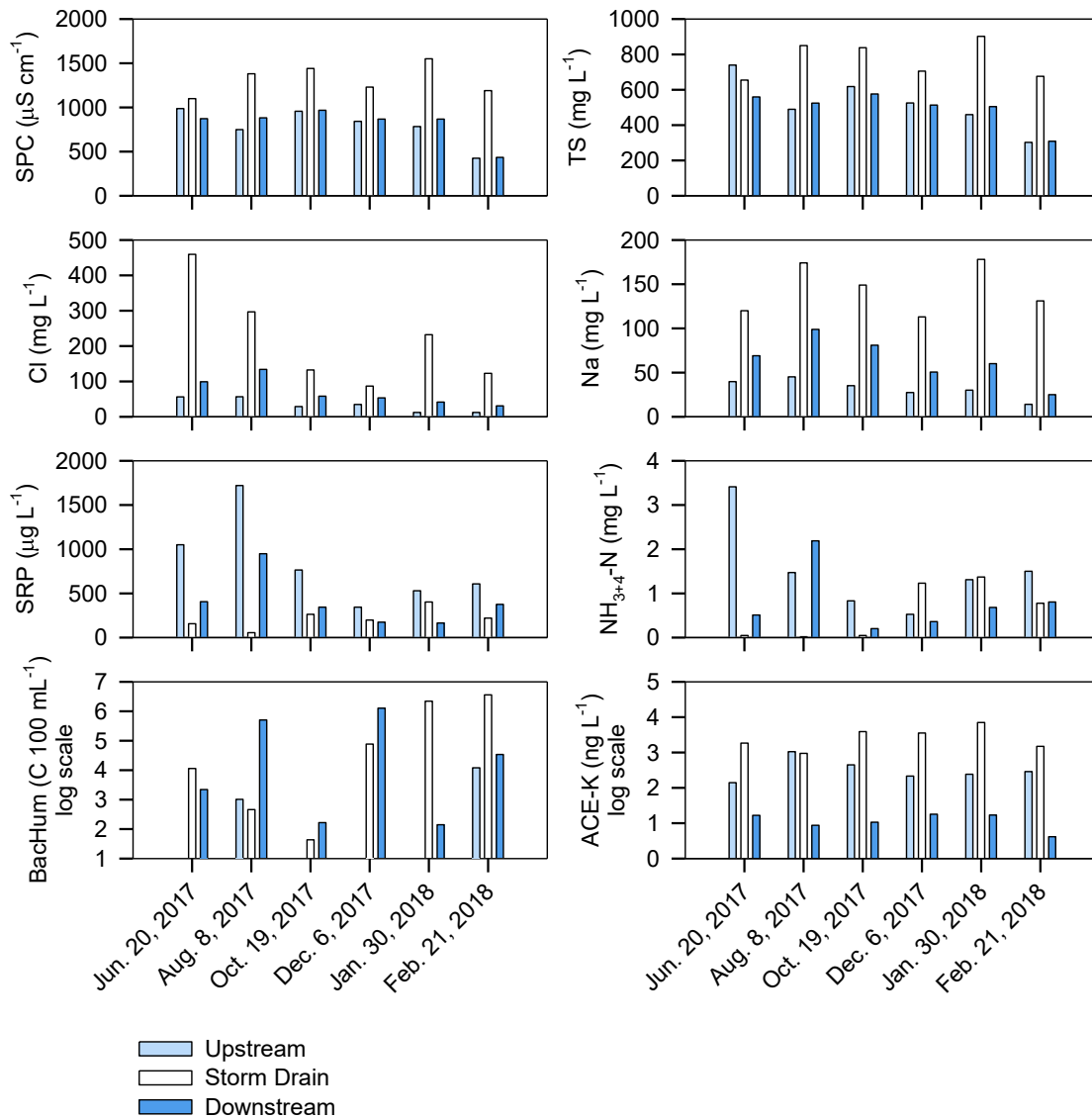


**Figure 2-10** - Bar graphs of the measurements or concentrations of specific conductance (SPC), total solids (TS), chloride (Cl), sodium (Na), soluble reactive phosphorus (SRP), ammonia and ammonium-nitrogen ( $\text{NH}_{3+4}\text{-N}$ ), BacHum, and ACE-K at the upstream, storm drain, and downstream sites at Site B over six sampling occasions between June 20, 2017 and February 21, 2018. Note that some data are displayed using a log scale (exponents shown).

**Table 2-1** - Land-use information (drainage, lakes, and wetland area; % agricultural or domestic; dwelling size), hydrometric information (annual temperature/precipitation), and hydrogeological characterization (overburden thickness, dominant material, and permeability) of Site A, Site B, and Site C. The number of buildings (including homes) was manually determined using Google Earth satellite imagery.

<b>Characteristic</b>	<b>Site A</b>	<b>Site B</b>	<b>Site C</b>
Drainage area (km <sup>2</sup> ) <sup>a</sup>	1.16	2.30	3.69
Lakes (km <sup>2</sup> ) <sup>a</sup>	0.00	0.00	0.00
Wetlands (km <sup>2</sup> ) <sup>a</sup>	0.00	0.00	0.24
Agricultural (%) <sup>a</sup>	60	71	78
Domestic/infrastructure (%) <sup>a</sup>	39	25	5
Dwelling size (persons home <sup>-1</sup> ) <sup>b</sup>	3.4	2.8	2.8
Homes/buildings	146	216	64
Annual mean temperature (°C) <sup>a</sup>	6.3	6.9	6.8
Annual precipitation (mm) <sup>a</sup>	953	984	909
Avg, overburden thickness (m) <sup>c</sup>	65	20	28
Overburden material <sup>c</sup>	clay	clay and silt	sandy silt
Permeability <sup>c</sup>	low	low	medium

<sup>a</sup>Ontario Flow Assessment Tool (OFAT); <sup>b</sup>Statistics Canada; <sup>c</sup>Ontario Geological Survey (OGS)



**Table 2-2** - Spearman Rank Order statistical test results for correlation coefficients ( $\rho$ ) obtained for Site A (SA), Site B (SB), and Site C (SC) upstream (US) and downstream (DS). Only significant ( $P < 0.05$ )  $\rho$  values are tabulated (bolded) between the nutrients TP, TDP, SRP, TN, NO<sub>3</sub>-N, NO<sub>2</sub>-N, and NH<sub>3+4</sub>-N and the FIB/tracers *E. coli*, BacGen, BacBov, BacHum, ACE-K, CAF, CBZ, GEM, IBU, NAP, and SMX. NS: not significant. The results were interpreted as: 0.2–0.4 = weak, 0.4–0.6 = moderate, and 0.6–0.8 = strong.

		TP		TDP		SRP		TN		NO <sub>3</sub> -N		NO <sub>2</sub> -N		NH <sub>3+4</sub> -N	
		US	DS	US	DS	US	DS	US	DS	US	DS	US	DS	US	DS
<i>E. coli</i>	SA	NS	<b>0.56</b>	NS	<b>0.48</b>	NS	NS	NS	<b>-0.62</b>	NS	<b>-0.63</b>	NS	NS	NS	NS
	SB	NS	NS	NS	NS	NS	NS	NS	NS	NS	NS	NS	NS	NS	<b>0.50</b>
	SC	<b>0.68</b>	NS	<b>0.69</b>	<b>0.57</b>	<b>0.70</b>	<b>0.60</b>	NS	NS	NS	NS	NS	<b>0.50</b>	NS	NS
BacGen	SA	<b>0.72</b>	<b>0.59</b>	<b>0.69</b>	NS	<b>0.64</b>	<b>0.49</b>	NS	NS	NS	NS	NS	NS	NS	NS
	SB	NS	NS	NS	NS	NS	NS	NS	NS	NS	NS	NS	<b>-0.69</b>	NS	<b>0.72</b>
	SC	<b>0.64</b>	<b>0.50</b>	<b>0.62</b>	NS	<b>0.61</b>	NS	NS	NS	NS	NS	NS	NS	NS	NS
BacBov	SA	--	NS	--	NS	--	<b>0.49</b>	--	NS	--	NS	--	NS	--	<b>0.76</b>
	SB	NS	NS	NS	NS	NS	NS	NS	NS	NS	NS	<b>-0.60</b>	<b>-0.57</b>	NS	<b>0.79</b>
	SC	NS	NS	NS	NS	NS	NS	NS	NS	NS	NS	NS	<b>0.76</b>	NS	NS
BacHum	SA	<b>0.69</b>	<b>0.55</b>	<b>0.69</b>	NS	<b>0.69</b>	NS	NS	NS	NS	NS	NS	NS	NS	NS
	SB	NS	NS	NS	NS	NS	NS	NS	NS	NS	NS	NS	NS	NS	NS
	SC	NS	<b>0.56</b>	NS	NS	NS	NS	NS	NS	NS	NS	NS	NS	<b>-0.64</b>	NS
ACE-K	SA	NS	NS	NS	NS	NS	NS	NS	NS	NS	NS	NS	NS	NS	NS
	SB	<b>0.49</b>	NS	NS	NS	NS	NS	NS	<b>-0.61</b>	NS	<b>-0.62</b>	NS	NS	NS	NS
	SC	NS	NS	NS	NS	NS	NS	<b>-0.55</b>	NS	<b>-0.58</b>	NS	<b>-0.72</b>	NS	NS	NS
CAF	SA	NS	NS	NS	NS	NS	NS	NS	NS	NS	NS	NS	NS	NS	NS
	SB	NS	<b>-0.49</b>	NS	<b>-0.54</b>	NS	NS	NS	NS	NS	NS	<b>0.49</b>	NS	NS	NS
	SC	NS	NS	NS	NS	NS	NS	NS	NS	NS	NS	NS	NS	<b>0.66</b>	NS
CBZ	SA	--	NS	--	NS	--	NS	--	NS	--	NS	--	NS	--	<b>-0.67</b>
	SB	<b>0.66</b>	NS	<b>0.64</b>	<b>0.50</b>	<b>0.63</b>	<b>0.60</b>	NS	<b>-0.64</b>	NS	<b>-0.53</b>	<b>0.65</b>	<b>0.66</b>	NS	NS
	SC	NS	NS	NS	NS	NS	NS	NS	NS	NS	NS	NS	NS	NS	NS

Table 2-2 Cont'd

		TP		TDP		SRP		TN		NO <sub>3</sub> -N		NO <sub>2</sub> -N		NH <sub>3+4</sub> -N	
		US	DS	US	DS	US	DS	US	US	DS	US	DS	US	DS	US
GEM	SA	--	NS	--	NS	--	NS	--	NS	--	NS	--	NS	--	NS
	SB	NS	NS	NS	NS	NS	NS	NS	<b>-0.52</b>	NS	NS	NS	NS	NS	NS
	SC	--	NS	--	NS	--	NS	--	NS	--	<b>0.65</b>	--	NS	--	NS
IBU	SA	NS	NS	NS	NS	NS	NS	NS	NS	NS	NS	NS	NS	NS	<b>0.5</b>
	SB	<b>0.50</b>	NS	<b>0.54</b>	NS	<b>0.49</b>	NS	NS	NS	NS	NS	NS	NS	NS	NS
	SC	--	NS	--	NS	--	NS	--	NS	--	NS	--	NS	--	NS
NAP	SA	NS	NS	NS	NS	NS	NS	NS	NS	NS	NS	NS	NS	NS	NS
	SB	NS	<b>-0.65</b>	NS	<b>-0.62</b>	NS	NS	NS	NS	NS	NS	<b>0.72</b>	NS	NS	NS
	SC	NS	NS	NS	NS	NS	NS	NS	NS	NS	NS	NS	NS	NS	NS
SMX	SA	NS	NS	NS	<b>-0.50</b>	NS	<b>-0.50</b>	NS	NS	NS	NS	NS	NS	NS	<b>-0.60</b>
	SB	NS	<b>-0.50</b>	NS	<b>-0.53</b>	NS	NS	NS	<b>0.5</b>	NS	NS	NS	NS	NS	NS
	SC	NS	NS	NS	NS	NS	NS	NS	NS	NS	NS	NS	<b>-0.64</b>	NS	NS

**Table 2-3** - Spearman Rank Order statistical test results for correlation coefficients ( $\rho$ ) obtained for Site A (SA), Site B (SB), and Site C (SC) upstream (US) and downstream (DS). Only significant ( $P < 0.05$ )  $\rho$  values are tabulated (bolded) between FIB/tracers *E. coli*, BacGen, BacBov, BacHum, ACE-K, CAF, CBZ, GEM, IBU, NAP, and SMX. NS: not significant. The results were interpreted as: 0.2–0.4 = weak, 0.4–0.6 = moderate, and 0.6–0.8 = strong.

		BacGen		BacBov		BacHum		ACE-K		CAF		CBZ		GEM		IBU		NAP		SMX	
		US	DS	US	DS	US	DS	US	DS	US	DS	US	DS	US	DS	US	DS	US	DS	US	DS
<i>E. coli</i>	SA	--	<b>0.56</b>	--	NS	--	NS	--	NS	--	NS	--	NS	--	NS	--	NS	--	NS	--	NS
	SB	<b>0.71</b>	NS	NS	NS	NS	NS	NS	NS	NS	NS	NS	NS	NS	NS	NS	NS	NS	NS	NS	NS
	SC	<b>0.64</b>	NS	NS	<b>0.57</b>	NS	NS	NS	NS	NS	NS	NS	NS	--	NS	--	NS	NS	NS	NS	NS
BacGen	SA			--	NS	--	<b>0.55</b>	--	NS	--	NS	--	NS	--	NS	--	NS	--	NS	--	NS
	SB			<b>0.79</b>	<b>0.67</b>	NS	<b>0.73</b>	NS	NS	NS	NS	NS	NS	NS	NS	NS	NS	NS	NS	NS	NS
	SC			NS	NS	NS	<b>0.79</b>	NS	<b>0.60</b>	NS	NS	NS	NS	--	NS	--	NS	NS	NS	NS	NS
BacBov	SA					--	NS	--	NS	--	NS	--	NS	--	NS	--	NS	--	NS	--	<b>-0.66</b>
	SB					NS	NS	NS	NS	NS	NS	NS	NS	NS	<b>-0.48</b>	NS	NS	<b>-0.55</b>	NS	NS	<b>0.65</b>
	SC					NS	NS	NS	NS	NS	NS	NS	NS	--	NS	--	NS	NS	NS	NS	NS
BacHum	SA							NS	NS	--	NS	--	NS	--	NS	--	NS	--	NS	--	NS
	SB							NS	NS	NS	NS	NS	NS	NS	NS	NS	NS	NS	NS	NS	NS
	SC							NS	NS	NS	NS	NS	NS	--	NS	--	NS	<b>-0.63</b>	NS	NS	NS
ACE-K	SA									--	NS	--	<b>0.66</b>	--	NS	--	NS	--	NS	--	NS
	SB									NS	NS	NS	NS	NS	<b>0.63</b>	<b>0.49</b>	NS	NS	<b>0.51</b>	NS	NS
	SC									NS	NS	NS	<b>0.62</b>	--	<b>0.57</b>	--	<b>-0.55</b>	NS	<b>-0.58</b>	NS	NS
CAF	SA											--	NS	--	NS	--	NS	--	NS	--	NS
	SB											<b>0.50</b>	NS	NS	NS	NS	<b>0.77</b>	NS	<b>0.59</b>	NS	NS
	SC											NS	NS	--	NS	--	NS	NS	NS	NS	NS

Table 2-3 Cont'd

		BacGen		BacBov		BacHum		ACE-K		CAF		CBZ		GEM		IBU		NAP		SMX		
		US	DS	US	DS	US	DS	US	DS	US	DS	US	DS	US	DS	US	DS	US	DS	US	DS	
CBZ	SA													--	NS	--	NS	--	NS	--	<b>0.51</b>	
	SB													NS	NS	NS	NS	<b>0.55</b>	NS	NS	NS	NS
	SC													--	NS	--	NS	NS	<b>-0.55</b>	NS	NS	NS
GEM	SA													--	<b>0.55</b>	--	NS	--	NS	--	NS	
	SB													NS	NS	NS	NS	<b>0.73</b>	NS	NS	NS	
	SC													--	NS	--	NS	--	NS	--	NS	
IBU	SA																	--	NS	--	NS	
	SB																	NS	<b>0.54</b>	NS	NS	
	SC																	--	<b>0.78</b>	--	<b>0.76</b>	
NAP	SA																			--	NS	
	SB																			NS	NS	
	SC																			<b>0.64</b>	NS	

## Chapter 3

# Using Passive Samplers POCIS and P-Traps to Measure Trace Acesulfame-K and Total Dissolved Phosphorus Concentrations in Headwater Streams

### 3.1 Introduction

The importance of environmental monitoring of headwater streams in rural hamlets with on-site wastewater disposal systems has been stressed in recent studies (Withers et al., 2011; Richards et al., 2016). Tracking wastewater can be accomplished by sampling for nutrients, like phosphorus (P), which may occur at elevated concentrations. However, P is also sourced from agricultural runoff, and found naturally in the environment. More recently, organic tracers that are human specific have successfully been used to monitor domestic wastewater effluent in surface and ground waters (Carrara et al., 2008; Robertson et al., 2013; Liu et al., 2014). The artificial sweetener acesulfame-K (ACE-K) has been found to be recalcitrant in ground and surface waters and has been referred to as an ideal domestic wastewater tracer (Buerge et al., 2009; Van Stempvoort et al., 2011b; Spoelstra et al., 2013, 2017).

Most environmental monitoring studies in rural headwater streams assessing domestic wastewater impacts are accomplished using a traditional grab sampling method. The alternative to grab sampling is the use of passive sampling techniques. Passive sampling techniques applied to low dilution headwater streams has many potential advantages: (1) lower detection limits; (2) time-weighted average (TWA) concentration that may be more representative of average

concentrations in the stream; (3) accumulation of target compound increases confidence that a target compound is present (Alvarez, 2010).

Polar Organic Chemical Integrative Samplers (POCIS) have previously been used to monitor various emerging organic contaminants in the environment including pesticides (Metre et al., 2017), per-fluorinated compounds (Kaserzon et al., 2014), pharmaceuticals and artificial sweeteners (Metcalf et al. 2014). The POCIS are usually designed by securing two large washers around the edges of two membranes holding a receiving phase. The POCIS are configured to apply solid phase extraction (SPE) techniques in the stream over a selected period of time (e.g. 14-28 days). A popular version of the POCIS uses OASIS HLB® sorbent (Waters) to accumulate polar organic contaminants that interact with the membranes (Metcalf et al., 2014; Sultana et al., 2017).

A less used passive sampler is the phosphorus trap (P-Trap) developed by Muller et al. (2008) that targets dissolved phosphorus. This sampler is similar in that it includes two membranes, this time secured with acrylic modified peepers, and a receiving phase within. The P-Trap receiving phase is iron-coated sand. If phosphorus interacts with the sampler, it will preferentially sorb onto the sand, where it would remain until extracted.

Passive sampling techniques are used to calculate time weighted average (TWA) concentrations rather than relying on “snapshot” concentrations obtained from grab samples. The TWA concentration ( $C_w$ ) is calculated using Equation 3.1 below, where  $M_s$  is the mass of the target analyte found in the sampler,  $R_s$  is the uptake rate (in  $L\ day^{-1}$ ), and  $t$  is the deployment time (days).

$$C_w = \frac{M_s}{R_s t} \quad (3.1)$$

Currently, the only published  $R_s$  values for ACE-K uptake using HLB POCIS and the P-Trap are  $0.08 \text{ L day}^{-1}$  (Sultana et al., 2017) and  $0.06 \text{ L}^{-1}$  (Muller et al., 2008) respectively.

### 3.1.1 Research Objectives

The main research objective of this study is to compare grab sampling to passive sampling in headwater streams in rural areas. To accomplish this, POCIS were deployed at upstream (US) and downstream (DS) locations for three rural hamlets to target the artificial sweetener acesulfame-K (ACE-K) during the spring, summer, and fall for a 14-day period; and grab samples collected on the first and last days. Finally, P-Traps and POCIS were deployed at the US and DS of one site, and grab samples were taken every other day for a 14-day period.

## 3.2 Methods

### 3.2.1 POCIS Specifications

The polar organic chemical integrated samplers (POCIS) were obtained pre-assembled from Environmental Sampling Technologies (EST) laboratories (St-Joseph, MO). The POCIS are comprised of 200 mg of OASIS® Hydrophilic-Lipophilic Balance (HLB) sorbent (Waters) held between two  $0.1 \mu\text{m}$  polyethersulfone (PES) membranes, which are encased by two washers and bolted tight. The POCIS were stored at room temperature in an air tight canister until deployment (Figure D-1).

### 3.2.2 P-Trap Specifications

The receiving phase for the P-Traps was prepared at the University of Waterloo according to a modified method published by Muller et al. (2008). Briefly, 1000 g of crystalline quartz (OK-75) grains obtained from U.S. Silica were soaked in 1M HCl overnight, subsequently rinsed with ultrapure water (Milli-Q A10 water system: 18.2 MΩ cm @ 25 °C) five times and separated into five 200 g batches. A ferric nitrate ( $\text{Fe}(\text{NO}_3)_2 \cdot 9\text{H}_2\text{O}$ ) solution was made by dissolving 160 g of Fe nonahydrate in 2000 mL of ultrapure water. A 1M sodium hydroxide (NaOH) solution was made by dissolving 40 g of NaOH into 1000 mL of ultrapure water.

Each batch (200 g) of sand was coated by adding 500 mL of the ferric nitrate solution in a beaker set up with a continuous stirrer. For a period of approximately two hours, 300 mL of the 1M NaOH solution was added by peristaltic pump while the solution was continuously stirred. The pH was adjusted to 7 and the sand and precipitate were left to settle to allow supernatant water to be decanted from the mixture. The final slurry was left to dry for 3 days at 50 °C and then homogenized.

The P-traps were made by modifying small acrylic dialysis plates (12 slots  $\sim 8 \text{ cm}^2$ , 1 cm thick) by cutting the solid back of the main piece to make the plate double sided. In short, the two sheets of filter membrane were sealed between two outer lids to encase iron-coated sand in the slots (Figure D-2). Each slot represents one replicate. After the traps were finished they were stored in ultrapure water until installation in the field.



### 3.2.3 Field Site Characterization and Study Design

For specific field-site descriptions and map, see Chapter 2. Site-specific records of air temperature and barometric pressure were not available; therefore, historical records from the UW Weather Station (43° 28' 25.6" N and 80° 33' 27.5" W) were used for this study.

#### 3.2.3.1 Cage assembly

For this study, wired cages (30.5×30.5×10.2 cm) were used to keep the passive samplers in place. The configuration within the cages for the seasonal study (SS) and two-week study (TWS) were different. For the SS, three POCIS were secured in the cage, along with a temperature logger (TidBit). For the TWS, four POCIS and a P-Trap were secured in a cage, along with two temperature loggers. A second cage contained the second P-Trap which was installed next to the other cage. Two level loggers were also installed for the TWS to obtain water level data. All components were secured using zip ties and placed so that all membranes were parallel (Figure D-3).

#### 3.2.3.2 Seasonal study

First, a seasonal study (SS) was conducted over three 2-week periods: (1) May 17–31, 2017 (spring); (2) July 12–26, 2017 (summer); and (3) November 15–29, 2017 (fall). These sampling excursions overlapped with six grab-sampling dates in Chapter 2, and the same sample locations were used: Site A (SA) upstream (US)/downstream (DS), Site B (SB) US/DS, and Site C (SC) US/DS. When grab samples were collected for Chapter 2 on these dates, POCIS were installed where/when possible on May 17, July 12, and November 15, 2017 and retrieved after 14 days. POCIS were not installed at SA–US during the spring and summer, nor at SA–DS during the

summer due to low flow conditions. Upon retrieval from the stream, each POCIS was rinsed with stream water, and gently cleaned to remove debris. Each POCIS was wrapped in foil and secured in a sample bag. The POCIS were placed on ice during transport and transferred to a -22 °C freezer until analysis. During each deployment and retrieval, a field blank was exposed to air while the sample POCIS were exposed to air. Between the deployment and retrieval, the blank was wrapped in foil and kept in a freezer at -22 °C.

### 3.2.3.3 Two-week study

For the two-week study (TWS), one site was selected to focus on more intensive grab sampling during the two-week period. Site A was selected due to the inference of little to no impacts at the US and higher impacts at the DS of TDP and ACE-K (*see* Chapter 2). For this sub-study, the cages included four POCIS, two P-Traps, and two temperature loggers. Furthermore, two level loggers (Solinst) were installed in the substrate next to the cages to obtain water level information. One of the P-Traps was removed on Day 8 (of 14) to obtain more information on the uptake during the two-weeks. The cages at the US location were installed a few meters downstream than the POCIS deployed in the SS to ensure the water was deep enough to cover the cages. The change in stream location may have affected the concentrations of TDP and ACE-K compared to those collected in the SS. This new installation location is impacted by water flowing along a ditch adjacent to an agricultural field and a road, along with potential impacts by a storm drain connected to a nearby elementary school (*see* Chapter 2 for more description). Grab samples were collected every other day at approximately the same time on Days 0, 2, 4, 6, 8, 10, 12, and 14 at both the US and DS sites.

### 3.2.4 Field Sampling Methods

The grab sample data used for comparison to the passive sampler data for the seasonal study were the same as reported in Chapter 2 on the deployment/retrieval dates. For this study, the following analytes and parameters were tested and used for data comparison: temperature, pH, DO, DOC, alkalinity, turbidity, SPC, TS, Cl, SO<sub>4</sub>, Ca, K, Mg, Na, TP, TDP, SRP, TN, NO<sub>3</sub>-N, NO<sub>2</sub>-N, NH<sub>3+4</sub>-N, and ACE-K (*see* Table 3-1).

For the two-week study, the SA-US samples were collected slightly downstream than for the samples collected in the SS (as mentioned above). The samples were collected using a bucket that was rinsed three times with site-specific water prior to collection. Grab samples were collected in duplicate for this study. A YSI handheld device (Hoskin Scientific) with multi-probes was used to measure temperature, dissolved oxygen, turbidity, and specific conductivity (SPC). Unfiltered samples were collected for pH, alkalinity, total solids, and total phosphorus. Filtered samples were collected for nutrients (TDP, SRP, TN, NO<sub>2+3</sub>-N, NO<sub>3</sub>-N, NH<sub>3+4</sub>-N), major cations (Ca, K, Mg, Na), DOC, and anions (Cl, SO<sub>4</sub>), as described in Chapter 2 (Section 2.2.2). The trace metal and DOC samples were acidified to a pH < 2 using nitric acid and sulfuric acid respectively. Samples for ACE-K were filtered using 0.2 µm PVDF filters and collected in 5 mL centrifuge tubes. All samples were stored on ice during transportation and samples were either sent in a cooler to the Ministry of Environment, Conservation and Parks Laboratory Services Branch (MECP LaSB, Etobicoke, ON) for analysis, or submitted to the University of Waterloo (UW) for analysis as described previously in Chapter 2. Samples for ACE-K and anions were stored in a freezer at -22 °C and DOC samples refrigerated at 4 °C.

### 3.2.5 Laboratory Methods

The laboratory analytical methods used for the SS and TWS were the same as those followed in Chapter 2. The alkalinity, total solids, nutrients, and major cations were analyzed at the Etobicoke (ON) MECP LaSB, and the TP and TDP at the Dorset (ON) MECP LaSB. The alkalinity (as  $\text{mg L}^{-1} \text{CaCO}_3$ ) was analyzed by titration (MOE, 2015b), total solids by gravimetry (MOE, 2014c), major cations by inductively coupled plasma-optical emission spectroscopy (ICP-OES) (MOE, 2014a), and dissolved nutrients by colourimetry (MOE, 2015a). The anion, DOC, and ACE-K samples were analyzed at UW. The anion samples were thawed, diluted 100 times, and run using an IC technique with a Dionex ICS-5000+ (Mississauga, Canada). The DOC samples were diluted 7.5 times and run using a TOC Analyzer method with an Aurora 1030W.

### 3.2.6 Solutes and Solvents

The native compound for the artificial sweetener ACE-K was purchased from Sigma-Aldrich (Oakville, Canada) and the isotope-labelled compound ACE-K-d4 was obtained from Toronto Research Chemicals Inc. (Canada). Ultrapure water was generated by a MilliQ A10 water system ( $18.2 \text{ M}\Omega \text{ cm @ } 25 \text{ }^\circ\text{C}$ ), and HPLC-grade methanol was purchased from Fisher Scientific™ (Toronto, ON). An internal standard (IS) stock solution was made by serial dilution in ultrapure water. The standard stock solutions were prepared by dissolving the powder to obtain an initial concentration of  $1 \text{ g L}^{-1}$ . Serial dilution was used to obtain a final concentration of  $1 \text{ }\mu\text{g L}^{-1}$ . The IS and stock solutions were used to spike quality control (QC) samples, to obtain a calibration curve, and continuing calibration verification (CCV) samples.

### 3.2.7 POCIS Extraction and Sample Preparation

The POCIS extractions were accomplished using a similar method previously published (Li et al., 2010; Sultana et al., 2017). The POCIS were thawed to room temperature, and the bolts were removed. The OASIS® HLB sorbent was transferred to a 50 mL centrifuge tube and the membranes rinsed with HPLC grade methanol. The final initial sample volume was 10 mL. The centrifuge tubes were vortexed and placed on a rotator overnight to ensure the samples were well-mixed. Empty SPE cartridges with the frit were washed with 3×1 mL methanol. The samples were vortexed and loaded to the empty cartridges. The eluate was collected in a 15 mL centrifuge tube. The 50 mL cartridges were then topped off with another 3 mL of methanol, vortexed, and loaded into the cartridges, this time loading the HLB sorbent into the empty cartridges. The cartridges were vacuumed dry and the sorbent was eluted with 2×1 mL methanol under gravity. The cartridges were vacuumed dry and the 15 mL centrifuge tubes were removed from the manifold. The final eluate was 15 mL per sample. A 5 mL aliquot was transferred to 7 mL amber glass vials and evaporated down under gentle N<sub>2</sub> stream. The samples were then reconstituted to 1 mL with ultrapure water. Samples were vortexed on high for 2 minutes and transferred to IC-MS/MS sample vials and directly analyzed using IC-MS methods (see below). For each batch, a set of QC samples were also subject to the same process. The QC samples were prepared by soaking membranes in ultrapure water, then transferring the membranes to centrifuge tubes with 200 mg HLB sorbent (Waters) and spiking to known concentrations using the stock solutions. Note that a known volume of IS was added to all QC and unknown samples prior to analysis.

### 3.2.8 ACE-K Analysis

The diluted ACE-K grab samples and POCIS extracts were analyzed using ion-chromatography tandem mass-spectrometry (IC-MS/MS) techniques previously described in Chapter 2. The grab samples were thawed and diluted two times with ultrapure water to help mitigate matrix effects. The analytical method using ion chromatography coupled with mass spectrometry (IC-MS/MS) (Van Stempvoort et al., 2011b), with modifications described by and optimized source parameters reported by Saurette et al. (2017). In short, the samples were analyzed by direct injection in a Dionex ICS-500 (Sunnyvale, CA, USA), followed by injection into an Agilent 6460 QQQ (Mississauga, ON, CA) operating in negative electrospray ionization (ESI<sup>-</sup>) mode with multiple reaction monitoring (MRM). In the IC, the samples were passed through a Dionex IonPac™ AG20 RFIC™ (2×50 mm) guard column, followed by a Dionex RFIC™ IonPac® A520 (2×250 mm) analytical column. The MRM transitions (m/z) were 162.1→81.8 for the ACE-K target analyte and 162.1→78.0 for the ACE-K IS, and the ACE-K retention time was approximately 5.7 minutes.

### 3.2.9 P-Trap Extraction and Analysis

After P-Trap collection, each slot was cut open and the sand was transferred to glass vials. Any remaining sand was rinsed out of the slot with ultrapure water. The vials were transferred to the oven heated at 50-70 °C for three days until the sand dried. The phosphorus was extracted from the sand with concentrated HCl and mixed. A volume of 500 µL was diluted with 9500 µL of ultrapure water. The samples were analyzed at UW using a standard inductively coupled plasma-optical emission spectrometry (ICP-OES) method (USEPA, 2018) on an iCap 6000 (Thermo Fisher). The MDL for this method is 0.1 mg L<sup>-1</sup> P.

### 3.3 Results

#### 3.3.1 QA/QC Results

##### 3.3.1.1 Water vs. ambient temperature

The water temperature data recorded by the temperature loggers were plotted against the air temperature data (Figure 3-1). This information was used to determine whether the POCIS may have been out of the water during the deployment. During the spring and summer 2017 deployments, the water temperature more closely followed the air temperature compared to winter 2017; therefore, it was difficult to discern whether the POCIS were exposed to the air during the warmer seasons. In the spring deployment, the surface water temperature line overlapped the air temperature line between May 19-21, 2017 at SA-DS, SC-US and SC-DS. This may be related to latent heat absorbed by the water from the high air temperature recorded for the two previous days or may indicate that the POCIS were not submerged in the stream. The spring 2017 SA-DS POCIS showed physical evidence of being above the water level for some part of the study periods (Figure D-4); however, based on the graph, the length of time the POCIS was not submerged remains unclear. Furthermore, when the fall 2017 SB-US cage was collected, it was caught in debris and at least half the cage was out of the water. Based on the graphs, the recorded water temperature at SB-US seems to more closely follow the pattern for the remaining five surface water temperature lines, and not the air temperature line. For the 2-week study plot, the water temperature followed a different trend compared to the air temperature at the US, as the water is cooler (more groundwater influence), indicating the POCIS were submerged in the stream. At the DS, it was more difficult to discern if the POCIS had been

exposed to air as the temperature differential was minimal. However, this site was visited every other day during deployment, and there was no evidence of it being exposed during the field visits.

### 3.3.1.2 ACE-K grab samples

The QA/QC results for the seasonal ACE-K samples were reported in Supplementary Information A in Chapter 2. The QA/QC results for the 2-week study ACE-K samples are reported here. Two batches of samples were analyzed using the IC-MS/MS. Each batch contained a standard curve using seven standards with concentrations between 0.05 and 50  $\mu\text{g L}^{-1}$ . The accuracy of the standards ranged between 75% and 119%, with an average accuracy and RSD% of  $96 \pm 12\%$ . Blank samples were run between samples, and there was no carryover of the target analyte between samples. The  $r^2$  values for both curves were greater than 0.99999. Continuing calibration verification (CCV) samples were also run ( $n=8$ ) with concentrations between 0.5 and 10  $\mu\text{g L}^{-1}$ . Method quality controls were added between samples for QA/QC purposes. These samples were spiked to final concentrations between 0.5 and 10  $\mu\text{g L}^{-1}$ . The accuracy of these samples ( $n=8$ ) ranged between 93% and 152%, with a mean and RSD% of  $115 \pm 16\%$ . The absolute IS recoveries for these QC samples ranged between 33% and 40%, with a mean and RSD% of  $36 \pm 8\%$ . However, the relative IS recoveries for these spiked samples ranged between 88% and 109%, with a mean recovery and RSD% of  $101 \pm 7\%$ . The samples ( $n=32$ ) had absolute IS recoveries between 44% and 82%, with a mean and RSD% of  $59 \pm 14\%$ . Like the spiked QC samples, the samples had relatively low absolute IS recoveries and better relative IS recoveries. The samples had relative IS recoveries between 69% and 129%, with a



mean and RSD% of  $100 \pm 11\%$ . In both batches, the retention times for the target analyte was 5.7 minutes. The MDL for these samples was the same as used in Chapter 2:  $140 \text{ ng L}^{-1}$ ; this MDL takes the dilution factor (2) into consideration.

### 3.3.1.3 ACE-K POCIS samples

The reconstituted POCIS extracts were analyzed in three separate batches on the IC-MS/MS. Each batch had a standard calibration curve ( $n=7$ ) of prepared standards with concentrations between  $0.05$  and  $50 \text{ } \mu\text{g L}^{-1}$ . The  $r^2$  values for the batches were greater than  $0.9997$  and the accuracy of the standards was between  $89\%$  and  $138\%$  (the lowest standard was removed for quantification) and a mean and RSD% of  $105\% \pm 15\%$ . Ultrapure blanks were run between each sample to minimize carryover between samples. There was no carryover observed in these samples. The CCV samples run with concentrations between  $0.1$  and  $10 \text{ } \mu\text{g L}^{-1}$  had a mean and RSD% of  $99\% \pm 13\%$ , and a range between  $76\%$  and  $124\%$ . The QC samples were prepared and followed the same laboratory process as the unknown samples. For each batch a blank and three spiked samples were analyzed. The spiked concentrations were  $0.5$ ,  $1$ , and  $2 \text{ } \mu\text{g L}^{-1}$ . These concentrations are similar to the concentrations detected in the unknown samples, which had a range of  $0.28$  and  $4.2 \text{ } \mu\text{g L}^{-1}$ . The QC samples had accuracies between  $96\%$  and  $136\%$ , with a mean and RSD% between  $110\% \pm 11\%$ . The measured vs. expected QC concentrations were plotted, and a regression line was fit through the data (Figure 3-2). The coefficient of correlation was calculated as  $0.9936$ , which showed that the method used to remove the analyte from the HLB sorbent, followed by the evaporation and reconstitution step, was likely adequate for this study. The absolute IS recoveries for these samples were between  $61\%$  and  $97\%$  and had a mean

and RSD% of  $82 \pm 14\%$ . The samples ( $n=16$ ) had low absolute IS recoveries between 29% and 69% and a mean and RSD% of  $45 \pm 22\%$ . The relative IS recoveries were much better, with a range between 63% and 148%, and an improved mean and RSD% of  $100 \pm 20\%$ . Field blank samples ( $n=4$ ) were also prepared and run to determine the method MDL, which was estimated as three times the Blank concentrations. All four Field Blanks were used to calculate an MDL of  $2 \text{ ng L}^{-1}$ , which is much lower than the grab sample MDL.

#### 3.3.1.4 TDP concentrations measured in grab samples and P-Traps

The TDP concentrations for the grab samples were carried out at the MECP LaSB (Dorset, ON), which applies their own standard QA/QC procedures. All grab sample TDP concentrations were reported with no noted issues. The diluted P-Trap extracts had uncorrected reported concentrations between 40.7 (Field Blank) and  $184.3 \text{ } \mu\text{g L}^{-1}$ . One sample was less than the MDL ( $0.09 \text{ mg L}^{-1}$ ) but was accepted as it was within 10% of the MDL. All samples had raw P concentrations greater than the Field Blank sample.

### 3.3.2 Seasonal Study (POCIS) Results

#### 3.3.2.1 General water quality

The general water quality results for the seasonal study were reported as part of the annual sampling study described in Chapter 2. The data points for the select grab samples collected on the first and last day of each deployment period were averaged and tabulated in Table 3-1. The temperature of the stream water varied over the seasons. The fall POCIS deployment had the coolest average temperature range (between 2.0 and 6.9 °C), followed by spring (between 9.8 and 16.7 °C), which was similar to the warmest samples collected in summer (between 14.7 and

17.6 °C). The average range of pH was not as variable, with an overall average range of 7.79 and 8.45.

### 3.3.2.2 ACE-K grab sample vs. passive sample results

The average ACE-K concentrations of the grab samples for the spring, summer, and fall deployment periods at the US and DS of SA, SB, and SC were graphed to compare with the TWA POCIS concentrations (Figure 3-3). The average (n=2) grab sample concentrations were always at least two orders of magnitude greater than the TWA POCIS concentrations. The range of POCIS ACE-K concentrations was between < 2 and 11 ng L<sup>-1</sup> compared to the grab sample concentration range of < 140 and 2100 ng L<sup>-1</sup>. The POCIS installed at the DS all had either similar (< 2 ng L<sup>-1</sup>) or greater TWA concentrations compared to the US. This is comparable to the observations made in Chapter 2. The spring sample results for SC show that there were concentrations < MDL for both the grab and passive samples.

Corrected  $R_s$  values were calculated for each season (i.e. spring, summer, fall) and sample site (i.e. SA-US, SA-DS, SB-US, SB-DS, SC-US, SC-DS) using the mass of ACE-K (ng) sorbed onto each POCIS and the mean concentrations for the grab samples collected during deployment and retrieval (n=2). The resulting  $R_s$  values were variable and between 0.000004 and 0.001764 day L<sup>-1</sup>, and mean annual  $R_s$  values between 0.00149 and 0.000828 day L<sup>-1</sup> (Figure 3-4).

### 3.3.3 Two-week Study (POCIS, P-Trap) Results

#### 3.3.3.1 General water quality

The general water quality parameters measured in this two-week study were averaged and tabulated in Table 3-2. The average temperatures for the US and DS were 8.6 °C and 12.3 °C, and the average pH values for the US and DS were 8.20 and 8.36 respectively. Most of the water quality measurements were similar between the sites, with the exception of turbidity, TS, Cl, and Na. The turbidity was higher at SA-US, with an average of 3.4 NTU compared to 0.9 NTU for the DS. The TS, Cl, and Na measurements were generally greater at SA-DS, with values of 765 mg L<sup>-1</sup> (US = 591 mg L<sup>-1</sup>), 182 mg L<sup>-1</sup> (US = 100 mg L<sup>-1</sup>), and 125 mg L<sup>-1</sup> (US = 59.1 mg L<sup>-1</sup>) respectively. The SRP and NH<sub>3+4</sub>-N averages were greater at SA-US: 26.6 µg L<sup>-1</sup> and 0.13 mg L<sup>-1</sup> compared to 15.9 µg L<sup>-1</sup> and 0.08 mg L<sup>-1</sup> at SA-DS.

#### 3.3.3.2 ACE-K grab sample vs. passive sample results

The TWA ACE-K concentrations from the two-week study for POCIS at SA-US and DS were not similar to the grab sample results (Figure 3-5). For SA-US, the mean grab sample concentration was 415 ng L<sup>-1</sup>, which is approximately 160 times greater than the TWA value of 2.6 ng L<sup>-1</sup>. Similarly, the SA-DS mean grab sample concentration of 917 ng L<sup>-1</sup> was 161 times greater than the TWA result of 5.7 ng L<sup>-1</sup>.

#### 3.3.3.3 TDP grab sample vs. passive sample results

The TWA TDP concentrations for the first 8 days, and total 14 days were plotted with the TDP grab sample results (Figure 3-6). For the 8-day P-Traps, the TDP was overestimated compared to

the mean grab samples. At the US, the P-Trap had a TWA of  $40.2 \mu\text{g L}^{-1}$  compared to mean grab sample concentration of  $22.9 \mu\text{g L}^{-1}$ . The DS P-Trap TWA was higher at  $53.6 \mu\text{g L}^{-1}$ , compared to an TDP grab sample concentration of  $26.0 \mu\text{g L}^{-1}$ . For the full 2-week deployment, the P-Trap TWA for the US was  $29.4 \mu\text{g L}^{-1}$ , which was similar to the mean concentration of  $27.1 \mu\text{g L}^{-1}$  in the grab samples. The DS TWA was  $45.5 \mu\text{g L}^{-1}$ , compared to the mean grab sample concentration of  $31.4 \mu\text{g L}^{-1}$ .

### 3.4 Discussion

#### 3.4.1 Confidence in TWA POCIS Concentrations

Based on the comparison between ACE-K grab sample concentrations and the calculated TWA concentrations using POCIS, there is little confidence that the POCIS are useful for this target analyte, especially in small headwater streams. The application of POCIS in shallow water can have limitations because of the potential exposure of POCIS to air over the extended period of deployment. The data obtained from the temperature loggers were used to infer whether they were, but there were instances when this was unclear. For example, the spring 2017 deployment at SA-DS was considered incomplete because the POCIS showed evidence of being only half-submerged. Unfortunately, it remains unclear whether, or for how long, the POCIS were out of the stream (Figure 3-1). If the POCIS was out of the water, then the  $t$  (days) would be reduced, which would increase the TWA concentration.

The ACE-K  $R_s$  of  $0.08 \text{ L day}^{-1}$  was determined by Sultana et al. (2017) using a static renewal experiment previously described by MacLeod et al. (2007). Briefly, a volume of deionized water was spiked with a known concentration of ACE-K, and POCIS was left to

interact with the water. Water samples were analyzed to determine the rate of uptake of ACE-K by the POCIS over time. The experiment was conducted at a temperature of 15 °C and at a pH of 6.5. This combination is similar to the temperature and pH ranges of the waters in this study during the spring and summer deployments, but not the winter. The effect of temperature within the range of 5-25 °C on the sampling rate is expected to be less than two-fold (Li et al., 2010b). The pH of the surface waters in this study are also higher than 6.5. However, Li et al. (2011) found that the effect of pH does not greatly influence the  $R_s$  values for HLB sorbent POCIS between the pH range of 3-9.

Moreover, some studies have noted that laboratory-derived  $R_s$  values may not be representative of the field  $R_s$  values which may cause uncertainty in the obtained results (e.g. Li et al. 2010b; Morin et al. 2013; Sultana et al. 2017). The physiochemical properties of target compounds and the environmental conditions of the sites of deployment are key to understanding how these values change. The field conditions that may alter the sampling rate include pH, temperature, biofouling, and dissolved organic carbon (DOC), and water flow/turbidity (Alvarez, 2010). The DOC in the sample medium was found to only slightly affect the sampling rate (Li et al., 2011). Water flow/turbidity for polar organic compounds in POCIS was assessed by Li et al. (2010b) through a field experiment, and found that the effect only changes the  $R_s$  by a factor of less than two. The effect of biofouling on the POCIS are not fully understood and require more attention for future research; a study found that there was an increase in  $R_s$  of 55% for biofouled POCIS (for alkylated phenols), which would decrease the TWA concentration (Harman et al., 2009). Biofouling occurred to some degree at all sites in this study. However, SB-US was subject to the most fouling during all three deployments. At this site, there were many insects latched

onto the POCIS membranes, and layers of mud filled the cage and around the POCIS devices. This could explain why the SC-US POCIS results were low ( $< 2 \text{ ng L}^{-1}$ ). The fouling would decrease the diffusion across the membranes, decreasing the field  $R_s$ , which would increase the TWA concentration. Underestimated concentrations of organic contaminants using POCIS compared to grab sampling has been reported in a study where the surface waters had low concentrations compared to the spiked laboratory water used to calculate the  $R_s$  value (Criquet et al., 2017). Although these changes in water quality are a possible explanation of the low TWA concentrations calculated, the  $R_s$  value would need to be orders of magnitude lower to obtain similar concentrations to the grab samples.

The calculated  $R_s$  values for the seasonal study were all less than the literature value of  $0.08 \text{ day L}^{-1}$ . However, it is unclear whether these calculated values are representative of the true field uptake rate values. Previous studies have assessed the use of performance reference compounds (PRCs) to help determine a more field-representative  $R_s$  value (Huckins, 2010; Dietschweiler et al., 2012). By spiking the receiving phase with another compound that will dissipate in the water, and using the assumption of isotropic diffusion, both the PRC mass loss and the target analyte uptake will be equally affected by the surface water exposure conditions. Using PRCs in these rural headwater streams may have helped determine a more accurate TWA concentration.

Originally, the extraction method was thought to have potentially reduced the mass of ACE-K removed from the sorbent. However, the QA/QC samples in this study showed that the extraction method was likely valid (Figure 3-2), and that perhaps there is limited ACE-K adsorbed onto the POCIS receiving phase. In the only other ACE-K POCIS study identified,

Sultana et al. (2017) calculated ACE-K TWA concentrations between 4 and 33 ng L<sup>-1</sup> compared to 128 and 213 ng L<sup>-1</sup> for sucralose. These ACE-K concentrations are lower than reported in previous studies on treated WWTP effluent (e.g. Liu et al., 2014). The HLB sorbent that is prepacked into the POCIS has been shown to have low recovery for ACE-K (Jian-ye et al., 2016). A more suitable sorbent would be a Poly-Sery PWAX sorbent, which has shown good recovery in river water samples near 100% (Gan et al., 2013). The evaluation of the most appropriate receiving phase was not conducted in this study and warrants further investigation.

### **3.4.2 Confidence in P-Trap TWA Concentrations**

The P-Traps that were deployed for the longer time-period (14 days) had TWA concentrations that more closely approximated the grab sample concentrations (Figure 3-6). This observation suggests that passive samplers deployed for a longer time may be more representative of the average surface water concentrations in the stream. However, the TWA concentrations are limited by the  $R_s$  constant used for the calculations.

The  $R_s$  value was obtained from Muller et al. (2008). The uptake rate was measured by static renewal, but the temperature and pH of the simulated water is unknown. Theoretically, uptake rate constants are related to the diffusion across the membrane, the surface area of the membrane, and the water boundary layer thickness (e.g. Bartelt-Hunt et al., 2011). The sand was coated with Fe following a method published in the same study that experimentally determined the  $R_s$  value used in the calculations (Muller et al., 2008). However, there may be changes in the modified surface area or varying diffusion coefficients for the sands since both the modified peeper and the sand were not produced by a certified supplier.



### 3.5 Conclusions

Overall, the P-Traps performed better than POCIS for the target analytes in this study. The application of the P-Trap over a longer time-period were in closer agreement with the average TDP grab sample concentration in the stream. However, there are reservations with the TWA concentrations calculated in this study related to concentrations close to the analytical method MDL and using uptake rates from previous studies. Future work applying this passive sampling technique should include an experimental study to determine uptake rates with simulated surface water.

The performance by the POCIS in targeting ACE-K within the stream stressed the importance of selecting the best receiving phase for the targeted analytes. Future research applying POCIS should also consider experimentally determining uptake rate constants experimentally and correct for field conditions (e.g. flow, temperature, fouling) by using performance reference compounds. In this study, an advantage to the POCIS was the lower MDL compared to the grab samples. The field blanks had consistent MDLs of  $2 \text{ ng L}^{-1}$  compared to  $140 \text{ ng L}^{-1}$  for the diluted grab samples.

This exercise in applying passive sampling techniques provided insight into the application of POCIS and P-Traps in shallow headwater streams. In the seasonal study, there was evidence of fouling which may have prevented uptake by the POCIS during deployment, reducing the TWA concentrations. The use of passive sampling techniques in rural headwater streams may be beneficial due to the lower MDLs, especially if the correct receiving phase is selected, there is a contrast between the air and water temperature (e.g. during the fall), and there is adequate flow to prevent excessive fouling.

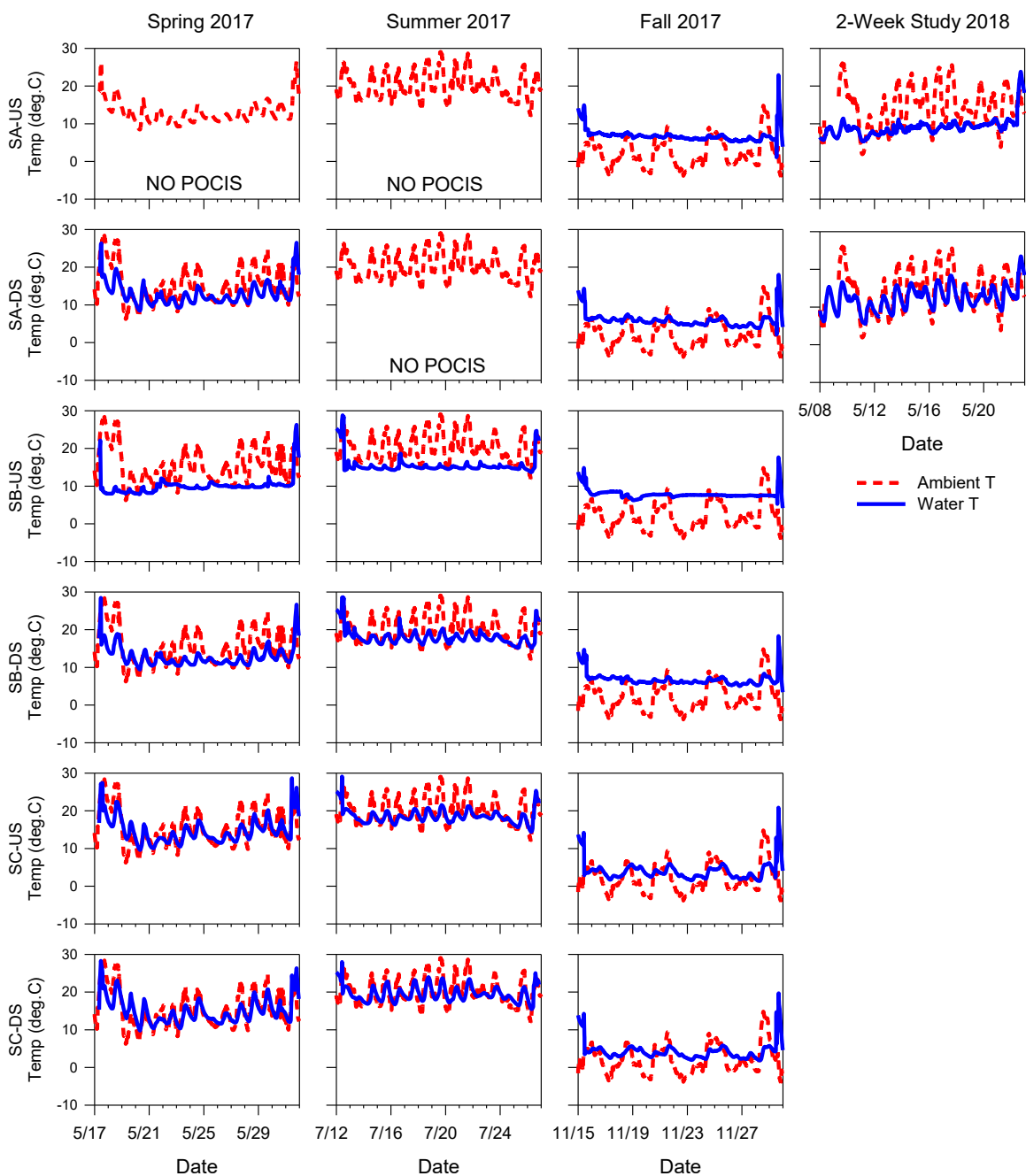


**Figure 3-1** - Multi-line plots of the ambient air temperature (red) and water temperature (blue) through the sampling period. The first column displays the Spring 2017 seasonal POCIS deployment (May 17-31, 2017). The second column displays the Summer 2017 seasonal POCIS deployment (July 12-26, 2017). The third column displays the Fall 2017 seasonal POCIS deployment (November 15-29, 2017). The fourth column displays the 2-week study results for SA only (May 8-22, 2018). The rows represent sample sites, from the top: SA-US, SA-DS, SB-US, SB-DS, SC-US, and SC-DS. The graphs without a blue line were not subject to POCIS deployment.

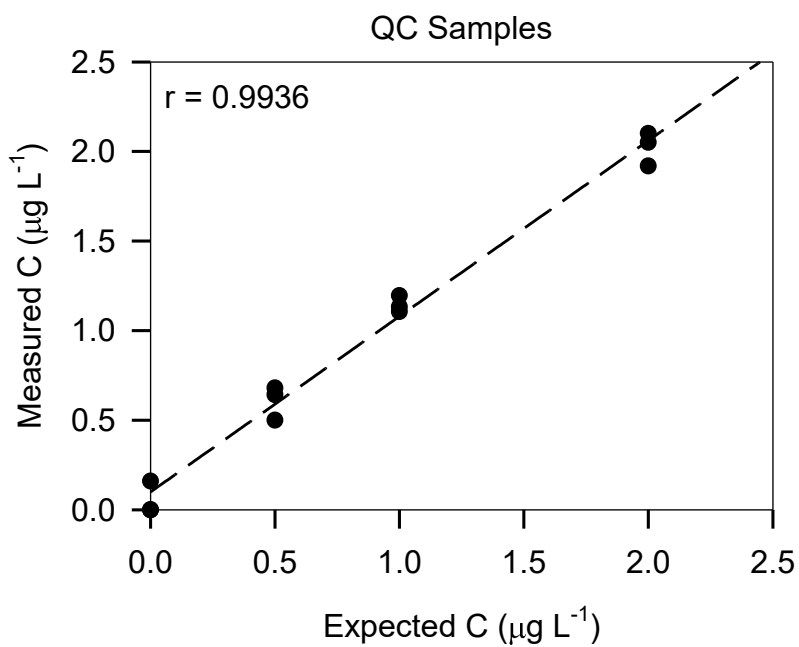


**Figure 3-2** - Scatter plot showing the measured vs. expected concentrations of the QC samples (Blank, 0.5, 1, and 2 µg L<sup>-1</sup>) analyzed with the three POCIS batches. A regression line was fit through the data, with a correlation coefficient value of 0.9936.

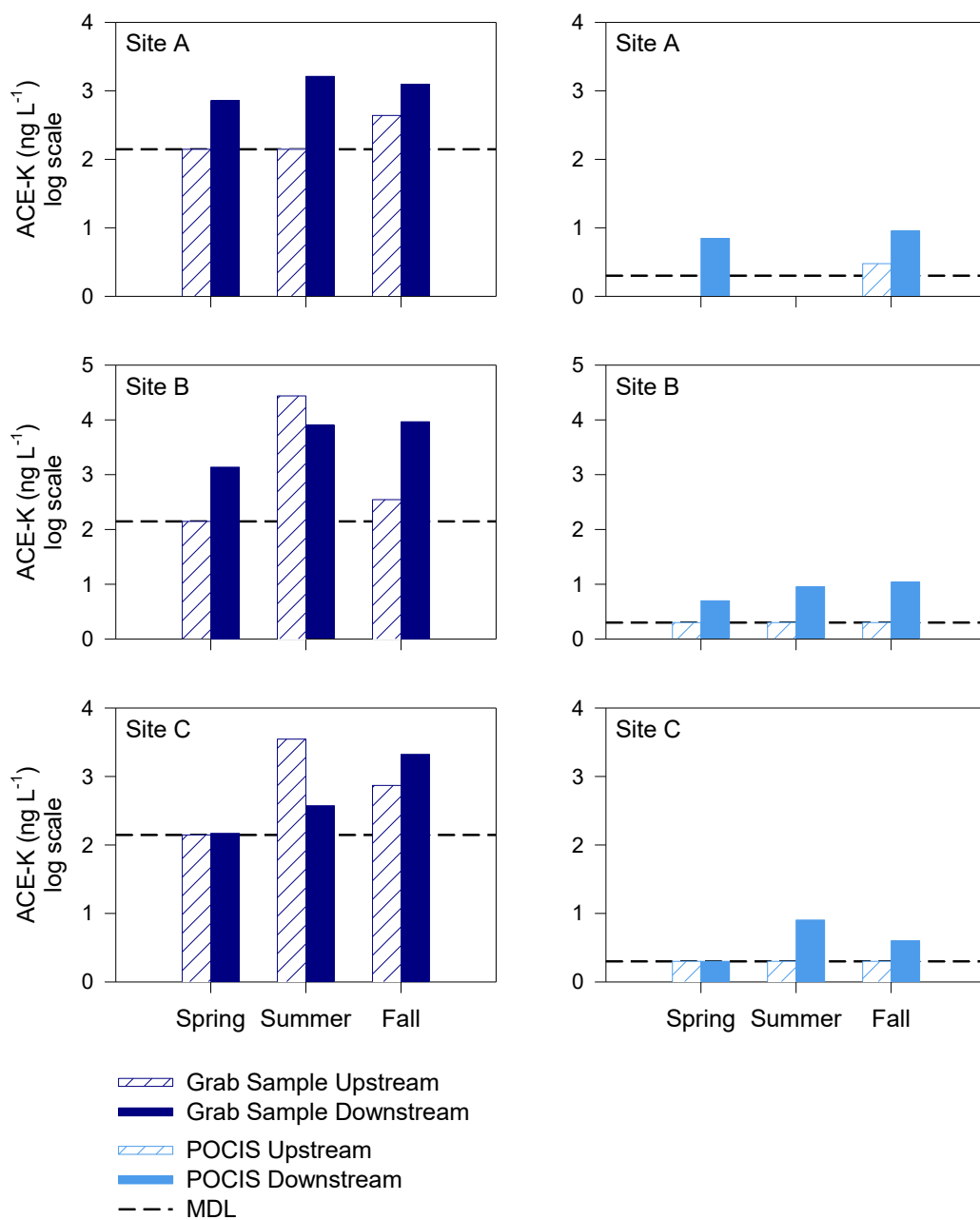


**Figure 3-3** – Bar graphs of the average grab sample and POCIS ACE-K concentrations for the Spring, Summer, and Fall 2017 seasonal study excursions. The grab sample and POCIS MDLs are displayed with dashed and solid lines respectively. POCIS were not deployed at SA-US during the Spring and Summer, nor at SA-DS during the Summer (denoted with “NA”)

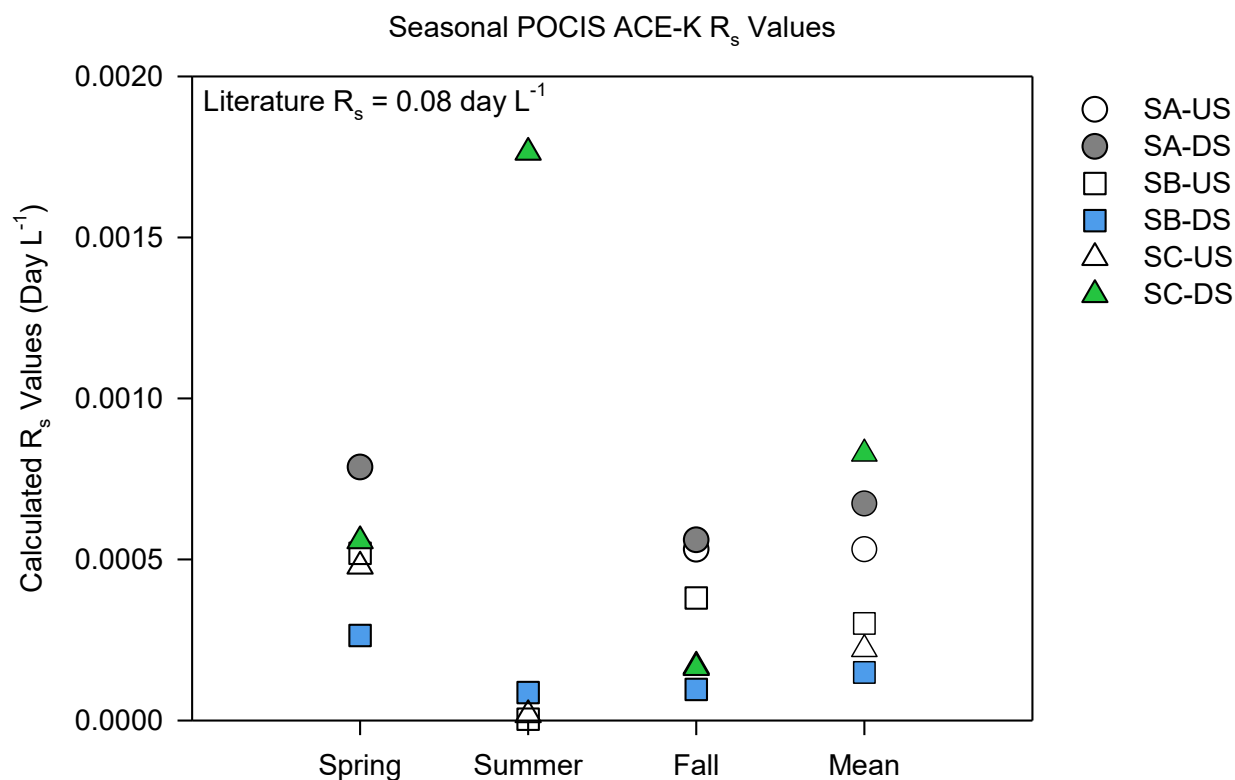


**Figure 3-4** – Scatter-plot of the calculated seasonal POCIS  $R_s$  values for ACE-K during the spring, summer, and fall 2017 for SA-US, SA-DS, SB-US, SB-DS, SC-US, and SC-DS. The mean calculated  $R_s$  values are also displayed. The values were calculated using the mass (ng) of ACE-K measured in each POCIS sample and the mean grab sample ACE-K concentrations for each deployment/retrieval.

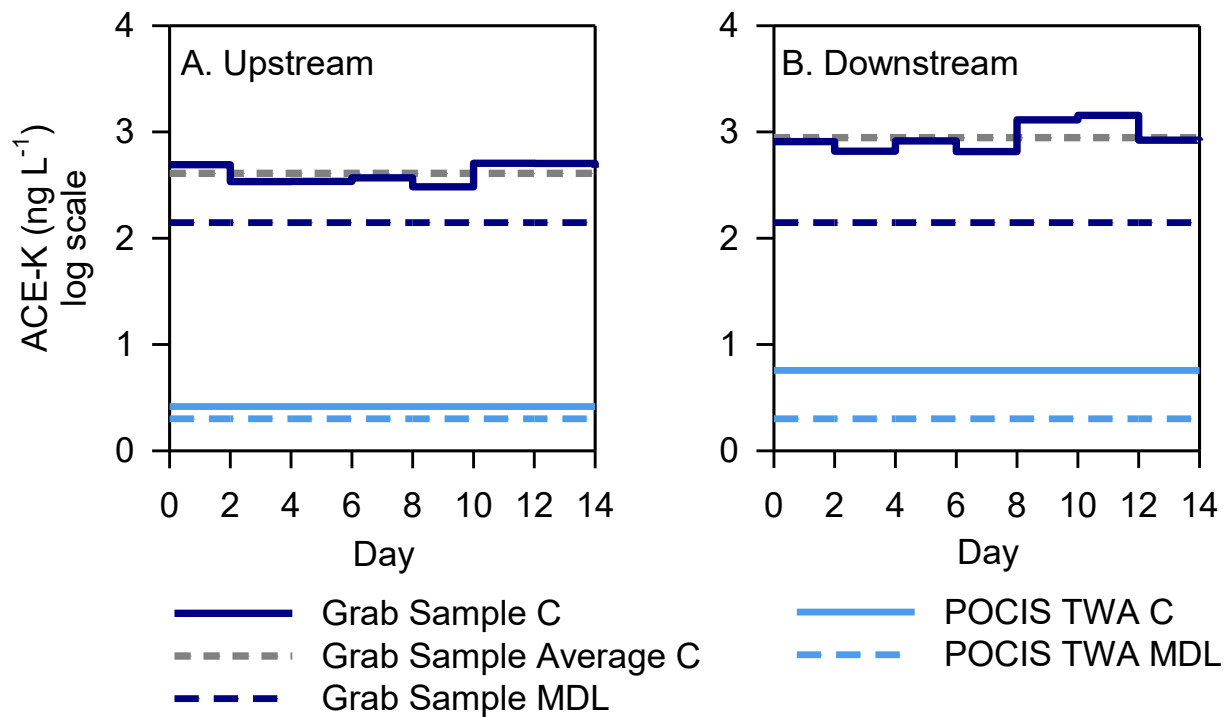


**Figure 3-5** – Stair plots of the ACE-K grab sample concentrations (blue solid line) collected on Day 0, 2, 4, 6, 8, 10, 12, and 14 during the 2-week study at SA-US (A) and SA-DS (B). The solid lines represent the grab sample concentrations (dark blue) and the POCIS TWA concentrations (light blue), and dashed lines show the respective MDLs and average grab sample concentrations.

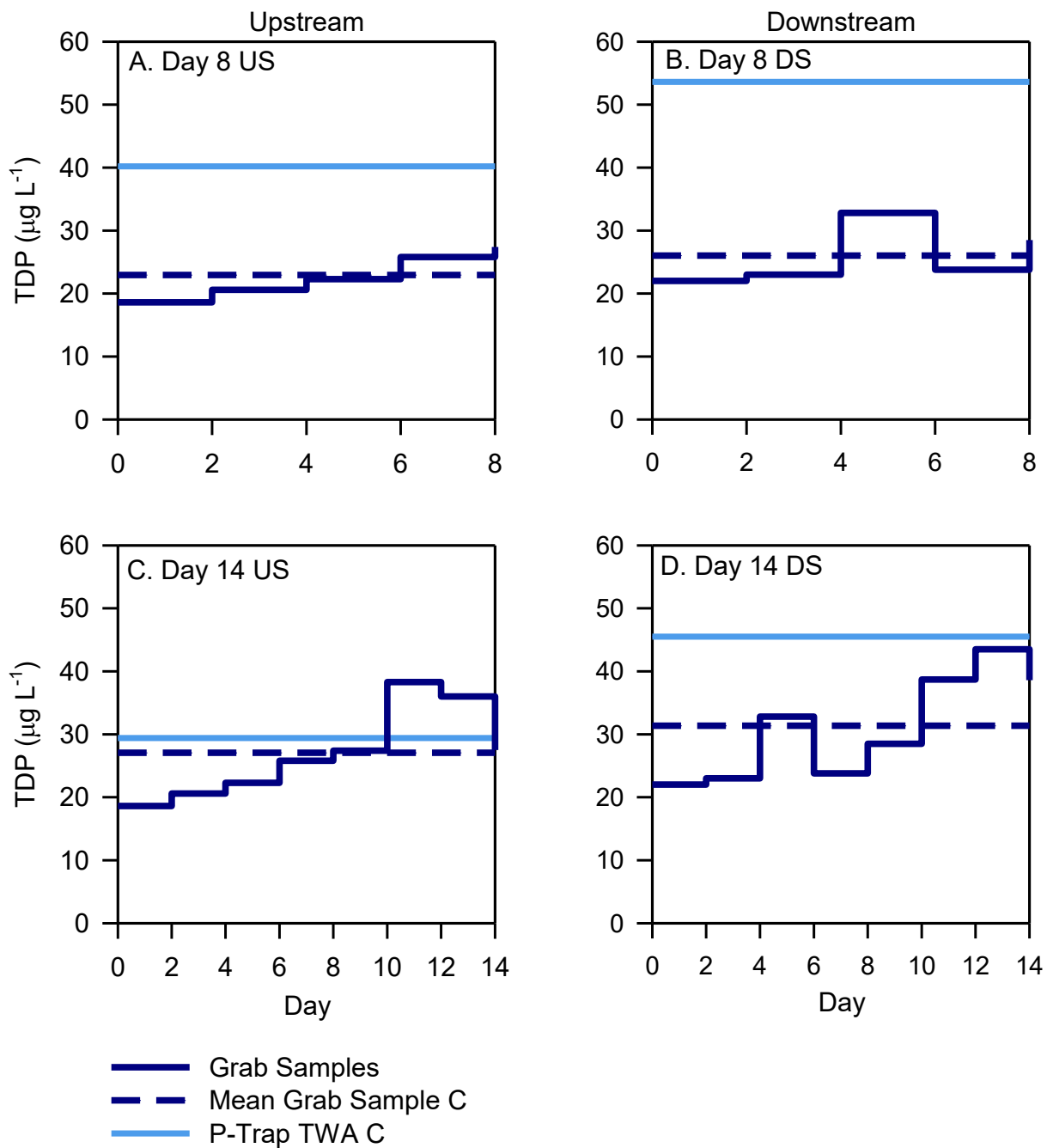


**Figure 3-6** – Stair plots of the TWA TDP and grab sample TDP concentrations for SA-US and SB-DS. The TWA concentrations calculated for the first 8 days (A and B), and for 14 days (C and D) were plotted as red solid lines. The solid blue line and dashed blue line represent the grab sample concentrations and the mean respectively.

**Table 3-1** – Average measurements/concentrations for the parameters measured in the field or laboratory for target water quality indicators, including includes the average concentrations for samples retrieved in Spring 2017, Summer 2017, and Fall 2017, for SA, SB, and SC US and DS samples where applicable. Samples for SA-US during Spring 2017 and Summer 2017, along with SA-DS in Summer 2017 were not included because POCIS were not deployed at these sites during the sampling excursions. The ACE-K mean concentrations are italicized.

		Spring 2017					Summer 2017				Fall 2017					
	Units	SA-DS	SB-US	SB-DS	SC-US	SC-DS	SB-US	SB-DS	SC-US	SC-DS	SA-US	SA-DS	SB-US	SB-DS	SC-US	SC-DS
Temp.	°C	16.1	9.75	15.4	15.9	16.7	14.7	17.4	17.0	17.6	5.65	4.35	6.90	5.50	2.00	2.60
pH	units	8.45	7.85	8.11	8.06	8.35	7.94	8.09	7.98	8.05	7.79	7.93	7.92	8.00	8.37	8.01
DO	mg L <sup>-1</sup>	14.7	8.87	9.79	9.90	12.7	5.93	7.77	8.03	7.90	11.6	13.5	9.9	11.3	10.9	12.1
SPC	µS cm <sup>-1</sup>	1007	798	829	625	625	1047	904	621	827	780	1102	819	813	700	918
Turb.	NTU	1.7	7.1	6.1	5.8	7.8	13	1	1.1	4.3	0.9	1.3	7.0	4.1	0.7	3.3
Alk.	mg L <sup>-1</sup>	216	264	245	260	233	370	259	269	292	326	335	372	323	310	307
DOC	mg L <sup>-1</sup>	3.6	6.6	4.0	5.2	4.1	15.3	36.3	32.1	18.6	31.1	27.7	NA	23.0	23.8	23.5
TS	mg L <sup>-1</sup>	729	614	569	462	474	770	576	482	590	455	647	541	499	468	604
Cl	mg L <sup>-1</sup>	213	37	103	24	35	99	117	143	92	15	73	27	37	27	81
SO <sub>4</sub>	mg L <sup>-1</sup>	32	24	13	11	7	36	7	17	11	9	17	18	21	23	38
Ca	mg L <sup>-1</sup>	78	94	84	86	78	128	79	93	103	108	114	108	103	101	107
K	mg L <sup>-1</sup>	3	6	3	2	2	26	5	2	3	1	3	13	6	3	6
Mg	mg L <sup>-1</sup>	20	26	22	23	21	33	23	29	30	26	27	28	24	26	28
Na	mg L <sup>-1</sup>	112	31	64	28.3	43	48	91	15	50	10	98	31	52	16	52
TP	µg L <sup>-1</sup>	90	574	352	85	149	1915	560	146	142	28	48	492	270	37	251
TDP	µg L <sup>-1</sup>	68	497	301	55	95	1630	447	125	115	19	42	384	219	30	234
SRP	µg L <sup>-1</sup>	61	430	255	48	82	1420	386	111	99	20	30	356	278	25	167
TN	mg L <sup>-1</sup>	8.9	20	7.2	5.3	4.9	11.9	3.5	3.5	1.6	8.9	6.0	6.1	4.3	3.2	5.5
NO <sub>3</sub> -N	mg L <sup>-1</sup>	7.4	15.8	6.3	4.9	4.2	6.4	2.2	3.3	1.2	8.7	6.0	4.0	3.5	3.2	5.3
NO <sub>2</sub> -N	mg L <sup>-1</sup>	0.07	0.25	0.19	0.07	0.09	1.00	0.28	0.02	0.04	0.01	0.03	0.15	0.11	0.02	0.02
NH <sub>3+4</sub> -N	mg L <sup>-1</sup>	0.07	1.62	0.34	0.05	0.20	2.69	0.53	0.03	0.06	0.04	0.06	1.04	0.34	0.03	0.03
<i>ACE-K</i>	<i>ng L<sup>-1</sup></i>	<i>719</i>	<i>&lt; 140</i>	<i>1370</i>	<i>&lt; 140</i>	<i>148</i>	<i>27400</i>	<i>8040</i>	<i>3500</i>	<i>375</i>	<i>437</i>	<i>1250</i>	<i>350</i>	<i>9260</i>	<i>739</i>	<i>2100</i>



**Table 3-2** – Table showing the daily grab sample averages for Days 1, 2, 4, 6, 8, 10, 12, and 14 for SA-US and SA-DS during the 2-week study for a variety of water quality parameter measurements or concentrations. The weekly average for each parameter is also calculated. The ACE-K and TDP concentrations are italicized.

		UPSTREAM									DOWNSTREAM								
		0	2	4	6	8	10	12	14	Average	0	2	4	6	8	10	12	14	Average
Temp.	°C	8.0	8.6	6.8	7.9	8.3	9.1	9.7	10.5	8.6	13.0	12.1	9.3	12.9	10.1	13.2	15.3	12.2	12.3
pH	units	8.14	8.24	8.13	8.16	8.18	8.20	8.25	8.31	8.20	8.41	8.39	8.24	8.20	8.30	8.43	8.46	8.43	8.36
DO	mg L <sup>-1</sup>	11.7	10.6	10.9	10.6	10.9	11.4	10.3	9.9	10.8	15.4	13.4	17.4	16.2	11.9	14.2	13.6	10.6	14.1
SPC	µS cm <sup>-1</sup>	801	841	1016	918	918	946	1057	922	927	1108	1094	1156	933	1290	998	1042	1219	1105
Turb.	NTU	0.3	2.8	2.1	0.4	0.1	0.5	20.1	0.8	3.4	0.5	0.9	0.6	0.9	0.8	1.0	0.8	2.2	0.9
Alk.	mg L <sup>-1</sup>	276	282	283	280	289	288	288	262	281	275	288	274	272	313	300	288	287	287
TS	mg L <sup>-1</sup>	518	579	584	598	599	634	633	591	592	720	731	777	782	811	807	760	733	765
Cl	mg L <sup>-1</sup>	118	82	75	81	76	133	158	100	103	156	119	193	208	214	160	161	242	182
SO4	mg L <sup>-1</sup>	22.7	17.0	18.9	17.1	47.3	16.2	47.6	20.9	25.9	16.3	18.4	15.5	14.5	27.6	19.3	24.0	25.2	20.1
Ca	mg L <sup>-1</sup>	81	103	105	105	111	114	110	108	105	101	102	111	109	118	114	110	108	109
K	mg L <sup>-1</sup>	4.09	3.89	3.92	4.6	5.74	4.99	5.61	5.145	4.75	3.09	3.14	3.60	3.64	4.02	3.94	3.75	3.75	3.62
Mg	mg L <sup>-1</sup>	11.9	24.1	24.8	25.1	25.5	24.6	23.1	22.2	22.6	23.9	23.6	25.7	25.6	25.6	25.1	23.3	22.2	24.3
Na	mg L <sup>-1</sup>	46.8	43.0	48.3	53.1	51.5	56.8	54.8	59.1	51.7	117	106	117	127	131	134	139	132	125
Fe	µg L <sup>-1</sup>	3	3	7	3	3	4	4	6	4	6	7	311	5	11	9	12	21	478
TP	µg L <sup>-1</sup>	22.8	29.3	29.8	30.1	27.3	67.1	49.0	35.1	36.3	34.5	48.5	45.0	42.2	45.1	39.6	44.8	49.1	43.6
<i>TDP</i>	<i>µg L<sup>-1</sup></i>	<i>18.6</i>	<i>20.6</i>	<i>22.3</i>	<i>25.8</i>	<i>27.4</i>	<i>38.3</i>	<i>36.0</i>	<i>27.5</i>	<i>27.1</i>	<i>22.0</i>	<i>23.0</i>	<i>32.8</i>	<i>23.8</i>	<i>28.5</i>	<i>38.7</i>	<i>43.5</i>	<i>38.6</i>	<i>31.4</i>
SRP	µg L <sup>-1</sup>	17.7	23.3	18.6	21.9	23.4	53.3	28.0	26.4	26.6	11.3	12.5	3.95	3.65	17.9	24.6	27.7	25.5	15.9
TN	mg L <sup>-1</sup>	11.8	11.7	12.9	12.9	11.8	12.5	12.8	11.2	12.2	6.90	7.12	7.28	6.90	6.83	6.76	5.05	4.88	6.46
NO <sub>3</sub> -N	mg L <sup>-1</sup>	10.1	10.9	10.9	11.3	11.6	10.8	10.7	9.4	10.7	6.8	6.5	7.5	6.5	6.3	6.0	4.4	4.2	6.0
NO <sub>2</sub> -N	mg L <sup>-1</sup>	0.03	0.03	0.03	0.03	0.03	0.04	0.06	0.07	0.04	0.03	0.05	0.04	0.04	0.05	0.06	0.06	0.07	0.05
NH <sub>3+4</sub> -N	mg L <sup>-1</sup>	0.04	0.04	0.02	0.03	0.01	0.02	0.82	0.07	0.13	0.06	0.03	0.02	0.03	0.28	0.12	0.06	0.05	0.08
<i>ACE-K</i>	<i>ng L<sup>-1</sup></i>	<i>491</i>	<i>341</i>	<i>342</i>	<i>370</i>	<i>304</i>	<i>508</i>	<i>505</i>	<i>460</i>	<i>415</i>	<i>811</i>	<i>659</i>	<i>824</i>	<i>653</i>	<i>1299</i>	<i>1430</i>	<i>836</i>	<i>828</i>	<i>917</i>

## Chapter 4

### Conclusions

#### 4.1 Summary of Findings

Environmental monitoring of rural headwater streams is important to help estimate load contributions of nutrients (P, N) sourced from agricultural runoff and septic systems.

Previous research has successfully shown the usefulness of using a suite of organic tracers to monitor wastewater in surface and ground water (Van Stempvoort et al., 2011b; Liu et al., 2014; Spoelstra et al., 2017; Richards et al., 2017a). Scientific exploration is required to determine innovative ways of tracking nutrient loads to their respective sources.

Additionally, rural areas are sometimes characterized by low dilution streams where organic tracer and nutrient concentrations may be low and difficult to confidently quantify (Richards et al., 2016). One innovative solution for determining concentrations of contaminants within surface waters is the use of passive sampling techniques (Muller et al., 2008; Metcalfe et al., 2014). However, more information on the performance of passive samplers in shallow headwater streams is required.

The findings of the second chapter, “Characterization of Non-point Source Contamination by Septic Systems in Rural Ontario Hamlets”, provide additional information on the use of organic compounds as tracers of domestic wastewater in rural headwater streams. Specifically, the occurrence of ACE-K at concentrations up to three orders of magnitude greater than the concentrations of pharmaceuticals, and the ubiquitous occurrence of host-specific *Bacteroides* in three rural streams, suggests that ACE-K and *Bacteroides* as co-tracers may be an effective tool for water managers to detect and mitigate septic system

impacts on streams in rural communities. The study also showed that there was increased contamination at the two hamlets with finer (e.g. clay/silt) overburden material compared to the hamlet with a coarser grained overburden material. A correlation analysis between the tracer concentrations and the nutrient concentrations did not exhibit many significant results; however, these findings highlight the difficulty in tracking non-point source contamination of nutrients in rural areas.

The findings of the third chapter, “Using Passive Samplers POCIS and P-Traps to Measure Trace Acesulfame-K and Total Dissolved Phosphorus Concentrations in Headwater Streams”, provide insight into the preliminary usage of passive sampling techniques in shallow headwater streams. The findings suggest that there is a potential for using the POCIS and the P-Trap for target organic tracers and P in rural headwater streams under certain conditions. The POCIS time weighted average concentrations were orders of magnitude lower than the average grab sample concentrations. These results highlight the importance of designing a passive sampler that will target the analytes of interest. The POCIS sorbent is more suitable for extracting pharmaceutical compounds (e.g. CBZ, GEM) rather than ACE-K. The P-Trap time weighted average concentrations were calculated based on samplers deployed for 8 days, and 2 weeks, and the samplers that were deployed for a longer time-period provided more representative of average dissolved P concentrations compared to the average grab sample concentrations.

#### **4.1 Future Research and Recommendations**

There was multi-faceted evidence of domestic wastewater impacting streams at all three hamlets in this study. Many homes that dispose of their waste by septic system also rely on

groundwater from domestic wells for their drinking water. Therefore, more research is warranted on assessing groundwater contamination in rural watersheds, especially on identifying potential drivers of contamination, including home density, overburden material, effect of high flow events, and the effect of preferential pathways (e.g. macro pores).

Additional research on applying passive sampling techniques in unconventional shallow streams is necessary to develop environmental monitoring approaches that provide representative concentrations of contaminants. One advantage to passive sampling is that it limits the field excursions required to obtain average stream water concentrations over an extended period of time. One recommendation for future installation in shallow streams is to install a weir which can be used to increase, monitor, and control stream flow to maintain adequate water depth over the sampling period. Additionally, POCIS extracts can be archived and different target analytes can be analyzed in the future.

Acesulfame-K is considered a conservative tracer that has been previously found in treated wastewater and may be considered a useful indicator of domestic wastewater impacts. The development of a passive sampler that adequately retains ACE-K over a long deployment period to obtain quantifiable concentrations of the tracer may be valuable for future monitoring programs. To obtain an accurate time weighted average concentration, the range in uptake rate constants for ACE-K should be expanded, including rates for different temperature, pH, and flow conditions. These rate constants can be acquired using laboratory experiments and can be verified or corrected using performance reference compounds in the field. Passive sampling technologies should be used in future monitoring programs, but there is currently no standard method on how to determine uptake rate constants. Overall, more

scientific application of these new technologies is required to help implement passive sampling in routine environmental monitoring programs in rural headwater streams.

## References

- Aislabie, J., Smith, J.J., Fraser, R., and McLeod, M., 2001, Leaching of bacterial indicators of faecal contamination through four New Zealand soils: *Aust. J. Soil Res.*, v. 39, p. 1397–1406, doi:10.1070/SR00086.
- Alvarez, D.A., 2010, Chapter 4 (Section D): Guidelines for the use of the Semipermeable Membrane Device (SPMD) and the Polar Organic Chemical Integrative Sampler (POCIS) in Environmental Monitoring Studies, *in* Collection of Water Data by Direct Measurement, p. 28.
- American Public Health Association (APHA), 2018, Method 9222: Membrane filter Technique for members of the coliform group, *in* Standard Methods For the Examination of Water and Wastewater, American Public Health Association, Standard Methods for the Examination of Water and Wastewater, doi:doi:10.2105/SMWW.2882.193.
- Aravena, R., Evans, M.L., and Cherry, J.A., 1993, Stable isotopes of oxygen and nitrogen in source identification of nitrate from septic systems: *Ground Water*, v. 31, p. 180–186, doi:10.1111/j.1745-6584.1993.tb01809.x.
- Arheimer, B., and Lide, R., 2000, Nitrogen and phosphorus concentrations from agricultural catchments — influence of spatial and temporal variables: *Journal of Hydrology*, v. 227, p. 140–159, doi:10.1016/S0022-1694(99)00177-8.
- Bartelt-Hunt, S.L., Snow, D.D., Damon-Powell, T., Brown, D., Prasal, G., Schwartz, M., and Kolok, A.S., 2011, Quantitative evaluation of laboratory uptake rates for pesticides, pharmaceuticals, and steroid hormones using POSIS: *Environmental Toxicology and*

Chemistry, v. 30, p. 1412–1420, doi:10.1002/etc.514.

- Baydan, E., Kaya, S., Cagiran, H., Yıldırım, E., Altıntaş, L., Yurdakok, B., Ekici, H., Aydın, F., and Küçükosmanoğlu, A., 2015, Investigation of veterinary drug residues in sea water, sediment, and wild fishes captured around fish farms in the Aegean Sea: Sulfonamides (Sulfamerazine, SMR; Sulfadimidine, SMT; Sulfamethoxazole, SMXZ; Sulfadimethoxine, SDMX): *Journal of Veterinary Pharmacology and Therapeutics*, v. 38, p. 112–113.
- Beven, K., and Germann, P., 1982, Macropores and water flow in soils: *Water Resources Research*, v. 18, p. 1311–1325, doi:10.1029/WR018i005p01311.
- Bitton, G., Farrah, S.R., Ruskin, R.H., Butner, J., and Chou, Y.J., 1983, Survival of pathogenic and indicator organisms in ground water: *Ground Water*, v. 21, p. 405–410, doi:10.1111/j.1745-6584.1983.tb00741.x.
- Blowes, D.W., and Gillham, R.W., 1988, The generation and quality of streamflow on inactive uranium tailings near Elliot Lake, Ontario: *Journal of Hydrology*, v. 97, p. 1–22, doi:10.1016/0022-1694(88)90062-5.
- Bonneau, J., Fletcher, T.D., Costelloe, J.F., and Burns, M.J., 2017, Stormwater infiltration and the ‘urban karst’ – A review: *Journal of Hydrology*, v. 552, p. 141–150, doi:10.1016/j.jhydrol.2017.06.043.
- Buerge, I.J., Buser, H.-R., Kahle, M., Müller, M.D., and Poiger, T., 2009, Ubiquitous occurrence of the artificial sweetener acesulfame in the aquatic environment: An ideal chemical marker of domestic wastewater in groundwater: *Environmental Science & Technology*, v. 43, p. 4381–4385, doi:10.1021/es900126x.

- Buerge, I.J., Keller, M., Buser, H.R., Müller, M.D., and Poiger, T., 2011, Saccharin and other artificial sweeteners in soils: Estimated inputs from agriculture and households, degradation, and leaching to groundwater: *Environmental Science & Technology*, v. 45, p. 615–621, doi:10.1021/es1031272.
- Buerge, I.J., Poiger, T., Müller, M.D., and Buser, H.R., 2003, Caffeine, an anthropogenic marker for wastewater contamination of surface waters: *Environmental Science & Technology*, v. 37, p. 691–700, doi:10.1021/es020125z.
- Canadian Council of Ministers of the Environment (CCME), 2004, Canadian water quality guidelines for the protection of aquatic Life: Phosphorus: Canadian guidance framework for the management of freshwater systems.
- Carey, R.O., and Migliaccio, K.W., 2009, Contribution of wastewater treatment plant effluents to nutrient dynamics in aquatic systems: A review: *Environmental Management*, v. 44, p. 205–217, doi:10.1007/s00267-009-9309-5.
- Carrara, C., Ptacek, C., Robertson, W.D., Blowes, D.W., Moncur, M.C., and Backus, S., 2008, Fate of pharmaceutical and trace organic compounds in three septic system plumes, Ontario, Canada: *Environmental Science & Technology*, v. 42, p. 2805–2811, doi:10.1021/es070344q.
- Chambers, P. et al., 1997, Impacts of municipal wastewater effluents on Canadian waters: A review: *Water Qual. Res. J. Canada*, v. 32, p. 659–713.
- Ciebin, B.W., Brodsky, M.H., Eddington, R., Horsnell, G., Choney, A., Palmateer, G., Ley, A., Joshi, R., and Shears, G., 1995, Comparative evaluation of modified m-FC and m-TEC media for membrane filter enumeration of *Escherichia coli* in water: *Applied and*



- Environmental Microbiology, v. 61, p. 3940–3942, doi:0099-2240.
- Clarke, B.O., Anumol, T., Barlaz, M., and Snyder, S.A., 2015, Investigating landfill leachate as a source of trace organic pollutants: Chemosphere, v. 127, p. 269–275, doi:10.1016/j.chemosphere.2015.02.030.
- Conley, D.J., Paerl, H.W., Howarth, R.W., Boesch, D.F., Seitzinger, S.P., Havens, K.E., Lancelot, C., and Likens, G.E., 2009, Controlling eutrophication : Nitrogen and phosphorus: Science, v. 233, p. 1014–1015, doi:10.1126/science.1167755.
- Conn, K.E., Barber, L.B., Brown, G.K., and Siegrist, R.L., 2006, Occurrence and fate of organic contaminants during onsite wastewater treatment: Environmental Science & Technology, v. 40, p. 7358–7366, doi:10.1021/es0605117.
- Conn, K.E., Habteselassie, M.Y., Blackwood, A.D., and Noble, R.T., 2011, Microbial water quality before and after the repair of a failing onsite wastewater treatment system adjacent to coastal waters: Journal of Applied Microbiology, v. 112, p. 214–224, doi:10.1111/j.1365-2672.2011.05183.x.
- Conn, K.E., Lowe, K.S., Drewes, J.E., Hoppe-Jones, C., and Tucholke, M.B., 2010, Occurrence of pharmaceuticals and consumer product chemicals in raw wastewater and septic tank effluent from single-family homes: Environmental Engineering Science, v. 27, p. 347–358, doi:10.1089/ees.2009.0364.
- Criquet, J., Dumoulin, D., Howsam, M., Mondamert, L., Goossens, J.-F., Prygiel, J., and Billon, G., 2017, Comparison of POCIS passive samplers vs. composite water sampling : A case study: Science of the Total Environment, v. 609, p. 982–991, doi:10.1016/j.scitotenv.2017.07.227.

- D'Alessio, M., Yoneyama, B., Kirs, M., Kisand, V., and Ray, C., 2015, Pharmaceutically active compounds : Their removal during slow sand filtration and their impact on slow sand filtration bacterial removal: *Science of the Total Environment*, v. 524–525, p. 124–135, doi:10.1016/j.scitotenv.2015.04.014.
- Dickenson, E.R.V., Snyder, S.A., Sedlak, D.L., and Drewes, J.E., 2011, Indicator compounds for assessment of wastewater effluent contributions to flow and water quality: *Water Research*, v. 45, p. 1199–1212, doi:10.1016/j.watres.2010.11.012.
- Domagalski, J.L., and Johnson, H.M., 2011, Subsurface transport of orthophosphate in five agricultural watersheds, USA: *Journal of Hydrology*, v. 409, p. 157–171, doi:10.1016/j.jhydrol.2011.08.014.
- Gan, Z., Sun, H., Wang, R., and Feng, B., 2013, A novel solid-phase extraction for the concentration of sweeteners in water and analysis by ion-pair liquid chromatography – triple quadrupole mass spectrometry: *Journal of Chromatography A*, v. 1274, p. 87–96, doi:10.1016/j.chroma.2012.11.081.
- Gibson, C.A., and Meyer, J.L., 2007, Nutrient uptake in a large urban river: *Journal of the American Water Resources Association*, v. 43, p. 576–587, doi:10.1111/j.1752-1688.2007.00041.x.
- Glassmeyer, S.T., Furlong, E.T., Kolpin, D.W., Cahill, J.D., Zaugg, S.D., Werner, S.T., Meyer, M.T., and Kryak, D.D., 2005, Transport of chemical and microbial compounds from known wastewater discharges: Potential for use as indicators of human fecal contamination: *Environmental Science & Technology*, v. 39, p. 5157–5169, doi:10.1021/es048120k.

- Godfrey, E., Woessner, W.W., and Benotti, M.J., 2007, Pharmaceuticals in on-site sewage effluent and ground water, *Western Montana: Ground Water*, v. 45, p. 263–271, doi:10.1111/j.1745-6584.2006.00288.x.
- Gruber, N., and Galloway, J.N., 2008, An Earth-system perspective of the global nitrogen cycle: *NATURE*, v. 451, p. 10–13, doi:10.1038/nature06592.
- Harman, C., Boyum, O., Thomas, K.V., and Grung, M., 2009, Small but different effect of fouling on the uptake rates of semipermeable membrane devices and polar organic chemical integrative samplers: *Environmental Toxicology and Chemistry*, v. 28, p. 2324–2332.
- Harman, J., Robertson, W.D., Cherry, J.A., and Zanini, L., 1996, Impacts on a sand aquifer from an old septic system: Nitrate and phosphate: *Ground Water*, v. 34, p. 1105–1114, doi:10.1111/j.1745-6584.1996.tb02177.x.
- Hoque, M.E., Cloutier, F., Arcieri, C., McInnes, M., Sultana, T., Murray, C., Vanrolleghem, P.A., and Metcalfe, C.D., 2014, Removal of selected pharmaceuticals, personal care products and artificial sweetener in an aerated sewage lagoon: *Science of the Total Environment*, v. 487, p. 801–812, doi:10.1016/j.scitotenv.2013.12.063.
- Hutchins, R.H.S., 2011, Dissolved Organic Matter in the Anthropogenically Impacted Grand River and Natural Burnt River Watersheds:
- International Joint Commission (IJC), 2018, Fertilizer Application Patterns and Trends and Their Implications for Water Quality in the Western Lake Erie Basin.:
- James, C.A., Miller-schulze, J.P., Ultican, S., Gipe, A.D., and Baker, J.E., 2016, Evaluating Contaminants of Emerging Concern as tracers of wastewater from septic systems: *Water*

- Research, v. 101, p. 241–251, doi:10.1016/j.watres.2016.05.046.
- Jarvie, H.P. et al., 2010, Streamwater phosphorus and nitrogen across a gradient in rural-agricultural land use intensity: *Agriculture, Ecosystems and Environment*, v. 135, p. 238–252, doi:10.1016/j.agee.2009.10.002.
- Jian-ye, G., Wei, S., Chen-Ling, Z., Yong-Tao, Z., Li, Z., and Fei, L., 2016, An innovative approach to sensitive artificial sweeteners analysis by ion chromatography - triple quadrupole mass spectrometry: *Chinese Journal of Analytical Chemistry*, v. 44, p. 361–366, doi:10.1016/S1872-2040(16)60914-3.
- Jiang, J., Lee, C., and Fang, M., 2014, Emerging organic contaminants in coastal waters : Anthropogenic impact , environmental release and ecological risk: *Marine Pollution Bulletin*, v. 85, p. 391–399, doi:10.1016/j.marpolbul.2013.12.045.
- Kaserzon, S.L., Hawker, D.W., Booij, K., O'Brien, D.S., Kennedy, K., Vermeirssen, E.L.M., and Mueller, J.F., 2014, Passive sampling of perfluorinated chemicals in water: In-situ calibration: *Environmental Pollution*, v. 186, p. 98–103, doi:10.1016/j.envpol.2013.11.030.
- Kaushal, S.S., and Belt, K.T., 2012, The urban watershed continuum: Evolving spatial and temporal dimensions: *Urban Ecosystem*, v. 15, p. 409–435, doi:10.1007/s11252-012-0226-7.
- Keegan, M., Kilroy, K., Nolan, D., Dubber, D., Johnston, M., Misstear, B.D.R., O'Flaherty, V., Barrett, M., and Gill, L.W., 2014, Assessment of the impact of traditional septic tank soakaway systems on water quality in Ireland: *Water Science & Technology*, v. 70, p. 634–641, doi:10.2166/wst.2014.227.

- Knappett, P.S.K. et al., 2012, Implications off fecal bacteria input from latrine-polluted ponds for wells in sandy aquifers: *Environmental Science & Technology*, v. 46, p. 1361–1370, doi:10.1021/es202773w.
- Lee, D.Y., Lee, H., Trevors, J.T., Weir, S.C., Thomas, J.L., and Habash, M., 2014, Characterization of sources and loadings of fecal pollutants using microbial source tracking assays in urban and rural areas of the Grand River Watershed, Southwestern Ontario: *Water Research*, v. 53, p. 121–131, doi:10.1016/j.watres.2014.01.003.
- Lee, D., Weir, S.C., Lee, H., and Trevors, J.T., 2010, Quantitative identification of fecal water pollution sources by TaqMan real-time PCR assays using Bacteroidales 16S rRNA genetic markers: *Appl. Microbiol. Biotechnol.*, v. 88, p. 1373–1383, doi:10.1007/s00253-010-2880-0.
- LESPRRT, 2008, Grand River Watershed Characterization Report.:
- Li, H., Helm, P.A., and Metcalfe, C.D., 2010a, Sampling in the great lakes for pharmaceuticals, personal care products, and endocrine-disrupting substances using the passive polar organic chemical integrative sampler: *Environmental Toxicology and Chemistry*, v. 29, p. 751–762, doi:10.1002/etc.104.
- Li, H., Helm, P.A., Paterson, G., and Metcalfe, C.D., 2011, The effects of dissolved organic matter and pH on sampling rates for polar organic chemical integrative samplers ( POCIS ): *Chemosphere*, v. 83, p. 271–280, doi:10.1016/j.chemosphere.2010.12.071.
- Li, H., Vermeirssen, E.L.M., Helm, P.A., and Metcalfe, C.D., 2010b, Controlled field evaluation of water flow rate effects on sampling polar compounds using polar organic chemical integrative samplers: *Environmental Toxicology and Chemistry*, v. 29, p.

2461–2469, doi:10.1002/etc.305.

Liu, Y., Blowes, D.W., Groza, L., Sabourin, M.J., and Ptacek, C.J., 2014, municipal wastewater in a receiving river: *Environmental Science Processes & Impacts*, v. 16, p. 2789–2795, doi:10.1039/c4em00237g.

Lusk, M.G., Toor, G.S., Yang, Y.-Y., Mechtensimer, S., De, M., and Obreza, T.A., 2017, A review of the fate and transport of nitrogen, phosphorus, pathogens, and trace organic chemicals in septic systems: *Environmental Science & Technology*, v. 47, p. 455–541, doi:10.1080/10643389.2017.1327787 A.

MacLeod, S.L., McClure, E.L., and Wong, C.S., 2007, Laboratory calibration and field deployment of the polar organic chemical integrative sampler for pharmaceuticals and personal care products in wastewater and surface water: *Environmental Toxicology & Chemistry*, v. 26, p. 2517–2529, doi:10.1897/07-238.1.

Marti, R. et al., 2013, Quantitative multi-year elucidation of fecal sources of waterborne pathogen contamination in the South Nation River basin using Bacteroidales microbial source tracking markers: *Water Research*, v. 47, p. 2315–2324, doi:10.1016/j.watres.2013.02.009.

Mazzella, N., Lissalde, S., Moreira, S., Mazellier, P., and Huckins, J.N., 2010, Evaluation of the use of performance reference compounds in an Oasis-HLB adsorbent based passive sampler for improving water concentration estimates of polar herbicides in freshwater: *Environ. Sci. Technol.*, v. 44, p. 1713–1719, doi:10.1021/es902256m.

Metcalfe, C., Hoque, M.E., Sultana, T., Murray, C., Helm, P., and Kleywegt, S., 2014, Monitoring for contaminants of emerging concern in drinking water using POCIS

passive samplers: *Environmental Science Processes & Impacts*, v. 16, p. 473–481,  
doi:10.1039/c3em00508a.

Van Metre, P.C., Alvarez, D.A., Mahler, B.J., Nowell, L., Sandstrom, M., and Moran, P.,  
2017, Complex mixtures of pesticides in Midwest U.S. streams indicated by POCIS  
time-integrating samplers: *Environmental Pollution*, v. 220, p. 431–440,  
doi:10.1016/j.envpol.2016.09.085.

Mihelcic, J.R., Fry, L.M., and Shaw, R., 2011, Global potential of phosphorus recovery from  
human urine and feces: *Chemosphere*, v. 84, p. 832–839,  
doi:10.1016/j.chemosphere.2011.02.046.

Minet, E.P., Goodhue, R., Meier-Augenstein, W., Kalin, R.M., Fenton, O., Richards, K.G.,  
and Coxon, C.E., 2017, Combining stable isotopes with contamination indicators: A  
method for improved investigation of nitrate sources and dynamics in aquifers with  
mixed nitrogen inputs: *Water Research*, v. 124, p. 85–96,  
doi:10.1016/j.watres.2017.07.041.

MOE, 2015a, DOP-E3036: The determination of total phosphorus by colourimetry.

MOE, 2014a, E3497: The determination of metals in water by inductively coupled plasma-  
optical emission spectroscopy (ICP-OES) using an Apex desolvation system.

MOE, 2014b, RNDNP-E2264: The determination of ammonia nitrogen, nitrite nitrogen,  
nitrite plus nitrate nitrogen and reactive ortho-phosphate in waters by colourimetry.

MOE, 2014c, SOLIDS-E3188: The determination of solids in liquid matrices by gravimetry.

MOE, 2015b, WATS-E3218: The determination of conductivity, pH, and alkalinity in water  
and effluents by potentiometry.

- Morin, N., Camilleri, J., Cren-Olive, C., Coquery, M., and Miege, C., 2013, Determination of uptake kinetics and sampling rates for 56 organic micropollutants using “pharmaceutical” POCIS: *Talanta*, v. 109, p. 61–73, doi:10.1016/j.talanta.2013.01.058.
- Muller, B., Stierli, R., and Gachter, R., 2008, A low-tech, low-cost passive sampler for the long-term monitoring of phosphate loads in rivers and streams: *Journal of Environmental Monitoring*, v. 10, p. 785–900, doi:10.1039/b806465b.
- Neilen, A.D., Chen, C.R., Parker, B.M., Faggotter, S.J., and Burford, M.A., 2017, Differences in nitrate and phosphorus export between wooded and grassed riparian zones from farmland to receiving waterways under varying rainfall conditions: *Science of the Total Environment*, v. 598, p. 188–197, doi:10.1016/j.scitotenv.2017.04.075.
- Odagiri, M., Schriewer, A., Hanley, K., Wuertz, S., Misra, P.R., Panigrahi, P., and Jenkins, M.W., 2015, Validation of Bacteroidales quantitative PCR assays targeting human and animal fecal contamination in the public and domestic domains in India: *Science of the Total Environment*, The, v. 502, p. 462–470, doi:10.1016/j.scitotenv.2014.09.040.
- Oliver, D.M., Clegg, C.D., Heathwaite, A.L., and Haygarth, P.M., 2007, Preferential attachment of *Escherichia coli* to different particle size fractions of an agricultural grassland soil: *Water Air Soil Pollut.*, v. 185, p. 369–375, doi:10.1007/s11270-007-9451-8.
- Ontario Geological Survey (OGS), 2010, *Surficial Geology of Southern Ontario: Project Summary and Technical Document.*
- Oppenheimer, J., Eaton, A., Badruzzaman, M., Haghani, A.W., and Jacangelo, J.G., 2011, Occurrence and suitability of sucralose as an indicator compound of wastewater loading



to surface waters in urbanized regions: *Water Research*, v. 45, p. 4019–4027,  
doi:10.1016/j.watres.2011.05.014.

Palmer-Felgate, E.J., Mortimer, R.J.G., Krom, M.D., and Jarvie, H.P., 2010, Impact of point-source pollution on phosphorus and nitrogen cycling in stream-bed sediments: *Environmental Science & Technology*, v. 44, p. 908–914.

Pang, L., Close, M., Goltz, M., Noonan, M., and Sinton, L., 2005, Filtration and transport of *Bacillus subtilis* spores and the F-RNA phage MS2 in a coarse alluvial gravel aquifer: Implications in the estimation of setback distances: *Journal of Contaminant Hydrology*, v. 77, p. 165–194, doi:10.1016/j.jconhyd.2004.12.006.

Peed, L.A., Nietch, C.T., Kelty, C.A., Meckes, M., Mooney, T., Sivaganesan, M., and Shanks, O.C., 2011, Combining land use information and small stream sampling with PCR-based methods for better characterization of diffuse sources of human fecal pollution: *Environmental Science & Technology*, v. 45, p. 5652–5659,  
doi:10.1021/es2003167.

Peeler, K.A., Opsahl, S.P., and Chanton, J.P., 2006, Tracking anthropogenic inputs using caffeine, indicator bacteria, and nutrients in rural freshwater and urban marine systems: *Environmental Science & Technology*, v. 40, p. 7616–7622, doi:10.1021/es061213c.

Ptacek, C.J., 1998, Geochemistry of a septic-system plume in a coastal barrier bar, Point Pelee, Ontario, Canada: *Journal of Contaminant Hydrology*, v. 33, p. 293–312,  
doi:10.1016/S0169-7722(98)00076-X.

Richards, S., Paterson, E., Withers, P.J.A., and Stutter, M., 2016, Septic tank discharges as multi-pollutant hotspots in catchments: *Science of the Total Environment*, v. 542, p.

854–863, doi:10.1016/j.scitotenv.2015.10.160.

Richards, S., Paterson, E., Withers, P.J.A., and Stutter, M., 2015, The contribution of household chemicals to environmental discharges via effluents : Combining chemical and behavioural data: *Journal of Environmental Management*, v. 150, p. 427–434, doi:10.1016/j.jenvman.2014.12.023.

Richards, S., Withers, P.J.A., Paterson, E., McRoberts, C.W., and Stutter, M., 2017a, Potential tracers for tracking septic tank effluent discharges in watercourses: *Environmental Pollution*, v. 228, p. 245–255, doi:10.1016/J.ENVPOL.2017.05.044.

Richards, S., Withers, P.J.A., Paterson, E., McRoberts, C.W., and Stutter, M., 2017b, Removal and attenuation of sewage effluent combined tracer signals of phosphorus, caffeine and saccharin in soil: *Environmental Pollution*, v. 223, p. 277–285, doi:10.1016/j.envpol.2017.01.024.

Ridley, C.M., Jamieson, R.C., Truelstrup Hansen, L., Yost, C.K., and Bezanson, G.S., 2014, Baseline and storm event monitoring of Bacteroidales marker concentrations and enteric pathogen presence in a rural Canadian watershed: *Water Research*, v. 60, p. 278–288, doi:10.1016/j.watres.2014.04.039.

Robertson, W.D., and Harman, J., 1999, Phosphate plume persistence at two decommissioned septic system sites: *Ground Water*, v. 37, p. 228–236, doi:10.1111/j.1745-6584.1999.tb00978.x.

Robertson, W.D., Schiff, S.L., and Ptacek, C.J., 1998, Review of phosphate mobility and persistence in 10 Septic system plumes: *Ground Water*, v. 36, p. 1000–1010, doi:10.1111/j.1745-6584.1998.tb02107.x.

- Robertson, W.D., Van Stempvoort, D.R., Solomon, D.K., Homewood, J., Brown, S.J., Spoelstra, J., and Schiff, S.L., 2013, Persistence of artificial sweeteners in a 15-year-old septic system plume: *Journal of Hydrology*, v. 477, p. 43–54, doi:10.1016/j.jhydrol.2012.10.048.
- Saurette, E.M., Groza, L.G., Blowes, D.W., and Ptacek, C.J., 2017, Storage and preservation of artificial sweeteners in groundwater samples: *Groundwater Monitoring & Remediation*, v. 37, p. 71–81, doi:10.1111/gwmr.12249.
- Schaider, L.A., Rodgers, K.M., and Rudel, R.A., 2017, Review of Organic Wastewater Compound Concentrations and Removal in Onsite Wastewater Treatment Systems:, doi:10.1021/acs.est.6b04778.
- Scheurer, M., Florian, R., Graf, C., Ruck, W., Lev, O., and Lange, F.T., 2011, Correlation of six anthropogenic markers in wastewater, surface water, bank filtrate, and soil aquifer treatment: *Journal of Environmental Monitoring*, v. 13, p. 966–973, doi:10.1039/c0em00701c.
- Schindler, D.W., 1977, Evolution of phosphorus limitation in lakes: *Science*, v. 195, p. 260–262.
- Schoumans, O.F., Chardon, W.J., Bechmann, M.E., Gascuel-Oudou, C., Hofman, G., Kronvang, B., Rubæk, G.H., Ulén, B., and Dorioz, J.-M., 2014, Mitigation options to reduce phosphorus losses from the agricultural sector and improve surface water quality : A review: *Science of the Total Environment*, v. 468–469, p. 1255–1266, doi:10.1016/j.scitotenv.2013.08.061.
- Schriewer, A. et al., 2010, Presence of Bacteroidales as a predictor of pathogens in surface

- waters of the central California Coast: *Applied & Environmental Microbiology*, v. 76, p. 5802–5814, doi:10.1128/AEM.00635-10.
- Sharp, J., 2010, The impacts of urbanization on groundwater systems and recharge: v. 1, 51-56 p., doi:10.4409/Am-004-10-0008.
- Sinton, L.W., 1986, Microbial contamination of alluvial gravel aquifers by septic tank effluent: *Water, Air, and Soil Pollution*, v. 28, p. 407–425, doi:10.1007/BF00583504.
- Sinton, L.W., 1980, Two antibiotic-resistant strains of *Escherichia coli* for tracing the movement of sewage in groundwater: *Journal of Hydrology (New Zealand)*, v. 19, p. 119–130, doi:10.1016/S0022-1694(96)03293-3.
- Snider, D.M., Roy, J.W., Robertson, W.D., Garda, D.I., and Spoelstra, J., 2017, Concentrations of artificial sweeteners and their Ratios with nutrients in septic system wastewater: *Groundwater Monitoring & Remediation*, v. 37, p. 94–102, doi:10.1111/gwmr.12229.
- Somnark, P., Chyerochana, N., Mongkolsuk, S., and Sirikanchana, K., 2018, Performance evaluation of Bacteroidales genetic markers for human and animal microbial source tracking in tropical agricultural: *Environmental Pollution*, v. 236, p. 100–110, doi:10.1016/j.envpol.2018.01.052.
- Sowah, R.A., Habteselassie, M.Y., Radcliffe, D.E., Bauske, E., and Risse, M., 2017, Isolating the impact of septic systems on fecal pollution in streams of suburban watersheds in Georgia, United States: *Water Research*, v. 108, p. 330–338, doi:10.1016/j.watres.2016.11.007.
- Spoelstra, J., Schiff, S.L., and Brown, S.J., 2013, Artificial sweeteners in a large Canadian

- river reflect human consumption in the watershed: *PLoS ONE*, v. 8,  
doi:10.1371/journal.pone.0082706.
- Spoelstra, J., Senger, N.D., and Schiff, S.L., 2017, Artificial sweeteners reveal septic system effluent in rural groundwater: *Journal of Environmental Quality*, v. 46, p. 1434–1443,  
doi:10.2134/jeq2017.06.0233.
- Stadler, L.B., Vela, J.D., Jain, S., Dick, G.J., and Love, N.G., 2017, Elucidating the impact of microbial community biodiversity on pharmaceutical biotransformation during wastewater treatment: *Microbial Biotechnology*, v. 11, p. 995–1007, doi:10.1111/1751-7915.12870.
- Van Stempvoort, D.R., Robertson, W.D., and Brown, S.J., 2011a, Artificial sweeteners in a large septic plume: *Ground Water Monitoring & Remediation*, v. 31, p. 95–102,  
doi:10.1111/j1745.
- Van Stempvoort, D.R., Roy, J.W., Brown, S.J., and Bickerton, G., 2011b, Artificial sweeteners as potential tracers in groundwater in urban environments: *Journal of Hydrology*, v. 401, p. 126–133, doi:10.1016/j.jhydrol.2011.02.013.
- Van Stempvoort, D.R., Roy, J.W., Grabuski, J., Brown, S.J., Bickerton, G., and Sverko, E., 2013, An artificial sweetener and pharmaceutical compounds as co-tracers of urban wastewater in groundwater: *Science of the Total Environment*, v. 461–462, p. 3480–359, doi:10.1016/j.scitotenv.2013.05.001.
- Sultana, T., Murray, C., Hoque, M.E., and Metcalfe, C.D., 2017, Monitoring contaminants of emerging concern from tertiary wastewater treatment plants using passive sampling modelled with performance reference compounds: *Environmental Monitoring &*

- Assessment, v. 189, p. 19, doi:10.1007/s10661-016-5706-4.
- Tambalo, D.D., Fremaux, B., Boa, T., and Yost, C.K., 2012, Persistence of host-associated Bacteroidales gene markers and their quantitative detection in an urban and agricultural mixed prairie watershed: *Water Research*, v. 6, p. 2891–2904, doi:10.1016/j.watres.2012.02.048.
- United States Environmental Protection Agency (USEPA), 2018, Method 6010D: Inductively coupled plasma-optical emission spectrometry.:
- Vermeirssen, Etienne, L.M., Dietschweiler, C., Escher, B.I., van der Voet, J., and Hollender, J., 2012, Transfer kinetics of polar organic compounds over polyethersulfone membranes in the passive samplers POCIS and Chemcatcher: *Environmental Science & Technology*, doi:10.1021/es3007854.
- Weiss, R.F., 1970, The solubility of nitrogen, oxygen and argon in water and seawater: *Deep-Sea Research*, v. 17, p. 721–735.
- Wilhelm, S.D., Schiff, S.L., and Robertson, W.D., 1994, Chemical fate and transport in a domestic septic system: Unsaturated and saturated zone geochemistry: *Environmental Toxicology and Chemistry*, v. 13, p. 193–203, doi:10.1002/etc.5620130203.
- Withers, P.J.A., Jarvie, H.P., and Stoate, C., 2011, Quantifying the impact of septic tank systems on eutrophication risk in rural headwaters: *Environment International*, v. 37, p. 644–653, doi:10.1016/j.envint.2011.01.002.
- Withers, P.J.A., and Sharpley, A.N., 2008, Characterization and apportionment of nutrient and sediment sources in catchments: *Journal of Contaminant Hydrology*, v. 350, p. 127–130, doi:10.1016/j.jhydrol.2007.10.054.

World Health Organization (WHO), 2001, Water Quality: Guidelines, Standards and Health:

London, UK, IWA Publishing.

YSI Environmental, 2005, Environmental Dissolved Oxygen Values Above 100% Air

Saturation.

## **Appendix A:**

### **QA/QC Results for Chapter 2**

#### *General Water Chemistry Analysis*

For the target anions Cl and SO<sub>4</sub>, five standards were run to produce calibration curves for each run, with concentrations between 0.12 and 3 mg L<sup>-1</sup> and between 0.6 and 15 mg L<sup>-1</sup> for Cl and SO<sub>4</sub> respectively. The mean accuracies for the calibration standards were 99.124% for Cl and 116.882% for SO<sub>4</sub>. The calibration curves had mean r<sup>2</sup> values of 0.9992 and 1.116 for Cl and SO<sub>4</sub> respectively. The MDLs were 0.0023 (Cl) and 0.0431 mg L<sup>-1</sup> (SO<sub>4</sub>). Blanks were run every five samples, and spiked QC samples were run after every five unknown samples. The major cation and trace metal samples were run with three QC samples, a blank, and a spiked sample between every 19 unknown samples (MOE, 2014a). The target analytes (MDL) were: Ag (9 µg L<sup>-1</sup>), Al (2 µg L<sup>-1</sup>), Ba (0.1 µg L<sup>-1</sup>), Be (0.1 µg L<sup>-1</sup>), Bi (5 µg L<sup>-1</sup>), Ca (0.05 mg L<sup>-1</sup>), Cd (0.9 µg L<sup>-1</sup>), Co (1 µg L<sup>-1</sup>), Cr (1 µg L<sup>-1</sup>), Cu (0.5 µg L<sup>-1</sup>), Fe (3 µg L<sup>-1</sup>), K (0.02 mg L<sup>-1</sup>), Li (5 µg L<sup>-1</sup>), Mg (0.01 mg L<sup>-1</sup>), Mn (0.5 µg L<sup>-1</sup>), Mo (2 µg L<sup>-1</sup>), Na (0.02 mg L<sup>-1</sup>), Ni (2 µg L<sup>-1</sup>), Pb (µg L<sup>-1</sup>), Sn (µg L<sup>-1</sup>), Sr (0.3 µg L<sup>-1</sup>), Ti (0.5 µg L<sup>-1</sup>), U (3 µg L<sup>-1</sup>), V (0.5 µg L<sup>-1</sup>), Zn (2 µg L<sup>-1</sup>), and Zr (1 µg L<sup>-1</sup>) (MOE, 2014a). The DOC samples were run with nine-point calibration curve (0-20 µg L<sup>-1</sup>); the mean r<sup>2</sup> value for the calibration curves was 0.9998. Blanks were run every eight samples. The MDL was 0.031 mg L<sup>-1</sup>. The runs for TN, NO<sub>2</sub>-N, NO<sub>2+3</sub>-N, and NH<sub>3+4</sub>-N were made up of eight standards, a blank, three QC samples, and thirty unknown samples (MOE, 2014b). The TP and TDP samples had an MDL of 0.18 µg L<sup>-1</sup>.



### *ACE-K Analysis*

Calibration standards for ACE-K ranged between 0.05 and 50  $\mu\text{g L}^{-1}$  and a five- to seven-point curve was used to analyze each sample batch. The mean accuracy (%) and RSD% for the calibration standards was  $125 \pm 39\%$ . The calibration standards were fitted to a linear curve with a mean  $r^2$  value of 0.9998 ( $n = 8$ ). Continuing calibration verification (CCV) samples were run between every five unknown samples. The mean accuracy and RSD% of the CCV samples was  $126 \pm 32\%$ . Spiked 50:50 by volume tap water and ultrapure water samples were run between every five samples as quality control (QC) samples with concentrations ranging between 0.5 and 5  $\mu\text{g L}^{-1}$ . The mean accuracy (%) and RSD% for these QC samples was  $132 \pm 37\%$ , which was similar to accuracies for the calibration standards and CCV samples. The mean absolute IS recovery and RSD% for these QC samples was  $53 \pm 17\%$ , which was similar to the absolute IS for the unknown samples:  $57 \pm 24\%$ . The relative IS recovery for the unknown samples was calculated based on the QC samples and accounted for matrix effects found in the environmental samples. The mean relative IS recovery and RSD% for the unknown samples was  $110 \pm 20\%$ . The method detection limit (MDL) was calculated by analyzing eight spiked blank samples and multiplying the standard deviation by the t value for the student's t test (d.o.f. = 7). The calculated MDL was multiplied by 2.0 to account for the dilution factor applied to the unknown samples prior to injection. The final MDL was calculated as 0.14  $\mu\text{g L}^{-1}$ .

### *Pharmaceutical Analysis*

Two calibration curves, a low range and a high range with eight to 12 points, were used to analyze the samples with concentration ranges between 0.01-10  $\mu\text{g L}^{-1}$  and 1-50  $\mu\text{g L}^{-1}$

respectively. The mean accuracy and RSD% for all calibration standards were: CAF  $100 \pm 11\%$ ; CBZ  $100 \pm 19\%$ ; GEM  $99 \pm 4\%$ ; IBU  $100 \pm 8\%$ ; NAP  $99 \pm 8\%$ ; and SMX  $103 \pm 11\%$ . Each calibration curve was fit with a linear regression curve with a  $1/x^2$  weighting. The mean  $r^2$  values for each analyte were: 0.9973 for CAF; 0.9969 for CBZ; 0.9996 for GEM; 0.9972 for IBU, 0.9953 for NAP; and 0.9977 for SMX. Furthermore, CCV samples were run between every five to ten unknown samples. The mean accuracy and RSD% for these samples were:  $103 \pm 46\%$  for CAF;  $97 \pm 13\%$  for CBZ;  $100 \pm 3\%$  for GEM;  $97 \pm 7\%$  for IBU;  $101 \pm 12\%$  for NAP; and  $97 \pm 14\%$  for SMX. The mean absolute IS recovery and RSD% for the CCV samples were: CAF  $104 \pm 16\%$ ; CBZ  $104 \pm 14\%$ ; GEM  $103 \pm 7$ ; IBU  $108 \pm 5\%$ ; NAP  $106 \pm 6\%$ ; and SMX  $111 \pm 14\%$ . QC samples and blanks were also extracted in each batch and added to each analytical run. The mean accuracy and RSD% for the spiked QC samples were consistent: CAF  $73 \pm 26$ ; CBZ  $73 \pm 19$ ; GEM  $74 \pm 13$ ; IBU  $72 \pm 25$ ; NAP  $74 \pm 10$ ; and SMX  $73 \pm 22$ . The mean absolute IS recoveries and RSD% for these QC samples were: CAF  $152 \pm 42$ ; CBZ  $119 \pm 26$ ; GEM  $95 \pm 24$ ; IBU  $100 \pm 16$ ; NAP  $95 \pm 25$ ; and SMX  $100 \pm 44$ . Some of the blanks had trace peaks, but none of the measured concentrations were greater than the MDLs. The mean absolute IS recoveries and RSD% for the method blanks were: CAF  $132 \pm 35$ ; CBZ  $118 \pm 29$ ; GEM  $99 \pm 30$ ; IBU  $103 \pm 16$ ; NAP  $95 \pm 29$ ; and SMX  $98 \pm 33$ . Blind spiked samples using the same matrix as the environmental samples were also assessed during each sample batch. The mean accuracy and RSD% for each analyte were similar to the QC samples: CAF  $85 \pm 23$ ; CBZ  $69 \pm 7$ ; GEM  $73 \pm 6$ ; IBU  $65 \pm 5$ ; NAP  $74 \pm 7$ ; and SMX  $64 \pm 12$ . The mean absolute IS and RSD% were: CAF  $132 \pm 35$ ; CBZ  $96 \pm 34$ ; GEM  $85 \pm 16$ ; IBU  $87 \pm 18$ ; NAP  $71 \pm 17$ ; and SMX  $88 \pm 32$ . The absolute IS recoveries for unknown samples were: CAF  $108 \pm 37$ ; CBZ  $89 \pm 32$ ; GEM  $80 \pm 28$ ; IBU  $82 \pm$

27; NAP  $59 \pm 32$ ; and SMX  $71 \pm 36$ . The mean relative IS recoveries and RSD% for unknown samples were: CAF  $103 \pm 37$ ; CBZ  $101 \pm 25$ ; GEM  $100 \pm 17$ ; IBU  $99 \pm 16$ ; NAP  $99 \pm 20$ ; and SMX  $99 \pm 29$ . The MDLs for each target analyte were calculated by passing spiked ultrapure water samples through the same SPE cartridges and analyzed seven times on the instrument using the same method. The calculated MDLs were then divided by 500 to account for the concentration factor used during the SPE process to obtain the following MDLs ( $\text{ng L}^{-1}$ ): 0.162 for CAF; 0.438 for CBZ; 0.032 for GEM; 0.228 for IBU; 0.254 for NAP; 0.394 for SMX.

## Appendix B: Additional Figures/Tables for Chapter 2

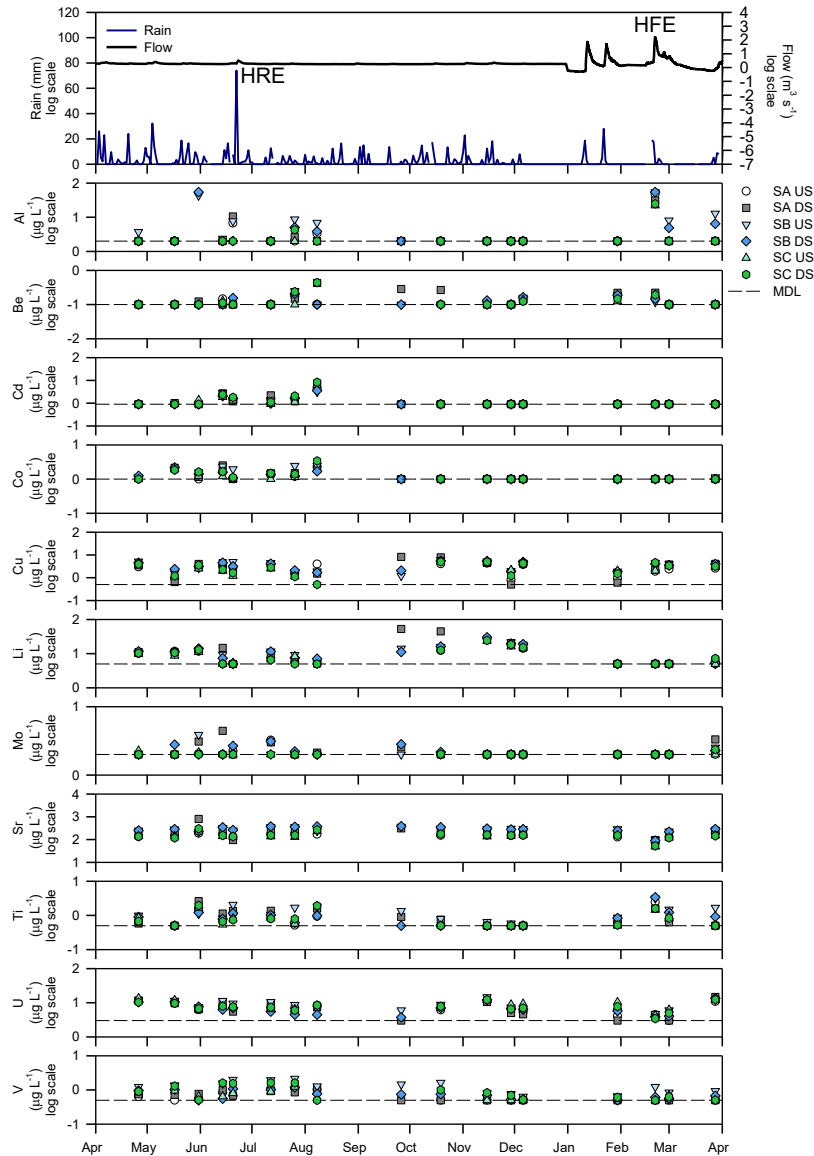


**Figure B-1** - Spatial-temporal multiple line plot displaying annual fluctuations in rain (mm) and flow ( $m^3 s^{-1}$ ) between April 1, 2017 and March 31, 2018, followed by multiple scatter plots displaying annual data for Site A (SA) upstream (US), SA downstream (DS), Site B (SB) US, SB DS, SC US, and SC DS for: Al, Be, Cd, Co, Cu, Li, Mo, Sr, Ti, U, and V. Note all parameter scales are displayed as log (exponents are shown). Dashed lines represent the MDLs. The high rainfall event (HRE) and high flow event (HFE) are noted on the multiple line plot.

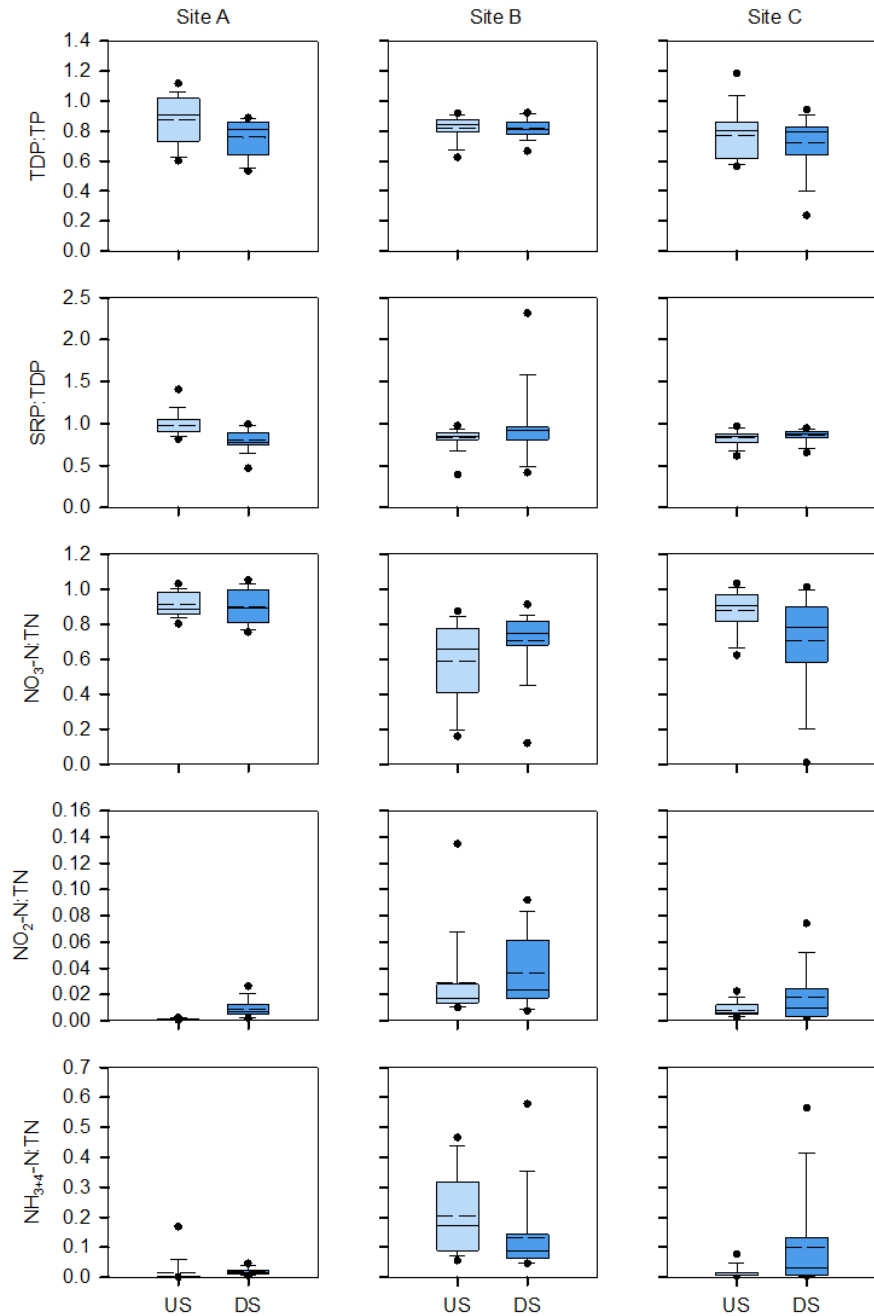


**Figure B-2** - Box and whisker plots of the annual proportions of TDP:TP, SRP:TDP, NO<sub>3</sub>-N:TN, NO<sub>2</sub>-N:TN, and NH<sub>3+4</sub>-N:TN for SA, SB, and SC US and DS concentrations. The solid and dashed lines represent the median and mean respectively. The dotted lines represent outliers in the dataset.

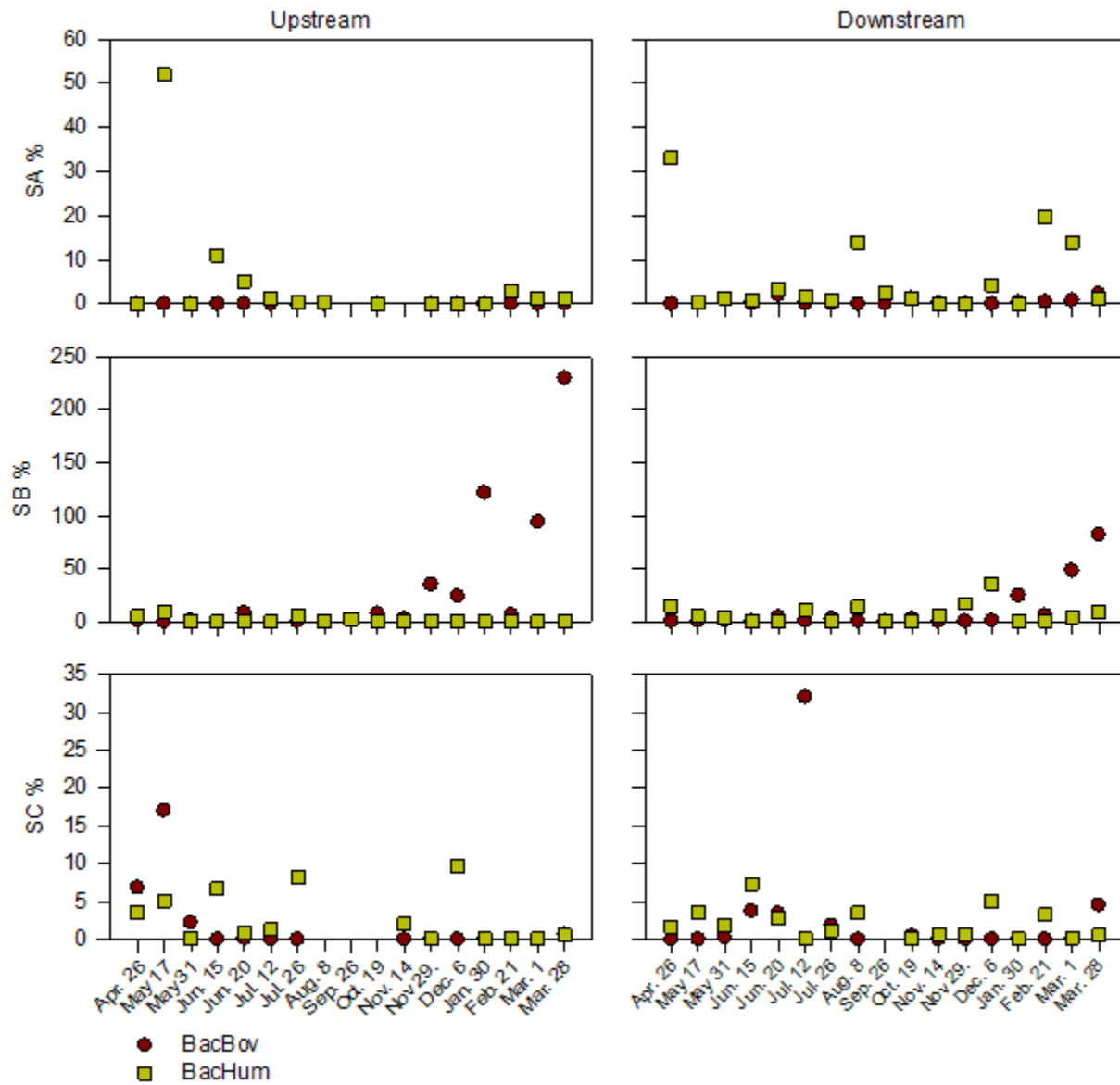


**Figure B-3** - Scatter plot displaying the proportion of BacGen that is BacBov (%) and BacHum (%) at the upstream and downstream of Site A (SA), Site B (SB), and Site C (SC) between April 26, 2017 and March 28, 2018.

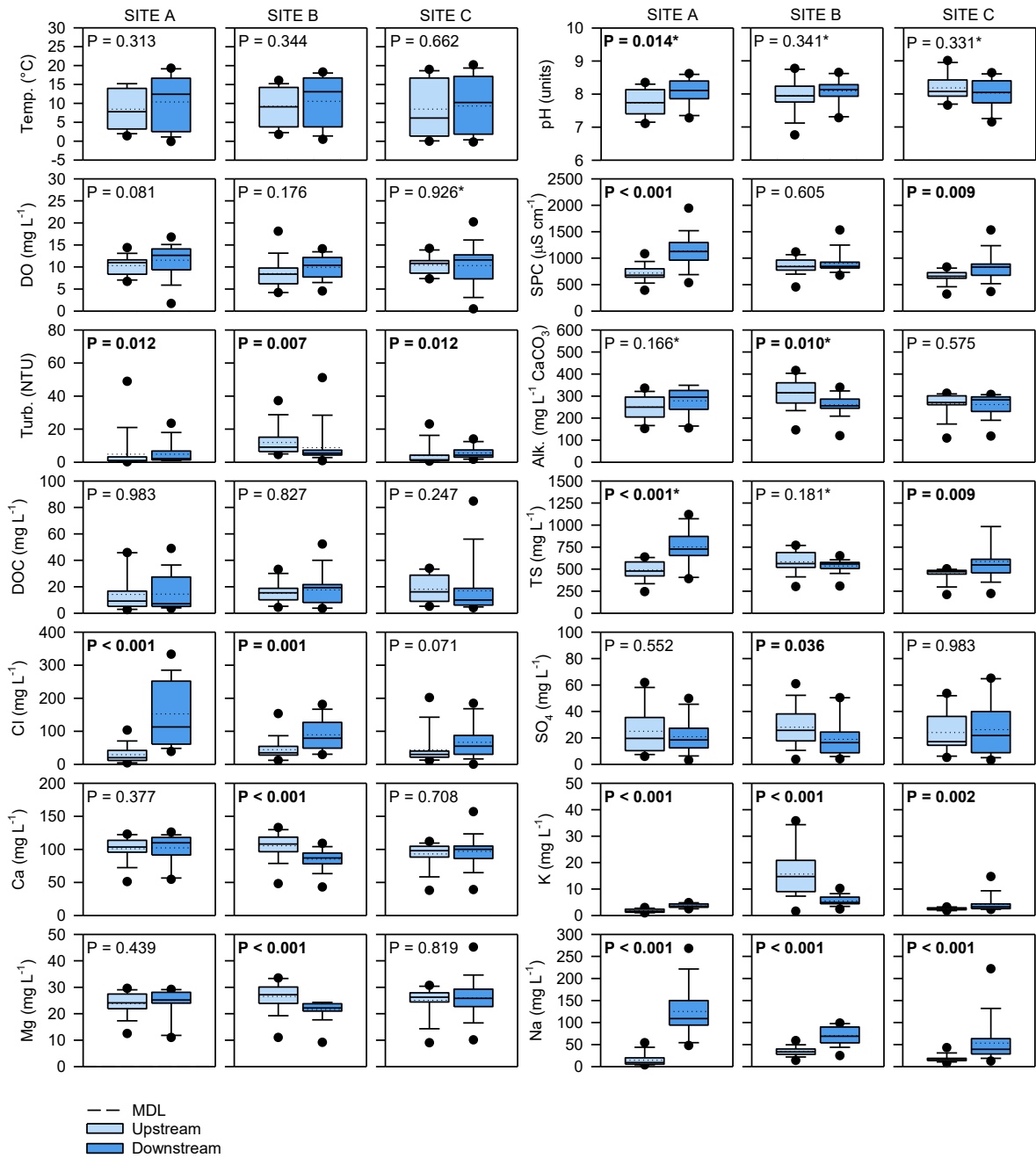


**Figure B-4** - Box and whisker plots displaying the annual measurements and concentrations of temperature, pH, DO, SPC, turbidity, alkalinity, DOC, TS, Cl, SO<sub>4</sub>, Ca, K, Mg, and Na at Sites A, B, and C upstream and downstream sites. The points represent outliers in the dataset and the dotted and solid lines represent the mean and median respectively. The MDLs were not displayed on the graphs as all data points were measured above the MDL. The P-values for the Mann Whitney Rank Sum Order tests are displayed on each graph, and the results obtained from a student's t-test are marked with an asterisk (\*). Bolded P-values are statistically significant ( $P < 0.05$ ).

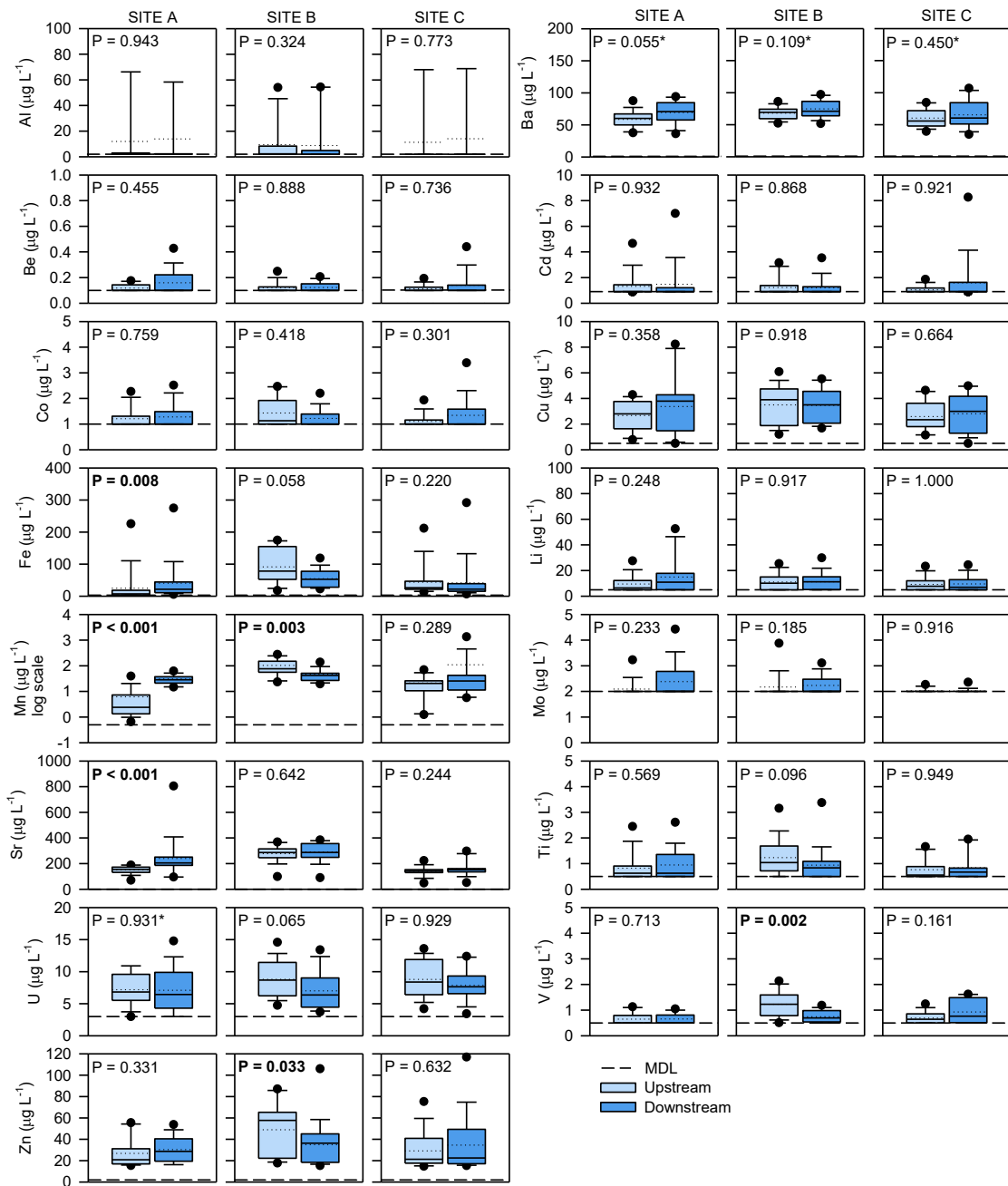


**Figure B-5** - Box and whisker plots displaying the annual concentrations of Al, Ba, Be, Cd, Co, Cu, Fe, Li, Mn, Mo, Sr, Ti, U, V, and Zn at Sites A, B, and C upstream and downstream sites. The points represent outliers in the dataset and the dotted and solid lines represent the mean and median respectively. The MDLs were not displayed on the graphs as all data points were measured above the MDL. The P-values for the Mann Whitney Rank Sum Order tests are displayed on each graph, and the results obtained from a student's t-test are marked with an asterisk (\*). Bolded P-values are statistically significant ( $P < 0.05$ ).



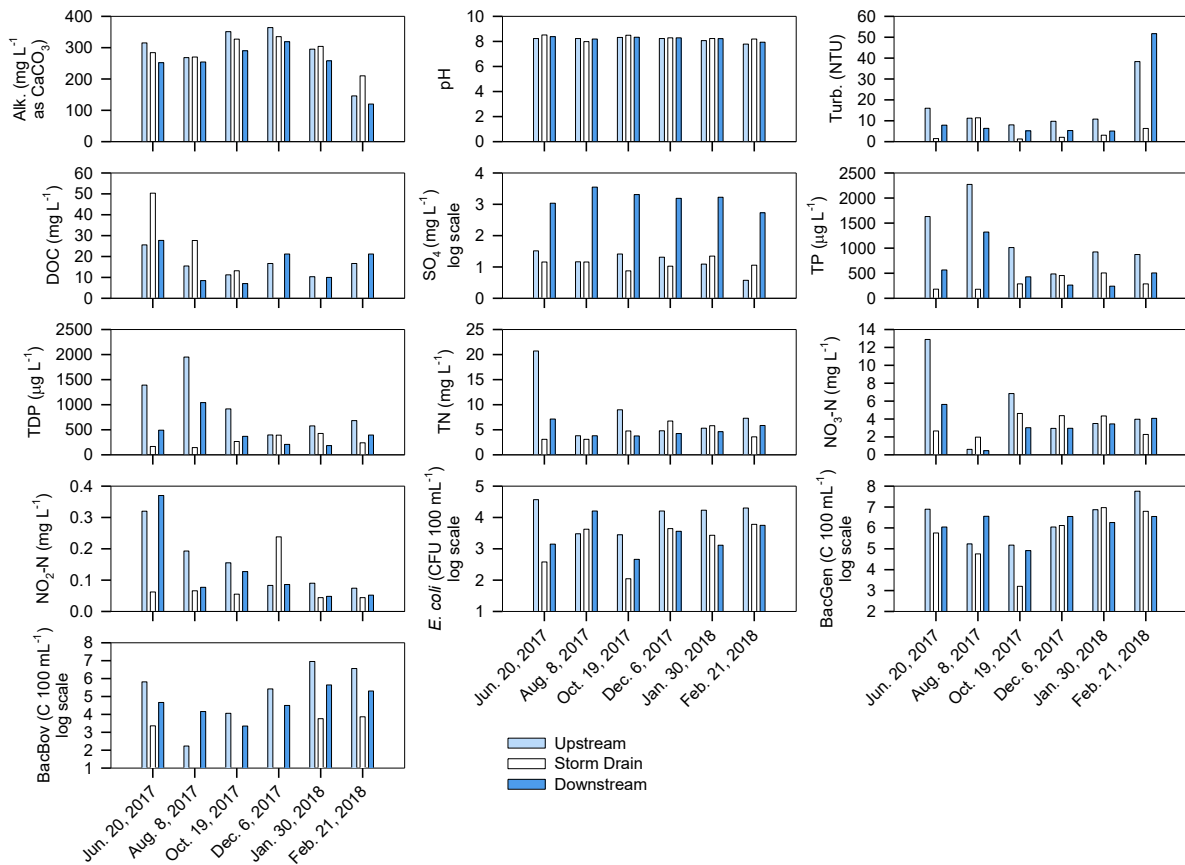


**Figure B-6** - Bar graphs showing the measurements or concentrations of alkalinity (Alk.), pH, turbidity (Turb.), dissolved organic carbon (DOC), sulfate (SO<sub>4</sub>), total phosphorus (TP), total dissolved phosphorus (TDP), total nitrogen (TN), nitrate-nitrogen (NO<sub>3</sub>-N), nitrite-nitrogen (NO<sub>2</sub>-N), *E. coli*, BacGen, and BacBov at the upstream, storm drain, and downstream sites at Site B over six sampling occasions between June 20, 2017 and February 21, 2018. Note that some data are displayed using a log scale. Samples were not taken for DOC on December 6, 2017, January 30, 2018, or February 21, 2018.

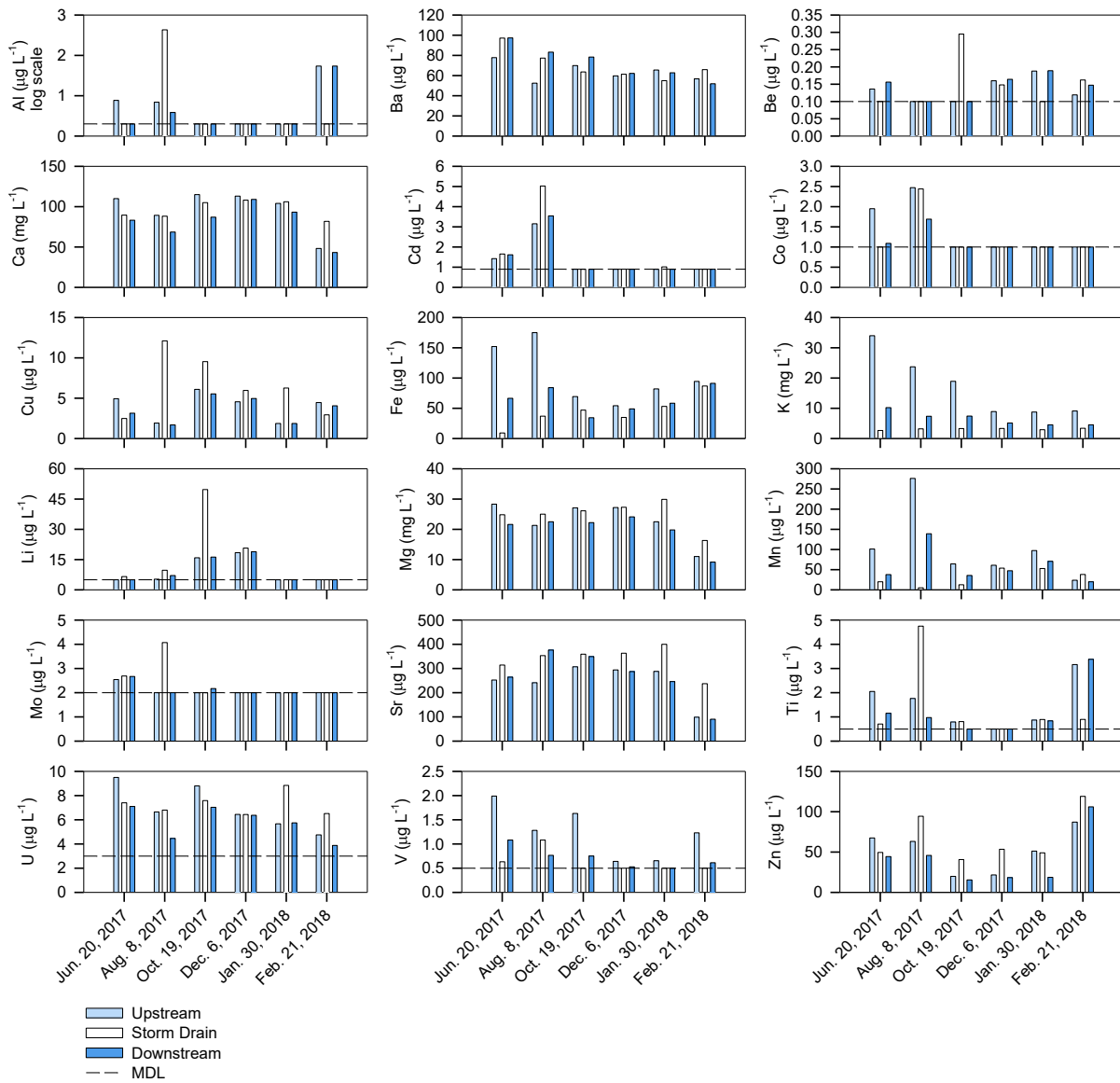


**Figure B-7** - Bar graphs showing the concentrations of trace metals: aluminum (Al), barium (Ba), beryllium (Be), calcium (Ca), cadmium (Cd), cobalt (Co), copper (Cu), iron (Fe), potassium (K), lithium (Li), magnesium (Mg), manganese (Mn), molybdenum (Mo), strontium (Sr), titanium (Ti), uranium (U), vanadium (V), and zinc (Zn) at the upstream, storm drain, and downstream sites at Site B over six sampling occasions between June 20, 2017 and February 21, 2018. Note that some data are displayed using a log scale. Measurements of silver, bismuth, chromium, nickel, lead, tin, and zirconium are not displayed as the concentrations were consistently below the MDLs. The MDLs on the graphs are displayed using a dashed line.

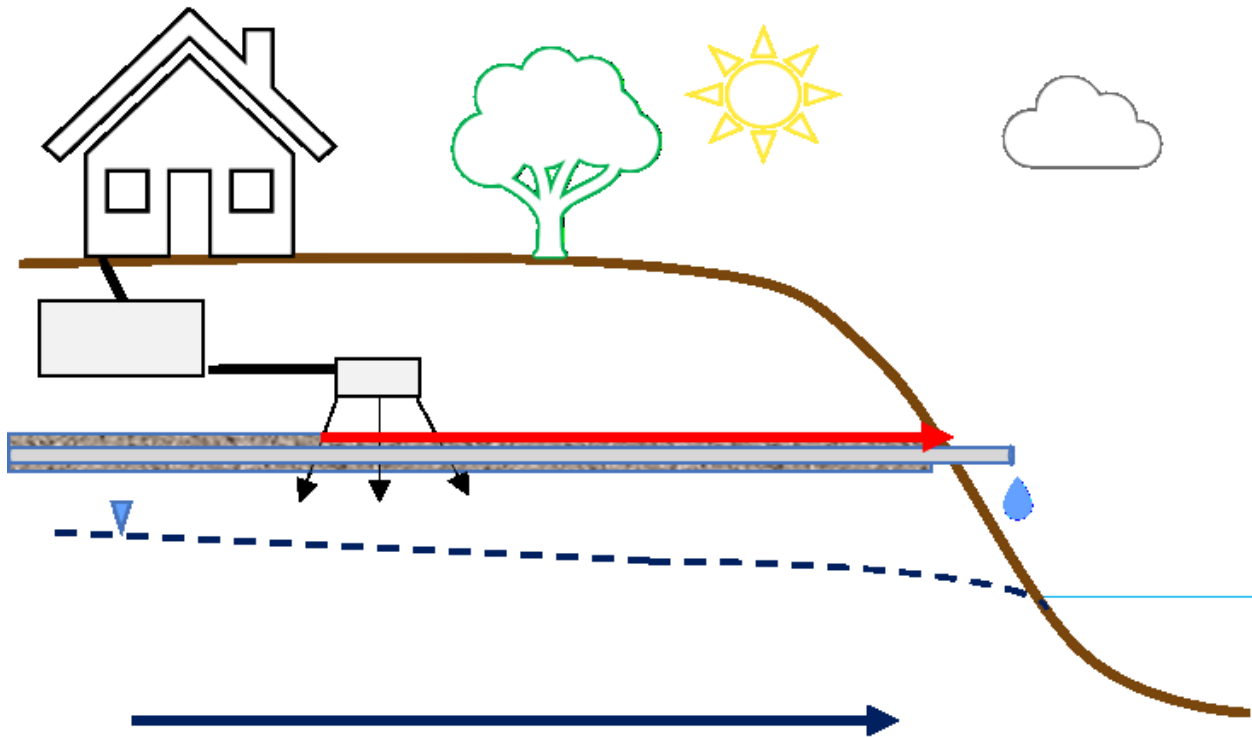


**Figure B-8** – Schematic of the higher-permeability pathways that may exist in hamlets and may be interacting with drain fields, providing preferential pathways for contaminants to reach surface waters prior to attenuation or removal.

**Table B-1** - Statistical summary table for general water quality, FIB, and organic tracer concentrations measured at Site A Upstream and Downstream sample sites. Min. = minimum; Max. = maximum; Med. = median; Std. Dev. = standard deviation; n = count. Results measured below detection limits for the target parameter are reported as < MDL.

		Upstream (n = 16)*					Downstream (n = 17)**				
For:	units:	Min.	Max.	Med.	Mean	Std. Dev.	Min.	Max.	Med.	Mean	Std. Dev.
Temp.	°C	1.4	15.2	7.8	8.5	4.9	-0.1	19.3	12.4	10.4	7.0
pH	units	7.11	8.35	7.74	7.74	0.40	7.28	8.62	8.11	8.10	0.38
DO	mg L <sup>-1</sup>	6.7	14.4	11.0	10.3	2.1	1.7	16.8	12.6	11.5	3.50
SPC	µS cm <sup>-1</sup>	393	1082	678	719	147	537	1944	1126	1136	297
Turb.	NTU	0.2	48.9	1.0	4.9	11.6	1.1	23.5	2.2	4.9	6.1
Alk.	mg L <sup>-1</sup> CaCO <sub>3</sub>	152	336	250	251	53	155	349	295	279	58
DOC	mg L <sup>-1</sup>	2.68	45.8	9.15	14.2	13.8	3.56	49.0	7.12	14.5	12.7
TS	mg L <sup>-1</sup>	244	637	479	490	105	391	1120	728	753	187
Cl	mg L <sup>-1</sup>	4.14	104	20.3	29.5	25.0	38.8	333	113	153	94.3
SO <sub>4</sub>	mg L <sup>-1</sup>	5.97	61.9	19.6	25.0	16.3	3.06	49.8	18.5	21.0	12.7
Ca	mg L <sup>-1</sup>	51.1	123	104	101	17.0	54.7	126	110	102	21.8
K	mg L <sup>-1</sup>	0.97	2.98	1.62	1.82	0.62	2.48	4.84	3.45	3.62	0.75
Na	mg L <sup>-1</sup>	3.82	54.2	9.17	14.8	13.5	47.7	268	109	125	54.0
Mg	mg L <sup>-1</sup>	12.5	29.6	24.1	23.9	4.12	11.0	29.2	25.2	24.1	5.43
Ag	µg L <sup>-1</sup>	< 9	< 9	< 9	< 9	0	< 9	< 9	< 9	< 9	0
Al	µg L <sup>-1</sup>	< 2	112	< 2	12	28	< 2	168	< 2	14.0	39.1
Ba	µg L <sup>-1</sup>	37.8	87.8	60.2	58.7	12.8	36.4	94.1	70.8	69.5	17.0
Be	µg L <sup>-1</sup>	< 0.1	0.175	< 0.1	0.119	0.027	< 0.1	0.428	< 0.1	0.160	0.091
Bi	µg L <sup>-1</sup>	< 5	< 5	< 5	< 5	0	< 5	< 5	< 5	< 5	0
Cd	µg L <sup>-1</sup>	< 0.9	4.67	< 0.9	1.33	0.94	< 0.9	7.01	< 0.90	1.49	1.47
Co	µg L <sup>-1</sup>	< 1	2.27	< 1	1.21	0.38	< 1	2.52	< 1.00	1.28	0.47
Cr	µg L <sup>-1</sup>	< 1	1.39	< 1	1.02	0.09	< 1	< 1	< 1	< 1	0
Cu	µg L <sup>-1</sup>	0.79	4.30	2.80	2.67	1.13	< 0.5	8.24	3.79	3.38	2.19
Fe	µg L <sup>-1</sup>	< 3	226	7.2	25.2	53.7	5.7	275	21.6	40.8	60.9
Li	µg L <sup>-1</sup>	< 5	27.6	6.4	9.6	6.1	< 5.0	52.6	10.9	14.9	13.8
Mn	µg L <sup>-1</sup>	0.66	39.9	2.40	6.25	9.32	14.8	62.4	28.4	30.9	12.8
Mo	µg L <sup>-1</sup>	< 2	3.23	< 2	2.10	0.30	< 2.0	4.43	< 2.0	2.38	0.67
Ni	µg L <sup>-1</sup>	< 2	< 2	< 2	< 2	0	< 2	< 2	< 2	< 2	0
Pb	µg L <sup>-1</sup>	< 7	< 7	< 7	< 7	0	< 7	< 7	< 7	< 7	0
Sn	µg L <sup>-1</sup>	< 9	< 9	< 9	< 9	0	< 9	< 9	< 9	< 9	0
Sr	µg L <sup>-1</sup>	71	189	154	151	28	95	805	205	241	150
Ti	µg L <sup>-1</sup>	< 0.5	2.45	0.63	0.82	0.52	< 0.5	2.61	0.63	0.95	0.57
U	µg L <sup>-1</sup>	< 3	10.9	6.83	7.19	2.39	1.99	14.8	6.44	6.99	3.45
V	µg L <sup>-1</sup>	< 0.5	1.13	< 0.5	0.65	0.23	< 0.5	1.05	0.50	0.66	0.19
Zn	µg L <sup>-1</sup>	15.5	55.5	20.9	26.9	12.8	16.2	53.9	28.7	30.4	11.9
Zr	µg L <sup>-1</sup>	< 1	< 1	< 1	< 1	0	< 1	< 1	< 1	< 1	0
<i>E. coli</i>	CFU 100 mL <sup>-1</sup>	> 4	4.3E+3	16	466	1.1E+3	660	5.1E+4	2.3E+3	5.9E+3	1.2E+4
BacGen	C 100 mL <sup>-1</sup>	150	1.4E+5	3.2E+3	1.4E+4	3.4E+4	5.2E+4	3.3E+6	2.3E+5	4.8E+5	7.4E+5
BacHum	C 100 mL <sup>-1</sup>	< 10	4.3E+3	42	403	1.1E+3	< 10	1.1E+6	4.8E+3	7.7E+4	2.5E+5
BacBov	C 100 mL <sup>-1</sup>	< 10	< 10	< 10	< 10	0	< 10	1.6E+4	290	2.3E+3	4.0E+3
ACE-K	ng L <sup>-1</sup>	< 140	562	150	228	133	350	2460	1033	1280	683
CAF	ng L <sup>-1</sup>	0.456	7.38	1.36	1.95	1.74	2.36	64.2	10.9	16.9	15.9

Table B-1 Cont'd											
		Upstream (n = 16)*					Downstream (n = 17)**				
For:	units:	Min.	Max.	Med.	Mean	Std. Dev.	Min.	Max.	Med.	Mean	Std. Dev.
CBZ	ng L <sup>-1</sup>	< 0.438	< 0.438	< 0.438	< 0.438	0	4.44	32.0	16.6	17.6	7.84
GEM	ng L <sup>-1</sup>	< 0.032	< 0.032	< 0.032	< 0.032	0	< 0.032	49.8	0.28	3.74	11.9
IBU	ng L <sup>-1</sup>	< 0.228	1.84	< 0.228	0.393	0.446	< 0.228	49.8	2.76	9.33	13.5
NAP	ng L <sup>-1</sup>	< 0.254	0.394	< 0.254	0.263	0.034	0.356	628	12.4	51.9	149
SMX	ng L <sup>-1</sup>	< 0.394	2.00	< 0.394	0.689	0.506	< 0.394	7.88	2.38	2.91	2.10
TP	µg L <sup>-1</sup>	13.6	362	36.5	64.1	86.1	42.0	235	62.0	85.4	53.0
TDP	µg L <sup>-1</sup>	12.8	232	33.7	49.3	54.7	24.6	160	51.8	63.1	34.6
SRP	µg L <sup>-1</sup>	11.6	210	33.4	45.5	48.1	16.4	147	43.2	51.8	31.9
TN	mg L <sup>-1</sup>	5.48	31.5	12.5	15.4	8.49	2.26	11	5.72	5.74	2.15
NO <sub>3</sub> -N	mg L <sup>-1</sup>	4.84	27.4	11.2	13.8	7.15	1.80	9.66	5.55	5.16	1.89
NO <sub>2</sub> -N	mg L <sup>-1</sup>	0.003	0.017	0.010	0.010	0.004	0.014	0.148	0.042	0.046	0.031
NH <sub>3+4</sub> -N	mg L <sup>-1</sup>	0.01	1.02	0.03	0.09	0.24	0.041	0.186	0.085	0.088	0.036

\*n = 13 for CAF, CBZ, and SMX

\*\*n = 16 for GEM and NAP

**Table B-2** - Statistical summary table for general water quality, FIB, and organic tracer concentrations measured at Site B Upstream and Downstream sample sites. Min. = minimum; Max. = maximum; Med. = median; Std. Dev. = standard deviation; n = count. measured below detection limits for the target parameter are reported as < MDL.

For:	units:	Upstream (n = 17)*					Downstream (n = 17)**				
		Min.	Max.	Med.	Mean	Std. Dev.	Min.	Max.	Med.	Mean	Std. Dev.
Temp.	°C	1.8	16.1	9.1	9.3	5.0	0.5	18.3	13.1	10.6	6.5
pH	units	6.76	8.77	7.94	7.94	0.48	7.28	8.65	8.13	8.09	0.37
DO	mg L <sup>-1</sup>	4.18	18.1	8.37	8.52	3.18	4.53	14.1	10.4	9.94	2.60
SPC	µS cm <sup>-1</sup>	455	1120	841	852	145	676	1530	845	905	187
Turb.	NTU	4.6	37.2	9.1	11.9	8.3	0.9	51.1	5.5	8.8	11.5
Alk.	mg L <sup>-1</sup> CaCO <sub>3</sub>	146	416	315	315	65	120	340	256	260	45
DOC	mg L <sup>-1</sup>	4.36	33.1	15.5	15.2	7.58	3.56	52.2	20.1	42.2	92.6
TS	mg L <sup>-1</sup>	302	770	563	584	121	308	651	558	536	70
Cl	mg L <sup>-1</sup>	12.2	153	34.9	44.4	31.3	29.4	181	79.1	89.4	44.4
SO <sub>4</sub>	mg L <sup>-1</sup>	3.73	61.0	25.7	28.1	13.9	4.13	50.4	16.5	19.0	13.6
Ca	mg L <sup>-1</sup>	48.1	133	108	106	19.4	43.1	109	87.0	85.3	14.7
K	mg L <sup>-1</sup>	1.6	35.8	14.7	15.7	8.9	2.40	10.2	4.93	5.54	1.81
Na	mg L <sup>-1</sup>	14.1	58.8	33.5	34.4	10.1	25.0	98.8	69.0	70.2	20.4
Mg	mg L <sup>-1</sup>	11.0	33.5	27.2	26.6	5.3	9.2	24.3	22.2	21.6	3.4
Ag	µg L <sup>-1</sup>	< 9	< 9	< 9	< 9	0	< 9	< 9	< 9	< 9	0
Al	µg L <sup>-1</sup>	< 2	54.2	2.4	9.6	14.7	< 2	54.5	< 2	8.9	16.7
Ba	µg L <sup>-1</sup>	52.4	86.1	69.3	68.2	9.1	51.9	97.3	71.1	74.8	13.3
Be	µg L <sup>-1</sup>	< 0.1	0.249	< 0.1	0.121	0.040	< 0.1	0.207	< 0.1	0.123	0.035
Bi	µg L <sup>-1</sup>	< 5	< 5	< 5	< 5	0	< 5	< 5	< 5	< 5	0
Cd	µg L <sup>-1</sup>	< 0.9	3.2	< 0.9	1.2	0.67	< 0.9	3.5	< 0.9	1.2	0.67
Co	µg L <sup>-1</sup>	< 1	2.5	1.1	1.4	0.55	< 1	2.2	< 1	1.2	0.33
Cr	µg L <sup>-1</sup>	< 1	< 1	< 1	< 1	0	< 1	< 1	< 1	< 1	0
Cu	µg L <sup>-1</sup>	1.21	6.09	3.90	3.50	1.50	1.69	5.53	3.50	3.47	1.26
Fe	µg L <sup>-1</sup>	17.8	175	78.3	91.7	52.0	22.8	119	52.6	54.8	27.5
Li	µg L <sup>-1</sup>	< 5	25.4	10.1	11.1	6.1	< 5	29.9	11.2	11.3	6.6
Mn	µg L <sup>-1</sup>	23.6	276	76.4	104	70.2	19.8	139	42.3	47.1	28.1
Mo	µg L <sup>-1</sup>	< 2	3.88	< 2	2.17	0.46	< 2	3.11	< 2	2.24	0.36
Ni	µg L <sup>-1</sup>	< 2	< 2	< 2	< 2	0	< 2	< 2	< 2	< 2	0
Pb	µg L <sup>-1</sup>	< 7	< 7	< 7	< 7	0	< 7	< 7	< 7	< 7	0
Sn	µg L <sup>-1</sup>	< 9	< 9	< 9	< 9	0	< 9	< 9	< 9	< 9	0
Sr	µg L <sup>-1</sup>	99	368	286	278	62	90	384	287	290	72
Ti	µg L <sup>-1</sup>	0.50	3.16	1.04	1.24	0.669	< 0.5	3.38	0.83	0.94	0.66
U	µg L <sup>-1</sup>	4.75	14.6	8.68	8.81	2.76	3.72	13.4	6.37	7.02	2.85
V	µg L <sup>-1</sup>	0.51	2.14	1.23	1.23	0.49	< 0.5	1.19	0.696	0.744	0.219
Zn	µg L <sup>-1</sup>	17.8	87.1	57.7	49.0	23.1	15.4	106	36.4	35.0	21.4
Zr	µg L <sup>-1</sup>	< 1	< 1	< 1	< 1	0	< 1	< 1	< 1	< 1	0
<i>E. coli</i>	CFU 100 mL <sup>-1</sup>	2.8E+3	1.6E+5	1.6E+4	2.9E+4	3.7E+4	4.6E+2	3.2E+4	4.3E+3	6.0E+3	7.4E+3
BacGen	C 100 mL <sup>-1</sup>	1.5E+5	5.7E+7	1.6E+6	7.1E+6	1.4E+7	8.2E+4	3.6E+6	1.4E+6	1.6E+6	1.2E+6
BacHum	C 100 mL <sup>-1</sup>	< 10	1.2E+5	1.1E+3	1.8E+4	3.4E+4	1.4E+2	1.3E+6	3.4E+4	1.7E+5	3.1E+5
BacBov	C 100 mL <sup>-1</sup>	170	4.4E+7	2.5E+4	4.3E+6	1.1E+7	7.6E+2	2.1E+6	1.2E+4	2.2E+5	5.1E+5
ACE-K	ng L <sup>-1</sup>	< 140	54300	288	3560	12700	535	14900	1550	3250	3880

	units:	Upstream (n = 17)*					Downstream (n = 17)**				
		Min.	Max.	Med.	Mean	Std. Dev.	Min.	Max.	Med.	Mean	Std. Dev.
CAF	ng L <sup>-1</sup>	2.18	46.7	11.4	16.2	13.0	5.70	109	31.2	45.2	34.0
CBZ	ng L <sup>-1</sup>	< 0.438	1.714	< 0.438	0.659	0.343	0.650	8.16	3.26	3.56	1.93
GEM	ng L <sup>-1</sup>	< 0.032	0.054	< 0.032	0.033	0.005	< 0.032	66.8	< 0.032	12.9	21.5
IBU	ng L <sup>-1</sup>	1.17	1160	22.2	90.2	267	< 0.228	82.0	35.6	34.3	27.5
NAP	ng L <sup>-1</sup>	< 0.254	55.2	0.426	6.62	14.9	9.00	105	47.0	50.8	26.3
SMX	ng L <sup>-1</sup>	< 0.394	0.612	< 0.394	0.409	0.053	< 0.394	11.1	2.35	3.86	3.54
TP	µg L <sup>-1</sup>	478	2270	872	1090	623	239	1320	370	438	252
TDP	µg L <sup>-1</sup>	362	1950	681	908	555	162	1040	314	359	202
SRP	µg L <sup>-1</sup>	316	1720	607	721	422	152	948	315	322	182
TN	mg L <sup>-1</sup>	3.8	20.7	9.71	11.38	5.66	3.00	7.35	4.41	4.98	1.45
NO <sub>3</sub> -N	mg L <sup>-1</sup>	0.602	16.4	4.42	7.26	5.22	0.456	6.46	3.45	3.62	1.58
NO <sub>2</sub> -N	mg L <sup>-1</sup>	0.074	1.31	0.193	0.299	0.292	0.048	0.37	0.119	0.161	0.103
NH <sub>3+4</sub> -N	mg L <sup>-1</sup>	0.525	5.51	1.47	2.03	1.37	0.202	2.19	0.359	0.591	0.474

\*n = 16 for CAF, CBZ, and SMX

\*\*n = 16 for CAF, CBZ, and SMX

**Table B-3** - Statistical summary table for general water quality, FIB, and organic tracer concentrations measured at Site C Upstream and Downstream sample sites. Min. = minimum; Max. = maximum; Med. = median; Std. Dev. = standard deviation; n = count. measured below detection limits for the target parameter are reported as < MDL.

For:	units:	Upstream (n = 14)*					Downstream (n = 16)**				
		Min.	Max.	Med.	Mean	Std. Dev.	Min.	Max.	Med.	Mean	Std. Dev.
Temp.	°C	0.0	19.0	6.2	8.5	7.4	-0.2	20.2	10.3	9.3	7.3
pH	units	7.66	9.01	8.08	8.19	0.40	7.15	8.64	8.05	8.03	0.42
DO	mg L <sup>-1</sup>	7.3	14.2	10.8	10.5	1.97	0.50	20.2	11.6	10.3	4.47
SPC	µS cm <sup>-1</sup>	320	832	659	654	114	367	1530	831	828	246
Turb.	NTU	0.6	23.1	1.4	4.0	5.9	1.7	14.0	4.3	5.6	3.5
Alk.	mg L <sup>-1</sup> CaCO <sub>3</sub>	109	313	271	267	49	118	307	283	262	47
DOC	mg L <sup>-1</sup>	5.16	33.9	16.2	18.2	9.89	4.12	84.8	9.98	17.0	19.9
TS	mg L <sup>-1</sup>	211	503	471	448	72	223	1530	549	588	268
Cl	mg L <sup>-1</sup>	11.6	202	30.0	44.1	46.9	0.21	185	55.1	66.9	48.4
SO <sub>4</sub>	mg L <sup>-1</sup>	5.21	53.7	17.2	24.1	15.1	3.22	65.2	21.8	26.3	19.5
Ca	mg L <sup>-1</sup>	37.9	112	98.1	93.3	17.7	39.1	157	100	97.1	22.9
K	mg L <sup>-1</sup>	1.84	3.22	2.31	2.45	0.44	2.28	14.70	3.29	4.25	2.96
Na	mg L <sup>-1</sup>	8.22	42.9	16.6	17.6	7.54	12.6	222	39.4	53.5	47.8
Mg	mg L <sup>-1</sup>	9.01	30.7	26.3	25.1	5.33	10.1	45.2	25.8	26.0	6.89
Ag	µg L <sup>-1</sup>	< 9	< 9	< 9	< 9	0	< 9	< 9	< 9	< 9	0
Al	µg L <sup>-1</sup>	< 2	114	< 2	11.4	28.9	< 2	172	< 2	14.2	41.1
Ba	µg L <sup>-1</sup>	39.7	84.7	55.9	60.4	13.6	35.0	107	60.5	65.5	20.6
Be	µg L <sup>-1</sup>	< 0.1	0.194	< 0.1	0.113	0.025	< 0.1	0.440	< 0.1	0.141	0.086
Bi	µg L <sup>-1</sup>	< 5	< 5	< 5	< 5	0	< 5	< 5	< 5	< 5	0
Cd	µg L <sup>-1</sup>	< 0.9	1.87	< 0.9	1.05	0.28	< 0.9	8.27	< 0.9	1.59	1.78
Co	µg L <sup>-1</sup>	< 1	1.94	< 1	1.11	0.24	< 1	3.39	< 1	1.34	0.60
Cr	µg L <sup>-1</sup>	< 1	< 1	< 1	< 1	0	< 1	< 1	< 1	< 1	0
Cu	µg L <sup>-1</sup>	1.15	4.63	2.34	2.59	1.12	< 0.5	4.99	2.99	2.81	1.45
Fe	µg L <sup>-1</sup>	12.8	212	26.3	44.1	49.3	7.0	292	22.0	41.8	66.1
Li	µg L <sup>-1</sup>	< 5	23.4	7.7	9.3	5.3	< 5	24.4	6.9	9.6	5.7
Mn	µg L <sup>-1</sup>	1.3	70.5	20.6	21.5	16.9	5.7	1350	25.7	110	321
Mo	µg L <sup>-1</sup>	< 2	2.27	< 2	2.03	0.08	< 2	2.36	< 2	2.02	0.09
Ni	µg L <sup>-1</sup>	< 2	< 2	< 2	< 2	0	< 2	2.29	< 2	2.02	0.07
Pb	µg L <sup>-1</sup>	< 7	< 7	< 7	< 7	0	< 7	< 7	< 7	< 7	0
Sn	µg L <sup>-1</sup>	< 9	< 9	< 9	< 9	0	< 9	< 9	< 9	< 9	0
Sr	µg L <sup>-1</sup>	49	224	141	140	34	53	298	152	158	55
Ti	µg L <sup>-1</sup>	< 0.5	1.66	0.55	0.76	0.36	< 0.5	1.950	0.668	0.842	0.489
U	µg L <sup>-1</sup>	4.21	13.60	8.38	8.80	2.71	3.43	12.40	7.64	7.87	2.30
V	µg L <sup>-1</sup>	< 0.5	1.24	0.645	0.696	0.216	< 0.5	1.62	0.763	0.930	0.438
Zn	µg L <sup>-1</sup>	14.8	75.4	21.3	29.2	16.5	15.4	117	22.6	34.6	25.4
Zr	µg L <sup>-1</sup>	< 1	< 1	< 1	< 1	0	< 1	< 1	< 1	< 1	0
<i>E. coli</i>	CFU 100 mL <sup>-1</sup>	< 4	1.2E+3	85	270	370	8	1.3E+3	230	420	430
BacGen	C 100 mL <sup>-1</sup>	9.2E+3	3.6E+5	5.2E+4	8.6E+4	9.9E+4	2.0E+4	1.0E+6	1.1E+5	1.9E+5	2.3E+5
BacHum	C 100 mL <sup>-1</sup>	< 10	3.0E+4	860	3.1E+3	7.5E+3	< 10	3.5E+4	1.4E+3	5.0E+3	8.6E+3
BacBov	C 100 mL <sup>-1</sup>	< 10	3.7E+3	10	450	1.0E+3	> 10	8.5E+3	< 10	1.7E+3	2.7E+3
ACE-K	ng L <sup>-1</sup>	< 140	6870	242	771	1700	< 140	3290	446	790	875



For:	units:	Upstream (n = 14)*					Downstream (n = 16)**				
		Min.	Max.	Med.	Mean	Std. Dev.	Min.	Max.	Med.	Mean	Std. Dev.
CAF	ng L <sup>-1</sup>	0.624	11.42	1.28	2.63	3.11	0.550	22.0	3.22	5.05	5.14
CBZ	ng L <sup>-1</sup>	< 0.438	1.058	< 0.438	0.494	0.178	< 0.438	6.18	< 0.438	1.04	1.41
GEM	ng L <sup>-1</sup>	< 0.032	< 0.032	< 0.032	< 0.032	0	< 0.032	0.1808	< 0.032	0.043	0.036
IBU	ng L <sup>-1</sup>	< 0.228	< 0.228	< 0.228	< 0.228	0	< 0.228	1.86	0.243	0.457	0.509
NAP	ng L <sup>-1</sup>	< 0.254	0.518	< 0.254	0.300	0.088	< 0.254	4.16	< 0.254	0.787	1.03
SMX	ng L <sup>-1</sup>	< 0.394	7.36	< 0.394	1.03	2.00	< 0.394	3.32	0.536	0.801	0.755
TP	µg L <sup>-1</sup>	29.6	239	65.4	87.0	61.4	48	382	145	167	98.7
TDP	µg L <sup>-1</sup>	17.4	150	54.8	66.8	45.1	23.8	360	110	124	91.5
SRP	µg L <sup>-1</sup>	15.6	130	41.7	55.5	38.8	17	259	100	105	71
TN	mg L <sup>-1</sup>	2.3	6.37	4.4	4.40	1.18	0.88	9.3	4.58	4.51	2.05
NO <sub>3</sub> -N	mg L <sup>-1</sup>	1.87	6.03	4.14	3.88	1.12	0.033	5.31	3.78	3.30	1.77
NO <sub>2</sub> -N	mg L <sup>-1</sup>	0.01	0.112	0.0235	0.036	0.027	0.012	0.330	0.028	0.080	0.100
NH <sub>3+4</sub> -N	mg L <sup>-1</sup>	0.019	0.229	0.041	0.056	0.051	0.016	3.26	0.079	0.466	0.858

\*n = 11 for CAF, CBZ, and SMX, n = 13 for GEM and NAP

\*\*n = 14 for SMX, n = 15 for CAF and CBZ

**Table B-4** - Table summarizing the Spearman Rank Order statistical test results for correlation coefficients ( $\rho$ ) obtained for Site A (SA) upstream (US) and downstream (DS) between the nutrient concentrations and the tracer concentrations. The tabulated values represent the output  $\rho$ -value with the P-value underneath for the correlation values between the nutrients TP, TDP, SRP, TN, NO<sub>3</sub>-N, NO<sub>2</sub>-N, and NH<sub>3+4</sub>-N and the FIB/tracers *E. coli*, BacGen, BacBov, BacHum, ACE-K, CAF, CBZ, GEM, IBU, NAP, and SMX. Significant values ( $P < 0.05$ ) are bolded. --: no output (< MDL). The results were interpreted as: 0.2–0.4 = weak, 0.4–0.6 = moderate, and 0.6–0.8 = strong.

		<i>E. coli</i>	BacGen	BacBov	BacHum	ACE-K	CAF	CBZ	GEM	IBU	NAP	SMX
TP	US	0.45 0.076	<b>0.72</b> <b>0.002</b>	-- --	<b>0.69</b> <b>0.004</b>	0.19 0.476	0.25 0.403	-- --	-- --	0.38 0.136	0.36 0.160	0.11 0.709
	DS	<b>0.56</b> <b>0.019</b>	<b>0.59</b> <b>0.012</b>	0.28 0.271	<b>0.55</b> <b>0.022</b>	-0.22 0.387	-0.12 0.632	-0.09 0.722	-0.31 0.233	-0.09 0.722	0.06 0.814	-0.46 0.061
TDP	US	0.36 0.160	<b>0.69</b> <b>0.004</b>	-- --	<b>0.69</b> <b>0.004</b>	-0.07 0.788	0.15 0.616	-- --	-- --	0.23 0.384	0.36 0.160	0.05 0.849
	DS	<b>0.48</b> <b>0.050</b>	0.43 0.087	0.41 0.102	0.35 0.169	-0.19 0.454	-0.22 0.393	-0.04 0.861	-0.11 0.664	-0.02 0.943	-0.06 0.822	<b>-0.50</b> <b>0.041</b>
SRP	US	0.34 0.194	<b>0.64</b> <b>0.010</b>	-- --	<b>0.69</b> <b>0.004</b>	-0.09 0.746	0.02 0.949	-- --	-- --	0.23 0.384	0.36 0.160	0.03 0.906
	DS	0.44 0.076	<b>0.49</b> <b>0.043</b>	<b>0.49</b> <b>0.047</b>	0.40 0.111	-0.16 0.521	-0.13 0.625	-0.07 0.780	-0.08 0.746	0.16 0.534	0.02 0.943	<b>-0.50</b> <b>0.038</b>
TN	US	-0.08 0.763	-0.06 0.812	-- --	0.23 0.403	-0.46 0.072	0.05 0.863	-- --	-- --	-0.32 0.220	-0.36 0.160	-0.05 0.849
	DS	<b>-0.62</b> <b>0.008</b>	-0.14 0.579	-0.28 0.275	-0.15 0.553	-0.25 0.321	-0.04 0.876	-0.42 0.091	-0.41 0.112	-0.13 0.625	0.08 0.754	0.25 0.331
NO <sub>3</sub> -N	US	-0.09 0.730	-0.15 0.593	-- --	0.15 0.584	-0.40 0.121	0.10 0.737	-- --	-- --	-0.32 0.228	-0.42 0.101	0.04 0.892
	DS	<b>-0.63</b> <b>0.006</b>	-0.27 0.298	-0.34 0.176	-0.38 0.134	-0.02 0.928	0.03 0.898	-0.27 0.288	-0.15 0.571	-0.062 0.809	0.024 0.926	0.37 0.142
NO <sub>2</sub> -N	US	0.45 0.076	0.27 0.325	-- --	0.42 0.113	-0.07 0.797	-0.21 0.481	-- --	-- --	0.17 0.512	0.31 0.238	0.20 0.504
	DS	0.44 0.076	0.33 0.189	-0.02 0.928	-0.09 0.715	-0.06 0.817	-0.22 0.387	0.24 0.346	-0.10 0.697	-0.18 0.478	0.17 0.533	-0.03 0.906
NH <sub>3+4</sub> -N	US	0.04 0.865	0.07 0.802	-- --	-0.15 0.584	0.17 0.512	-0.30 0.313	-- --	-- --	-0.8 0.771	0.42 0.101	-0.28 0.352
	DS	-0.04 0.876	0.44 0.080	<b>0.76</b> <b>&lt; 0.001</b>	0.38 0.131	-0.22 0.398	0.15 0.553	<b>-0.67</b> <b>0.003</b>	-0.30 0.252	<b>0.48</b> <b>0.050</b>	0.15 0.563	<b>-0.58</b> <b>0.014</b>

**Table B-5** - Table summarizing the Spearman Rank Order statistical test results for correlation coefficients ( $\rho$ ) obtained for Site B (SB) upstream (US) and downstream (DS) between the nutrient concentrations and the tracer concentrations. The tabulated values represent the output  $\rho$ -value with the P-value underneath for the correlation values between the nutrients TP, TDP, SRP, TN, NO<sub>3</sub>-N, NO<sub>2</sub>-N, and NH<sub>3+4</sub>-N and the FIB/tracers *E. coli*, BacGen, BacBov, BacHum, ACE-K, CAF, CBZ, GEM, IBU, NAP, and SMX. Significant values ( $P < 0.05$ ) are bolded. --: no output ( $< MDL$ ). The results were interpreted as: 0.2–0.4 = weak, 0.4–0.6 = moderate, and 0.6–0.8 = strong

		<i>E. coli</i>	BacGen	BacBov	BacHum	ACE-K	CAF	CBZ	GEM	IBU	NAP	SMX
TP	US	0.24 0.341	0.08 0.744	-0.21 0.420	0.02 0.928	<b>0.49</b> <b>0.046</b>	0.42 0.104	<b>0.66</b> <b>0.005</b>	0.26 0.316	<b>0.50</b> <b>0.040</b>	0.29 0.258	0.47 0.068
	DS	0.24 0.341	-0.06 0.802	-0.06 0.824	-0.19 0.449	-0.04 0.861	<b>-0.49</b> <b>0.050</b>	0.45 0.078	0.07 0.78	-0.30 0.237	<b>-0.65</b> <b>0.005</b>	<b>-0.50</b> <b>0.046</b>
TDP	US	0.11 0.666	-0.02 0.928	-0.33 0.186	0.14 0.579	0.45 0.072	0.37 0.153	<b>0.64</b> <b>0.007</b>	0.26 0.316	<b>0.54</b> <b>0.026</b>	0.31 0.214	0.41 0.115
	DS	0.24 0.336	-0.14 0.579	-0.20 0.437	-0.24 0.346	0.03 0.898	<b>-0.54</b> <b>0.032</b>	<b>0.50</b> <b>0.047</b>	0.19 0.454	-0.34 0.173	<b>-0.62</b> <b>0.008</b>	<b>-0.53</b> <b>0.034</b>
SRP	US	0.07 0.780	-0.04 0.883	-0.38 0.131	0.13 0.612	0.43 0.082	0.48 0.057	<b>0.63</b> <b>0.009</b>	0.26 0.316	<b>0.49</b> <b>0.045</b>	0.34 0.173	0.45 0.082
	DS	0.34 0.179	-0.28 0.266	-0.26 0.302	-0.169 0.509	0.26 0.316	-0.15 0.578	<b>0.60</b> <b>0.013</b>	0.36 0.157	-0.11 0.666	-0.35 0.166	-0.26 0.325
TN	US	0.28 0.280	0.03 0.898	-0.29 0.254	0.15 0.566	-0.23 0.377	0.02 0.935	0.31 0.233	0.38 0.126	-0.26 0.312	0.22 0.387	0.32 0.215
	DS	-0.17 0.515	-0.04 0.861	0.14 0.598	-0.03 0.891	<b>-0.61</b> <b>0.010</b>	-0.35 0.178	<b>-0.64</b> <b>0.007</b>	<b>-0.52</b> <b>0.034</b>	-0.41 0.104	-0.19 0.466	<b>0.51</b> <b>0.043</b>
NO <sub>3</sub> -N	US	-0.04 0.869	-0.14 0.598	-0.28 0.280	0.05 0.831	-0.37 0.137	-0.22 0.403	0.02 0.943	0.26 0.316	-0.37 0.145	0.03 0.898	-0.01 0.969
	DS	-0.34 0.182	-0.29 0.258	-0.09 0.730	-0.18 0.484	<b>-0.62</b> <b>0.008</b>	-0.23 0.378	<b>-0.53</b> <b>0.033</b>	-0.42 0.093	-0.27 0.288	-0.20 0.443	0.37 0.149
NO <sub>2</sub> -N	US	0.228 0.371	-0.22 0.387	<b>-0.60</b> <b>0.011</b>	0.16 0.521	0.31 0.218	<b>0.49</b> <b>0.050</b>	<b>0.65</b> <b>0.006</b>	0.20 0.426	0.13 0.618	<b>0.72</b> <b>0.001</b>	0.48 0.057
	DS	-0.17 0.502	<b>-0.69</b> <b>0.002</b>	<b>-0.57</b> <b>0.016</b>	-0.41 0.096	-0.04 0.876	-0.27 0.314	<b>0.66</b> <b>0.005</b>	0.04 0.869	-0.28 0.266	-0.33 0.193	-0.17 0.526
NH <sub>3+4</sub> -N	US	0.47 0.058	0.42 0.093	0.09 0.730	0.38 0.126	0.09 0.730	0.03 0.917	0.33 0.198	0.26 0.316	0.23 0.361	0.09 0.730	0.45 0.082
	DS	<b>0.50</b> <b>0.039</b>	<b>0.72</b> <b>0.001</b>	<b>0.79</b> <b>&lt; 0.001</b>	0.31 0.226	-0.04 0.869	-0.29 0.272	-0.40 0.118	-0.39 0.116	-0.30 0.242	-0.08 0.744	0.35 0.178

**Table B-6** - Spearman Rank Order statistical test results for correlation coefficients ( $\rho$ ) obtained for Site C (SC) upstream (US) and downstream (DS) between nutrient concentrations and tracer concentrations. The tabulated values represent the output  $\rho$ -value with the P-value underneath for the correlation values between the nutrients TP, TDP, SRP, TN, NO<sub>3</sub>-N, NO<sub>2</sub>-N, and NH<sub>3+4</sub>-N and the FIB/tracers *E. coli*, BacGen, BacBov, BacHum, ACE-K, CAF, CBZ, GEM, IBU, NAP, and SMX. Significant values ( $P < 0.05$ ) are bolded. --: no output ( $< MDL$ ). The results were interpreted as: 0.2–0.4 = weak, 0.4–0.6 = moderate, and 0.6–0.8 = strong

		<i>E. coli</i>	BacGen	BacBov	BacHum	ACE-K	CAF	CBZ	GEM	IBU	NAP	SMX
TP	US	<b>0.68</b> <b>0.008</b>	<b>0.64</b> <b>0.013</b>	-0.06 0.844	0.22 0.444	-0.30 0.293	-0.08 0.797	0.20 0.538	-- --	-- --	0.16 0.603	0.50 0.109
	DS	0.43 0.094	<b>0.50</b> <b>0.046</b>	0.23 0.378	<b>0.56</b> <b>0.024</b>	0.39 0.130	0.09 0.753	0.40 0.138	0.16 0.548	-0.38 0.143	-0.38 0.139	-0.18 0.532
TDP	US	<b>0.69</b> <b>0.006</b>	<b>0.62</b> <b>0.017</b>	-0.23 0.407	0.21 0.453	-0.14 0.626	-0.13 0.693	0.20 0.538	-- --	-- --	0.08 0.778	0.50 0.109
	DS	<b>0.57</b> <b>0.020</b>	0.39 0.136	0.30 0.257	0.39 0.133	0.27 0.303	0.14 0.602	0.24 0.381	0.26 0.325	-0.20 0.442	-0.32 0.220	0.05 0.856
SRP	US	<b>0.70</b> <b>0.004</b>	<b>0.61</b> <b>0.019</b>	-0.23 0.407	0.26 0.364	-0.17 0.542	-0.12 0.714	0.20 0.538	-- --	-- --	< 0.01 0.993	0.50 0.109
	DS	<b>0.60</b> <b>0.014</b>	0.37 0.149	0.31 0.238	0.43 0.094	0.24 0.354	0.08 0.763	0.20 0.465	0.19 0.463	-0.14 0.594	-0.29 0.272	0.07 0.808
TN	US	-0.33 0.231	-0.48 0.078	0.33 0.244	0.18 0.532	<b>-0.55</b> <b>0.039</b>	0.01 0.968	-0.20 0.538	-- --	-- --	-0.02 0.935	-0.40 0.210
	DS	0.36 0.167	-0.01 0.969	-0.07 0.788	-0.14 0.601	0.16 0.548	0.01 0.954	0.17 0.540	0.49 0.052	0.08 0.763	-0.09 0.721	0.03 0.916
NO <sub>3</sub> -N	US	-0.29 0.301	-0.22 0.435	0.27 0.340	0.36 0.201	<b>-0.58</b> <b>0.029</b>	-0.13 0.693	-0.30 0.353	-- --	-- --	-0.29 0.323	-0.50 0.109
	DS	0.24 0.372	0.12 0.648	-0.33 0.207	-0.07 0.780	0.23 0.384	0.05 0.852	0.12 0.657	<b>0.65</b> <b>0.006</b>	-0.02 0.935	-0.23 0.397	0.15 0.605
NO <sub>2</sub> -N	US	0.11 0.693	0.08 0.773	0.49 0.072	-0.01 0.964	<b>-0.72</b> <b>0.003</b>	0.36 0.257	0.30 0.353	-- --	-- --	< 0.01 0.993	0.20 0.538
	DS	<b>0.50</b> <b>0.046</b>	-0.28 0.282	<b>0.76</b> < <b>0.001</b>	-0.01 0.952	-0.11 0.680	-0.05 0.842	0.02 0.954	-0.11 0.680	-0.29 0.277	-0.20 0.456	<b>-0.64</b> <b>0.014</b>
NH <sub>3+4</sub> -N	US	-0.35 0.212	-0.32 0.264	-0.23 0.407	<b>-0.64</b> <b>0.014</b>	0.29 0.308	<b>0.66</b> <b>0.026</b>	0.30 0.353	-- --	-- --	0.52 0.067	0.50 0.109
	DS	0.29 0.267	0.12 0.656	0.44 0.087	0.08 0.771	-0.05 0.856	-0.01 0.954	0.09 0.743	-0.15 0.571	0.22 0.409	0.27 0.308	-0.19 0.511

## Appendix C: Equations for Calculations in Chapter 2

**Equation C.1** – Equation showing the calculation made to estimate NO<sub>3</sub>-N (NO<sub>3</sub>N) concentrations with the reported concentrations of NO<sub>2+3</sub>-N (NO<sub>2+3</sub>N) and NO<sub>2</sub>-N (NO<sub>2</sub>N) concentrations. Concentrations were reported as mg L<sup>-1</sup>.

$$\text{NO}_3\text{N} = \text{NO}_{2+3}\text{N} - \text{NO}_2\text{N}$$

**Equation C.2** – Equation showing the calculation made to estimate BacHum abundances with the reported abundance of BacGen and the proportion characterized as BacHum% (%). Final abundances were reported as C 100 mL<sup>-1</sup>.

$$\text{BacHum} = \frac{\text{BacGen} \cdot \text{BacHum}\%}{100}$$

**Equation C. 3** - Equation showing the calculation made to estimate BacBov abundances with the reported abundance of BacGen and the proportion characterized as BacBov% (%). Final abundances were reported as C 100 mL<sup>-1</sup>.

$$\text{BacBov} = \frac{\text{BacGen} \cdot \text{BacBov}\%}{100}$$

**Appendix D:  
Additional Figures/Tables for Chapter 3**

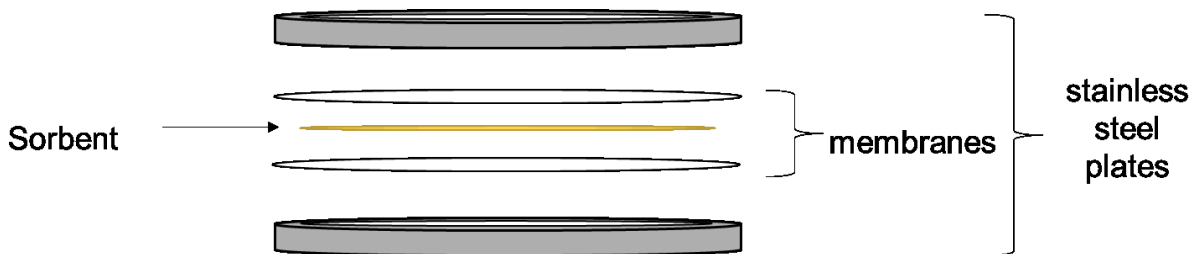


**Figure D-1** – Schematic of a POCIS with two stainless steel washers securing two filter membranes and a receiving phase (sorbent).

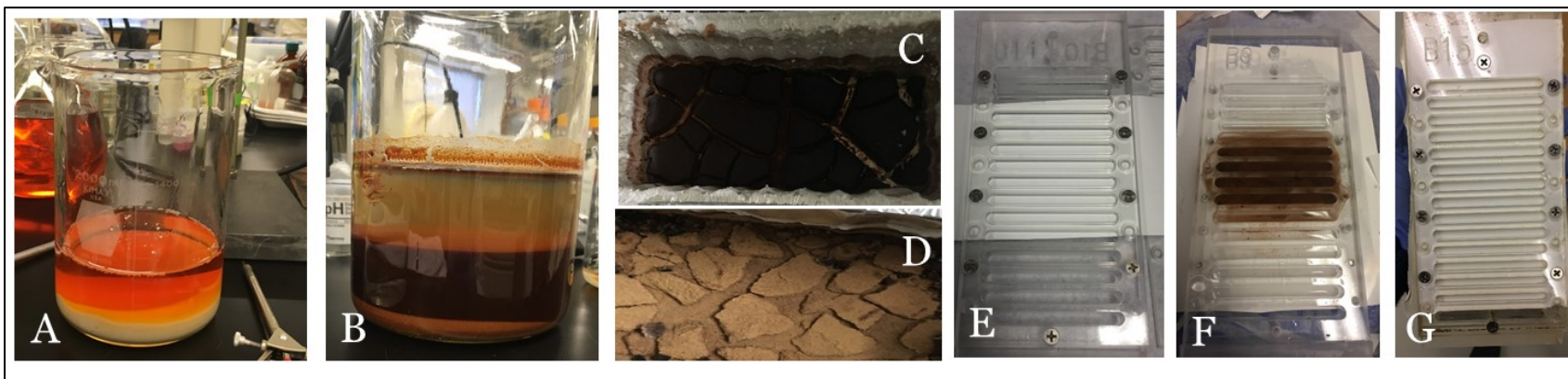


**Figure D-2** – A. mixture of sand and ferric nitrate; B. after the addition of NaOH; C. slurry after supernatant water was removed; D. dried Fe-coated sand; E. P-Trap outer plate overlain with filter membrane paper and secure to the main plate; F. addition of sand and ultrapure water into the P-Trap; G. addition of the second filter membrane paper and the outer plate. Photos taken by Maria Digaletos (2018).



**Figure D-3** -Placement of the passive samplers within a wire cage in a stream (SA-DS). The membranes of the POCIS and P-Traps are placed parallel to the flow of the stream to allow interaction with both sides of the samplers. Photos taken by Maria Digaletos (2017).





**Figure D-4** – Three POCIS removed from the stream (SA-DS) after a 14-day deployment. The POCIS may have been exposed to the air during a portion of the deployment period, as shown by the inconsistent lines and fouling on the membranes. Photos taken by Maria Digaletos (2017).